GDANSK UNIVERSITY OF TECHNOLOGY
FACULTY OF OCEAN ENGINEERING AND SHIP TECHNOLOGY
SECTION OF TRANSPORT TECHNICAL MEANS
OF TRANSPORT COMMITEE OF POLISH ACADEMY OF SCIENCES
UTILITY FOUNDATIONS SECTION
OF MECHANICAL ENGINEERING COMMITTEE OF POLISH ACADEMY OF SCIENCE

ISSN 1231 – 3998
ISBN 83 – 900666 – 2 – 9

Journal of

POLISH CIMAC

ENERGETIC ASPECTS

Vol. 8 **No. 1**

Gdansk, 2013

Science publication of Editorial Advisory Board of POLISH CIMAC

Editorial Office:

GDANSK UNIVERSITY OF TECHNOLOGY
Faculty of Ocean Engineering and Ship Technology
Department of Ship Power Plants
G. Narutowicza 11/12 80-233 GDANSK POLAND
tel. +48 58 347 29 73, e – mail: sek4oce@pg.gda.pl

www.polishcimac.pl

This journal is devoted to designing of diesel engines, gas turbines and ships' power transmission systems containing these engines and also machines and other appliances necessary to keep these engines in movement with special regard to their energetic and pro-ecological properties and also their durability, reliability, diagnostics and safety of their work and operation of diesel engines, gas turbines and also machines and other appliances necessary to keep these engines in movement with special regard to their energetic and pro-ecological properties, their durability, reliability, diagnostics and safety of their work, and, above all, rational (and optimal) control of the processes of their operation and specially rational service works (including control and diagnosing systems), analysing of properties and treatment of liquid fuels and lubricating oils, etc.

All papers have been reviewed

ISSN 1231 – 3998
ISBN 83 – 900666 – 2 – 9

Printed in Poland

CONTENTS

GDAŃSK UNIVERSITY OF TECHNOLOGY

Journal of POLISH CIMAC

Faculty of Ocean Engineering & Ship Technology
GDAŃSK UNIVERSITY OF TECHNOLOGY

STABILIZING PISTON SPEED WITH A LAYER OF CARBON NANOTUBES ON THE LATERAL SURFACE OF THE PISTON

Antoni Iskra, Maciej Babiak, Jarosław Kałużny

Poznan University of Technology
Institute of Combustion Engines and Transport
Piotrowo Street 3, 60-965 Poznań, Poland
tel.: +48 61 665 25 11, fax: +48 61 665 22 04
e-mail: antoni.iskra@put.poznan.pl

Michael Giersig

Freie Universitaet Berlin
Arnimallee 14, 14195 Berlin
tel.: 00493083853047, fax: 004983856299
e-mail: giersieg@physik.fu-berlin.de

Krzysztof Kempa

Boston College
Chestnut Hill MA, 02467 Boston
tel.: +1 617 552 3592, fax: +1 617 552 8478
email: kempa@bc.edu

Abstract

The paper presents the possibility of stabilizing higher harmonics of piston speed generated by torsional vibrations of the shaft. As a result of torsional vibrations, the transient speed of the piston deviates from the values resulting from the known formulae describing geometrical dependences of the piston position versus the angle of rotation of the crankshaft [1]. This phenomenon causes the desired effect of damping torsional vibrations. As it is known, in larger engines of the cylinder diameter exceeding 120mm and the number of in-line cylinders greater than or equal to 6, structural damping is insufficient and it becomes necessary to use torsional vibration dampers. In article [2] attention was drawn to the effect of damping higher harmonics of the moment generated by the engine whose lateral surfaces are coated with layers of nanotubes, which was not however, the main subject of the article. This work presents a preliminary analysis and determinants of the efficiency of vibration damping due to the impact of nanotubes on the reduction of the amplitude of higher harmonics of the moment generated by the engine. In addition, the possible mechanism of the phenomenon of vibration damping by a layer of nanotubes is presented. However, one should emphasize that at this stage the authors do not close the debate concerning the mechanical properties of the structures based on carbon nanotubes (CNTs), but in fact, they open up such a discussion. Besides the confirmed properties of nanotubes, such as extremely high tensile strength of properly structured fiber formed by CNTs, there is very little data concerning the properties of chaotic structures in which nanotubes combine in larger structures adopting any directions. No less important is the base on which nanotubes are grown, and it can be very different. The authors of the paper have presented preliminary results of a positive impact of selected properties of CNTs on the vibrations of the crankshaft.

Keywords: *friction in internal combustion engine, nanotubes layers, crankshaft torsional vibration*

1. Introduction

One of the methods of reducing friction losses in a combustion engine is coating the lateral surfaces of pistons with proper layers with a low coefficient of friction. This method assumes that in a combustion engine the lateral surface of the piston comes into direct contact with the cylinder bearing surface. As it is confirmed by the research and computer simulations, the described situation is a phenomenon of a relatively short duration, usually when the engine is started, following a longer standstill [3]. Consequently, in a properly designed piston-cylinder group, the friction losses depend to a small extent on coating the lateral surfaces of the piston with layers with a low coefficient of friction. The importance of these coatings is exposed in easier engine start, and first of all, in reducing abrasive wear, before a continuous oil film is formed on the cylinder bearing surface. However, it appears that coating the cylinder bearing surface with specific layers may lead to reducing vibrations of the crankshaft, and thus the whole sequence of drive transmission. Fig. 1 presents schematically and disproportionately the combination of the side-surface of a piston coated with a layer of carbon nanotubes with the cylinder bearing surface.

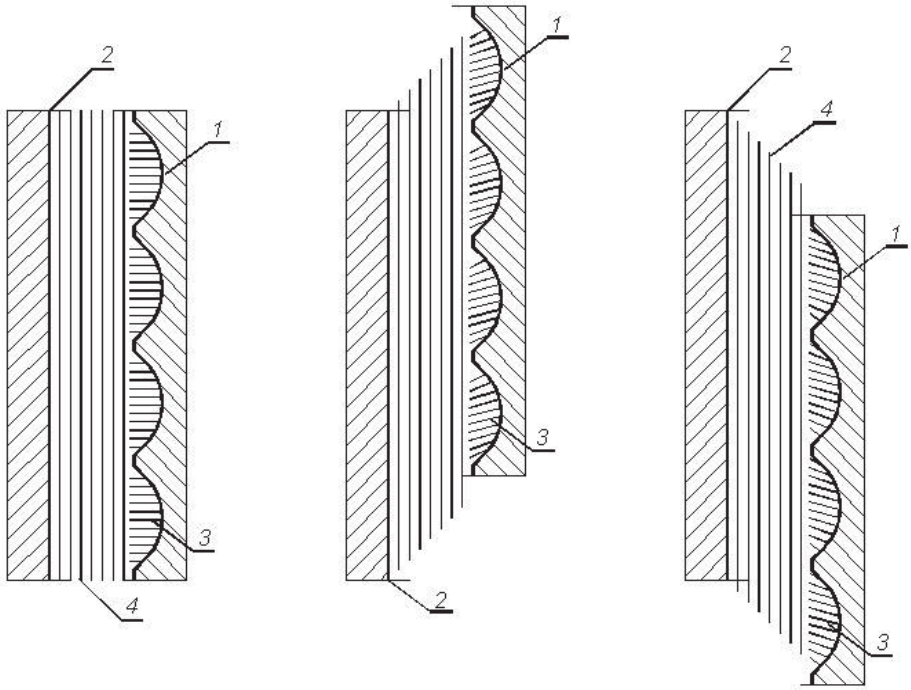

Fig. 1. The combination of the side-surface of a piston coated with a layer of carbon nanotubes with the cylinder bearing surface – description in the text

The structure of the lateral surface of piston 1 was outlined while taking into account only the trace of the curvature of the cutting tool that is left after finishing. Both on the lateral surface of the piston and on cylinder bearing surface 2 there is micro-roughness which is not relevant to the discussed issue, therefore, Fig. 1 pictures the plateau of these surfaces. In the grooves of the side-surface of the piston, there are embedded carbon nanotubes 3, which in fact form a chaotic structure. But in order to orientate the reader which direction the layer of nanotubes is deforming, they were pictured by horizontal lines. The layers of the oil film formed between the surfaces in contact was marked by vertical lines. The position of the piston on the left side in Fig. 1

corresponds to the zero relative velocity of the piston and sleeve. The middle diagram shows laminar motion of the oil film layers when the piston is ascending, and the diagram on the right side describes the piston motion in the opposite direction. As a result of the laminar movement of the oil film layers, within the contact area of a layer of nanotubes, there occurs a tangential force deforming nanotubes located in the grooves of the lateral surface of the piston. The deformation of the nanotube layer may be elastic, elastic-plastic or plastic. The results of the test carried out by the authors of this article confirm that the structure of randomly oriented nanotubes mainly exhibits elastic properties. This means that the energy of deformation of the nanotube layer is absorbed at the very moment when the piston accelerates, and when the piston slows down its speed in relation to the sleeve, the energy is transferred onto the piston and further onto the power receiver. As a result, there occurs suppression of higher harmonics describing the movement of the piston, which is equivalent to damping torsional vibration of the shaft. As it is known, the basic component of damping torsional vibrations in a classic internal combustion engine is generated by the viscous force of the oil film on the cylinder bearing surface. Unfortunately, such damping of torsional vibrations causes large energy losses because the change in the velocity of oil layers which are moved laminarily causes energy absorption, whether the piston accelerates or slows down; therefore, irrespective of the direction of the piston motion as well.

2. The course of engine's moment of resistance to motion

The actual course of the coupling moment of an internal combustion piston engine with a driving machine deviates considerably from the calculation values based on geometrical relationships. The reason lies in numerous phenomena, but the vibrations of the following unit: the engine shaft – the driving machine shaft are the most important. From a very extensive study, we selected the most representative measurement results of the coupling moment of a two-cylinder combustion engine with a driving machine and the obtained results are presented in Fig. 2-4.

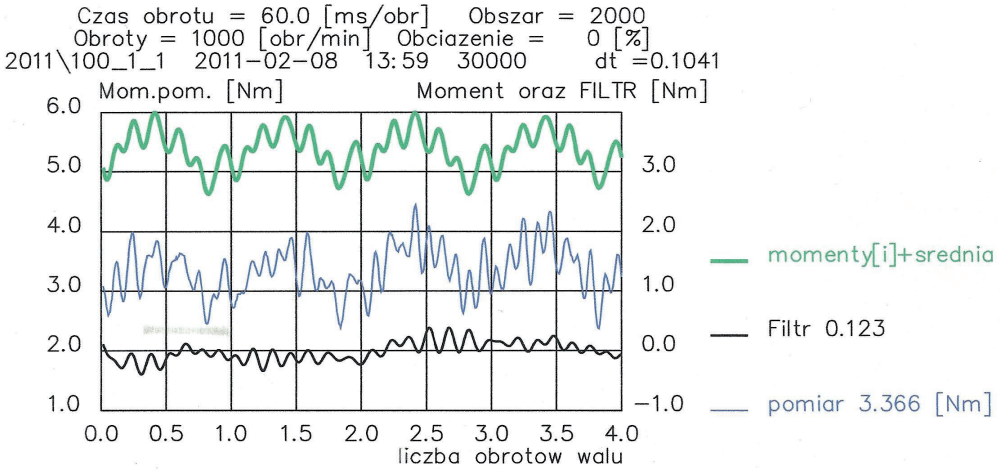

KEY: Czas obrotu- revolution time, obszar – area, obroty- revolutions, obciążenie – load, pomiar – measurement, Moment oraz filtr – torque and filter, liczba obrotów wału – crankshaft revolutions

Fig. 2. The course of the coupling moment of a two-cylinder combustion engine with the machine driving the engine at the angular velocity of 1000 rpm for standard pistons whose lateral surface is not coated with a layer of nanotubes, description in the text

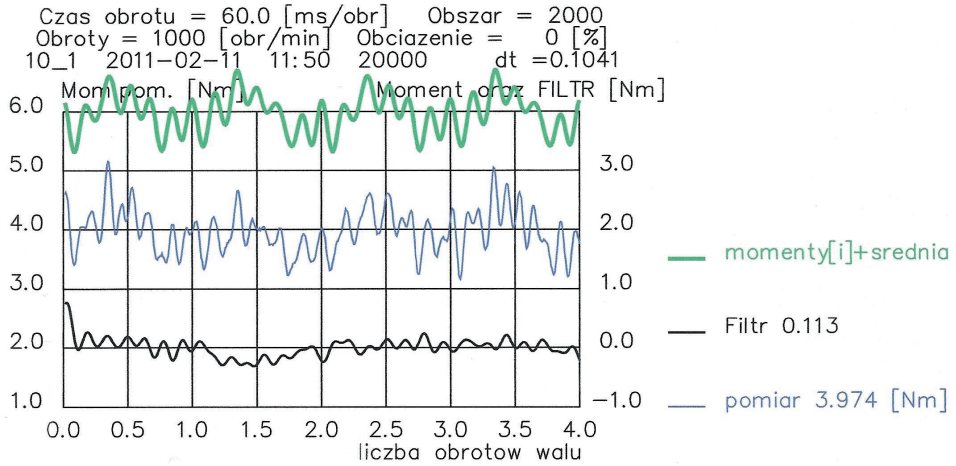

Fig. 3. The course of the coupling moment of a two-cylinder combustion engine with the machine driving the engine at the angular velocity of 1000 rpm after 10-minute grinding-in of nanotubes on the lateral surface of the piston

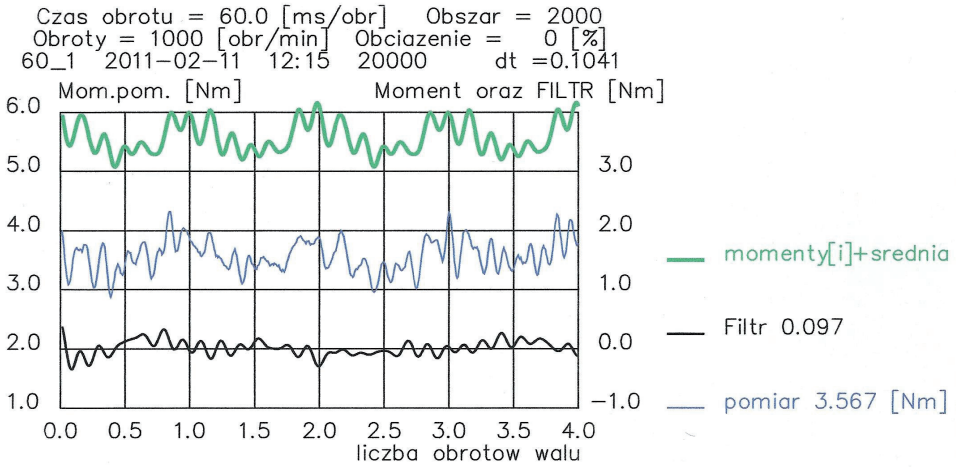

Fig. 4. The course of the coupling moment of a two-cylinder combustion engine with the machine driving the engine at the angular velocity of 1000 rpm after 60-minute grinding-in of nanotubes on the lateral surface of the piston

The following are marked in the drawings:

- the blue line – the course of the measured coupling moment, wherein the scale of the graph is described on the left vertical axis. The mean coupling moment is given on the right side of the drawing, next to the word "pomiar",
- the green line – the course of the processed signal of repeatable moment every two rotations of the crankshaft; the scale of the graph was described on the right vertical axis,
- the black line – the course of the filtered signal causing unrepeatability of the coupling moment at the rhythm of processes taking place in the engine, the scale of the graph was also described on the right vertical axis.

Due to the engine type and its modifications, the course of the coupling moment should in principle be repeatable every single rotation, but because of the difference in distance of two

double cranks from the driving machine there must occur certain differences in the generated moment of resistance related to the compression of the agent within cylinder volume. This results from differential susceptibility of drive transmission.

What is important is the answer to the question of the cause of unrepeatability of the measured coupling moment. As one can notice, in the case of full repeatability of the coupling moment the filtered signal shown as the black line in Fig. 2-4 should amount to 0. However, since the filtered signal shows variable values, one should accept a definition of a certain indicator which would be the measure of unrepeatability of the course of the coupling moment. The simplest and, as it seems, the most proper indicator of the unrepeatability of the coupling moment is the sum of deviations from the mean value in relation to the number of included values. In this case, the mean value is 0, and the deviation is always assumed positive. The indicator of unrepeatability of the courses of the coupling moment is to be referred to as α in later parts of the article.

As mentioned above, it is torsional vibrations that are the main cause of unrepeatability of the courses of the coupling moment. The frequency of these vibrations is dependent on the mass moments of inertia of the elements coupled with the shafts and the rigidity of the units connecting the shafts, and not on the angular speed of the set: combustion engine – driving machine. One can, therefore, put forward a hypothesis that the smaller the value of indicator α of unrepeatability of courses, the less the energy of torsional vibrations, and therefore less stress loading the engine's shaft.

In Fig. 2-4 the values of indicators α were marked next to the word „Filtr" on the right side of the graphs. The value of indicator α is given in [Nm]. More details of the process of evaluating the value of the filtered signal are provided presented in literature [2].

In the case of a standard piston engine in which the piston lateral surface is not coated with a layer of nanotubes, the value of indicator α was 0.123 [Nm] – Fig. 2. Coating the lateral surface of the pistons with a 5 μm layer of nanotubes brought about a decrease in the initial value of indicator α to the level of 0.113 Nm – Fig. 3. This value was obtained following a 10-minute running-in of the engine, since the moment when pistons coated with a layer of nanotubes were embedded. The shape and location of the layer of nanotubes is shown in Fig. 5.

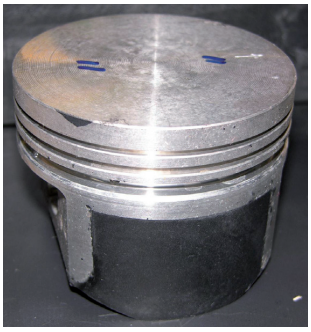

Fig. 5. The piston with a layer of nanotubes applied to the lateral surface prior to testing

Further grinding-in the layer of nanotubes on the lateral surface of the piston during the period of 30 minutes caused a systematic decrease in the average value of the coupling moment, followed by its stabilization. The course of the coupling moment that was obtained after 60 minutes is shown in Fig. 4. The value of indicator α after 60 minutes of movement decreased to 0.097 [Nm] so in relation to the value α for standard pistons, the decrease in free vibrations of the set was reduced by approximately 25%.

Having completed the testing, a disassembly of the engine was performed. Examination of the pistons demonstrated that the layer of nanotubes was worn off to the edges of vertices that were left as a result of machining – Fig. 6.

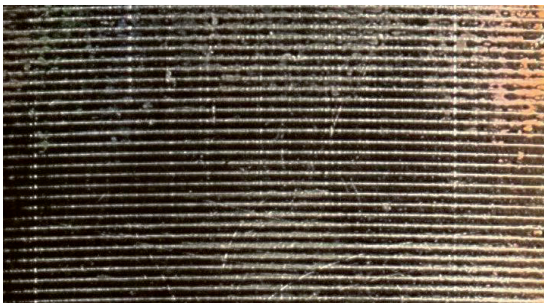

Fig 6. A section of the lateral surface of the piston following a 60min running process

One should emphasize that applying a layer of nanotubes on the surface of an aluminum alloy is a process that is still in its experimental phase, and first attempts to control such a process gave positive results in very few laboratories [4-14]. Fig. 7-8 present the structures of the chosen ways of growing nanotubes on the surface of a carrier.

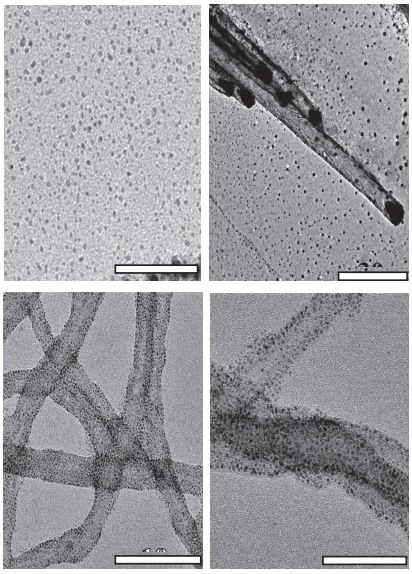

Fig. 7. Pictures from a transmission electron microscope presenting CNTs with the embedded platinum nanoparticles on them

Conducting the process of growth while applying a strong electric field allows for vertical growth of nanotubes, which is very important from the viewpoint of mechanical properties of the applied layers on the side-surfaces of pistons. The vertical growth of CNTs was presented in Fig.ures 8A), B) and C), whereas the anisotropic one in Fig. 8 D).

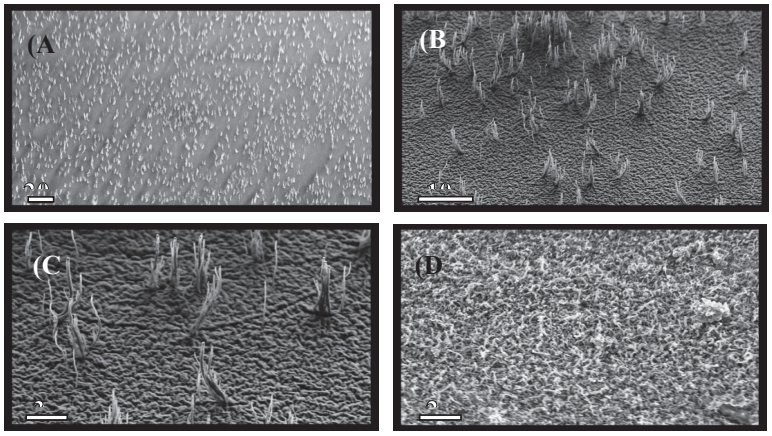

Fig. 8. Pictures from a scanning electron microscope (SEM) showing metal surface coated with CNTs with the embedded platinum nanoparticles on them

Current research focuses on growing more durable layers of CNTs of the desired mechanical properties on the surface of aluminum alloys.

3. Summary

The research presented in the article shows the possibility of using coverings of layers of nanotubes on the lateral surface of the aluminum alloy piston in order to reduce unwanted torsional vibrations in the sequence of drive transmission. Further tests modifying the structures of nanotubes are being carried out in order to reduce frictional resistance and to more effectively reduce the vibrations of the engine shaft. The experiments concerning applying various elements and chemical compounds on CNTs suggest that damping properties of nanotube layers and the frictional forces generated by them on the contacting point of oil film allow for obtaining significantly better performance of piston combustion engines. Frictional losses of pistons on the cylinder bearing surface will, however, depend first of all on the parameters of the oil film that is generated by properly designed lateral surface of the piston. Any layers applied to the lateral surfaces of pistons may reduce friction only in the phase of starting an engine, before oil film is formed on the cylinder bearing surface.

References

[1] Iskra, A., *Dynamika mechanizmów tłokowych silników spalinowych*, Wydawnictwo Politechniki Poznańskiej, pp. 1-271, Poznań 1995.

[2] Iskra, A., Babiak, M., Kałużny, J., Giersig, M., Kempa, K., *Comparing the resistance to motion of piston coated with a layer of nanotubes with standard piston*, Journal of KONES 2012, Paper ID: 095. European Science Society of Powertrain and Transport, pp. 225-233, Warsaw 2012.

[3] Iskra, A., *Studium konstrukcji i funkcjonalności pierścieni w grupie tłokowo-cylindrowej*, Wydawnictwo Politechniki Poznańskiej, pp. 1-334, Poznań 1996.

[4] Ciałkowski, M., Iskra, A., Giersig, M., Kempa, K., *Wysokoefektywny samochodowy reaktor katalityczny na bazie trójwymiarowych hierarchicznych nanostruktur węglowych*, Nr projektu: 3940/T02/2007/32, Poznań 2009.

[5] K. Kinoshita, *Electrochemical oxygen technology*, John Wiley & Sons: New York, 1992.R. Durand, R. Faure, F. Gloaguen and D. Aberdam; R. R. Adzic, F. C. Ansonand K. Kinoshita, Eds., The Electrochem. Soc. Inc.: Pennington, Vol. 95-26, p 27, 1996.
[6] Kabbabi, A., Gloaguen, F., Andolfatto, F., Durand, R., *J. Electroanal. Chem.,* 373, pp. 251-254, 1994.
[7] Frelink, T., Visscher, W., vanVeen, J. A. R., *J. Electroanal. Chem.,* 382, pp. 65-72, 1995.
[8] Takasu, Y., Ohashi, N., Zhang, X. G., Murakami, Y., Minagawa, H., Sato, S., Yahikozawa, K., *Electrochim. Acta,* 41, pp. 2595-2600, 1996.
[9] Cherstiouk, O. V., Simonov, P. A., Savinova, E. R., *Electrochim. Acta, 48*, pp. 3851-3860, 2003.
[10] Maillard, F., Eikerling, M., Cherstiouk, O. V., Schreier, S., Savinova, E. Stimming, U., *Faraday Discuss.,* 125, pp. 357-377, 2004.
[11] Arenz, M., Mayrhofer, K. J. J., Stamenkovic, V., Blizanac, B. B., Tomoyuki, T., Ross, P. N., Markovic, N. M., *J. Am. Chem. Soc., 127*, pp. 6819-6829, 2005.
[12] Tang, Z. C., Geng, D. S., Lu, G. X., *J. Colloid Interface Sci.*, 287, pp. 159-166, 2005.
[13] Mukerjee, S., McBreen, J., *J. Electroanal. Chem.*, *448*, pp. 163-171, 1998.
[14] Sun, Y., Zhuang, L., Lu, J., Hong, X., Liu, P. J., *Am. Chem. Soc.*, 129, 15465-15467, 2007.

GDAŃSK UNIVERSITY OF TECHNOLOGY

Journal of POLISH CIMAC

Faculty of Ocean Engineering & Ship Technology
GDAŃSK UNIVERSITY OF TECHNOLOGY

VIBRATION SIGNALS OF RECIPROCATING COMPRESSOR VALVES

Paweł Białek, Piotr Bielawski

Maritime University of Szczecin
ul. Podgórna 51/53, 70-205 Szczecin, Poland
tel.: +48 91 4318540, fax: +48 91 4318542
e-mail: p.bielawski@am.szczecin.pl

Abstract

This study deals with the problem of the diagnostics of self-acting valves installed in reciprocating machines. Piston compressors and their valves are characterized. Compressor diagnostic systems, those offered and used, are described, including their restrictions. The signal generated by closing the valve is estimated. The authors have examined the relationship between the vibration signal and the condition of plate delivery valve of an air compressor. Simulations were made of the spring and plate wear and valve assembly errors. It has been shown that there is a relation between the selected vibration measure, mean peak-to-peak value of vibration accelerations and the technical condition of the discharge valve and measurement point. The authors have concluded, that in case of plate valves, one should expect that values of vibration measures depend on the measurement point and will decrease depending on its technical condition. A rule of diagnostic inference was formulated.

Keywords: *technical diagnostic, reciprocating machines, self-acting valves, condition of discharge valve, vibration signal*

1. Introduction

Successful vibration-based diagnostics of rotor machines encourage manufacturers of diagnostic systems to develop and offer equipment and systems for piston (reciprocating) machines as well, including piston compressors. Various authors indicate possibilities of effective diagnostics of piston-crank mechanism components. However, certain problems occur when attempts are made to diagnose valves.

2. Compressors and their valves

There is a wide variety of design solutions in piston compressors. Also, various classifications exist. Depending on the piston-crank mechanism, there are compressors with and without crank mechanisms. Depending on the arrangement of cylinders (shape of the crankshaft) compressors can be of in-line, boxer, V-, star- and vane types. If we consider the shape of piston, there will be single-acting, double-acting, differential and stage-differential pistons. Due to piston guiding, compressors are with or without crossheads. Depending on the piston axis position, compressors may be horizontal or vertical.

The medium and required pressure lead to this classification [3]:

– non-critical use: low pressures, gases are not dangerous;
– semi-critical use: high pressures, gases are not dangerous;

– critical use: media are potentially dangerous.

Considering compressor dimensions, e.g. power N of compressor drive, compressors belong to these ranges: $N < 50$ kW, 50 kW$< N <$ 100 kW, $N >$ 100 kW [3].

The medium being compressed results in another classification: air compressors, hydrogen compressors etc.

For the control of compressor working process valves are used: self-acting and controlled (forced timing). Forced timing is used mainly for controlling the delivery rate of the compressor. The suction valve closing angle is controlled by an electronically controlled hydraulic cylinder. In most design solutions self-acting valves are used.

Self-acting valves are of various types [4]:

– plate valves; these valves, with a plate functioning as the sealing element made of metal or non-metallic materials; this type of valve is used in oil and gas, fertilizer and other industries;
– ring valve; instead of a valve plate, independent rings are used. The rings are opened and closed by springs adjusted to the working conditions. The materials for rings are carbon fiber-reinforced composites, characterized by very high tightness, impact resistance, resistance to plastic deformation and particles, etc. Their significant advantage is that cylinder liner sliding surface is not damaged in case of ring fracture. Rings can be covered with an anti-adhesive material. Ring valves are intended for most extreme working conditions: hydrogen or light gases (molecular weight < 8 kg/kmol) in refineries and oil and gas industry;
– mushroom valves; valves with a number of mushrooms in one assembly are used in compressors installed in natural gas transport systems where large quantities of gas are transferred at relatively low degree of compression, at low or medium flow rate, 180–600 rpm. These parameters allow to apply high lift (max. lift: 8 mm);
– concentric valve; used in single-acting compressors, concentric valves are the most effective solutions, comprising the whole piston surface. The suction and discharge valves are mounted in a joint body of cylinder head. Such solution is characterized by slight flow resistance and high durability. These valves are used in air and refrigerating compressors, sometimes in single-acting gas compressors;
– lamellar valve. Lamellar (tongue) valves are generally an integral part of cylinder head. The lamella of the suction and discharge valve is integrated on one joint plate of the valve seat.

3. Diagnostics of compressors

Depending on the scope of identification of machine condition, condition monitoring and diagnostics are distinguished. As various equipment may be used, condition monitoring and diagnostics can be executed as remote condition monitoring and diagnostics, in-site monitoring and diagnostics or distributed condition monitoring or diagnostics.

In practice [3], compressors are generally equipped with vibration transmitters sending signals to superior systems. TDC sensors are also installed in order to carry out measurements for various angles of the crankshaft by means of a portable measuring instrument. Vibration transmitters are usually mounted on the cylinder block. Major compressors are additionally equipped with vibration transmitters installed on the crosshead guide. Some compressors are fitted with indicator cocks, so that during their operation, if need arises, p–V diagrams can be drawn by portable measuring instruments. During diagnostic inference the measured signals as a function of crankshaft rotation angle are analyzed.

Those dealing with compressor diagnostics face a problem of identifying components of a vibration signal measured on the compressor cylinder. Normal vibration sources are impacts of the piston against cylinder liner and impacts of valves against the cylinder head, dependent on the

condition and loads. The difficulty lies in the fact that both impacts occur at a similar rotation angle of the crankshaft, Fig. 1. Other sources of vibration are possible. These activate themselves only after a defect occurs. In [3] a case is described where an increase of acceleration of cylinder vibration was considered as a symptom of incorrect valve condition, while inspection revealed that the cause was piston seizure in the cylinder.

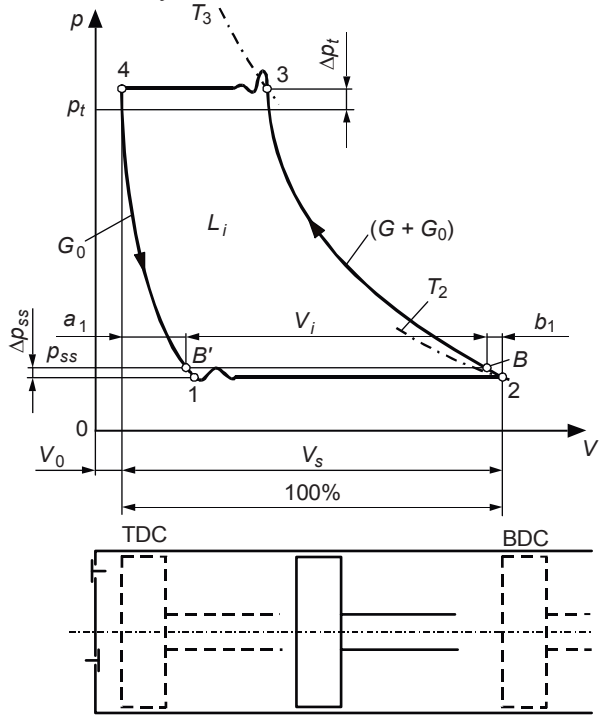

Fig. 1. P-v chart of a single-stage piston compressor: L_i – work of the circulation, TDC – top dead centre, BDC – bottom dead centre (own study on the basis of [2])

The problem of piston impact on the cylinder liner has been discussed in [1]. The impact of self-acting valves requires a separate analysis.

4. Examination of vibration signals from self-acting valves

The impact of valve plate against the valve seat depends on the pressure difference before and after the valve, valve spring tension, plate lift and "elasticity" of the plate and the seat. The mentioned quantities may change due to valve wear. As a result, the impact force may:

- increase, e.g. because of increased valve lift;
- decrease, e.g. due to decreased spring stiffness.

It should be expected that a diagnostic symptom of valves can be either an increase or decrease in the measure value of vibration generated by impacts in valves. The value of vibration measure also depends on the point of measurement. None of the authors on the subject indicates that the cylinder block is the best place for measuring vibration dependent on valve condition; points of measurement, however, are selected for their ease of mounting and conviction that the distance of vibration propagation of all possible sources is the shortest.

A vibration signal from a plate delivery valve was examined, Fig. 2.

The measurements aimed at examining the influence of changes in the technical condition of a discharge valve on the second cylinder of a three-cylinder single-stage air compressor on the vibration signals of the valve, valve plate and cylinder head, Fig. 3. Vibration accelerations were measured. Vibrations on the cylinder block were not measured as its construction made it impossible to measure vibrations by means of available transmitters.

Vibration accelerations as a function of time were measured in combination with a TDC signal from the second cylinder, Fig. 4.

One can conclude from Fig. 4 that:

– time signal of vibration has the highest value near the top dead centre, which means that that part of the signal is generated by the closing of delivery valve (see Fig. 1.),
– instantaneous values of that signal part are not constant, they change from cycle to cycle.

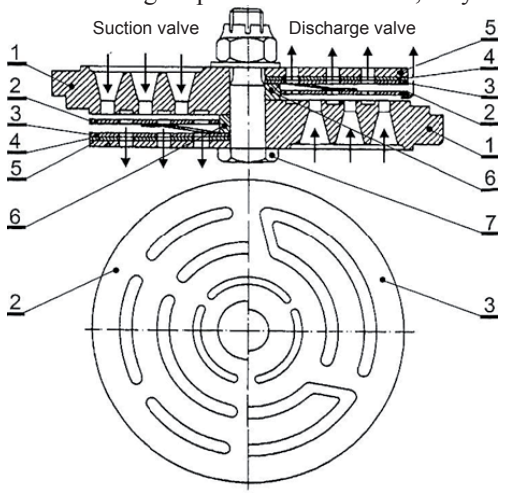

Fig. 2. Delivery and suction valves [2]: 1 – seat, 2 – plate, 3 – plate spring, 4 – damping plate, 5 – stop plate, 6 – guiding ring, 7 – bolt

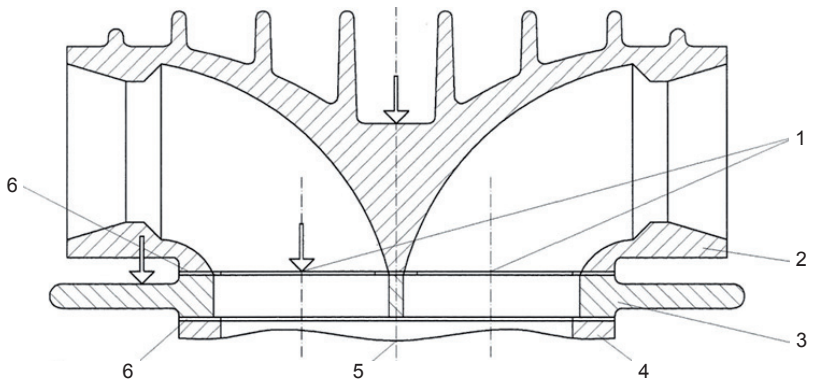

Fig. 3. A section across compressor components essential for vibration propagation (arrows show points where vibration transmitters were mounted): 1 – axes of valves, 2 – cylinder head, 3 – plate of the valve seat, 4 – cylinder block, 5 – axis of the piston movement, 6 – seal

Certain valve conditions were simulated in order to determine the influence of valve condition on the vibration signal. Then vibrations of the delivery valve bolt were measured. Tests were made without an external load of the compressor, i.e. with the cylinder cover removed and with low rotary speed. Simulated compressor conditions are given in Table 1. The peak-to-peak value of vibration was measured in a period much longer than one revolution. An example diagram is shown in Fig. 5.

The peak-to-peak values changing in time lead to a conclusion that after a time needed to stabilize the working conditions, the peak-to-peak value for simulated states reaches an average (constant value) and variable value Δ (difference between maximum and minimum values). Both values depend on the simulated condition of the valve. Table 2 contains simulated conditions and corresponding peak-to-peak values of vibration accelerations of the valve bolt.

Presented below in Table 3 are the peak-to-peak values of vibrations measured on the valve, valve plate and the cylinder head for one "normal" condition of the valve.

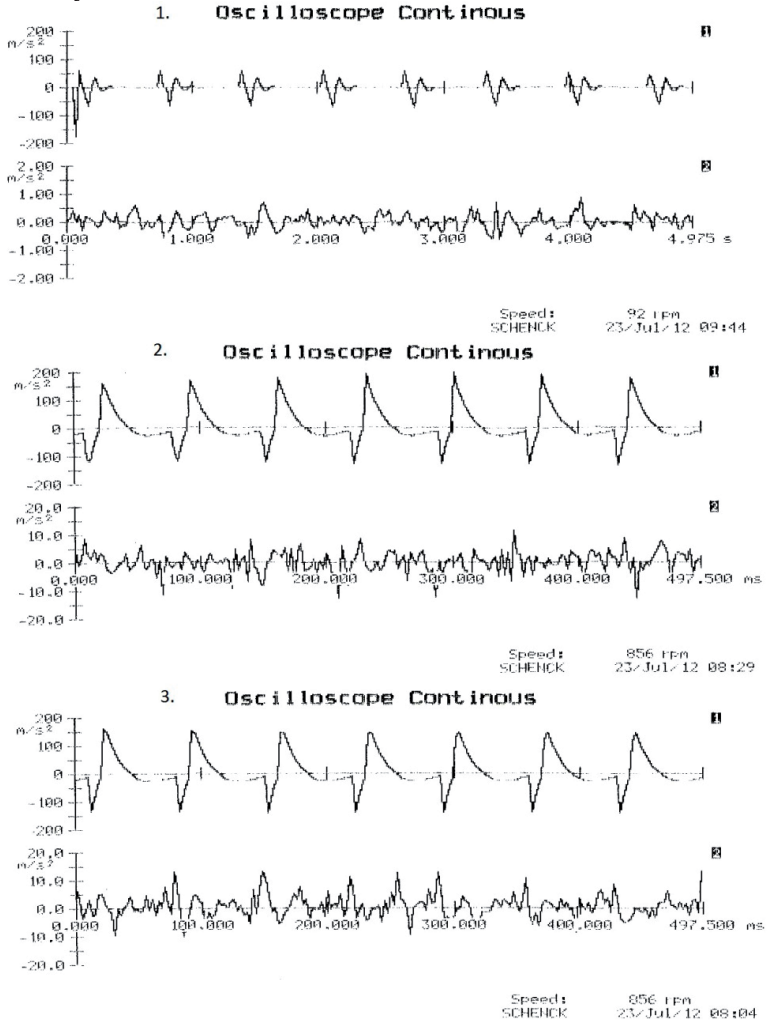

Fig. 4. Time / vibration acceleration diagrams and a corresponding TDC signal from the second cylinder, signal measured on: 1. valve bolt at 72 rpm and head removed, 2. valve plate at 856 rpm, 3. head at 856 rpm

Tab. 1. Measurements table

Item	Condition	Simulation
1	Normal	Valve is operational
2	Fracture A of valve plate	Radial "natural" fracture along 1/3 of the radius
3	Fracture B of valve plate	Lack of 1/3 external ring of valve plate
4	Fracture C of valve plate	Radial fracture along the whole radius length
5	High spring stiffness	3 springs
6	Low spring stiffness	1 spring
7	Suspension of valve plate	No valve plate
8	Spring wear	No spring
9	Backlash of two connected components	Loosened valve nut
10	Backlash in valve-plate connection	Loosened tightening ring

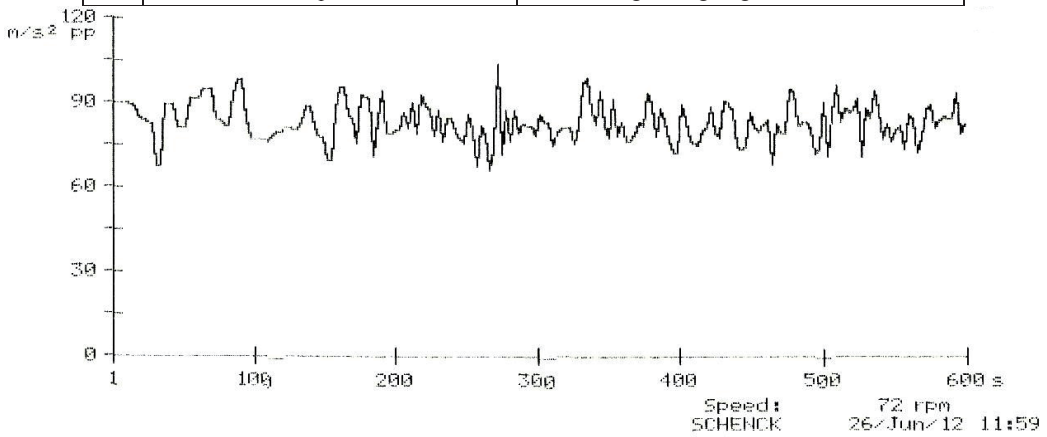

Fig. 5. Peak-to-peak values of vibration accelerations of an operational valve

Tab. 2. Measures of the time function of peak-to-peak values of vibration accelerations (valve bolt)

Condition	Constant value (mean) [m/s^2]	Δ [m/s^2]
Normal	79.2	38.7
Fracture A	61.6	37.5
Fracture B	4.15	(uncertain value)
Fracture C	55.6	34.4
High stiffness of spring	71.4	25.0
Low stiffness of spring	4.4	3.0
Suspension of valve plate	7.55	6.6
Spring wear	32.4	45.2
Backlash of two connected components	39.35	15.55
Backlash in valve-plate connection	69.975	25.7

Tab. 3. Peak-to-peak values of vibration accelerations generated by a valve working in the "normal" condition as a time function, for three measurement points

Measurement point:	Constant value (mean) [m/s^2]	Δ [m/s^2]
Valve bolt	79.2	38.7
Valve plate	11.4	10.0
Cylinder head	3.4	5.1

5. Conclusion

Simulated conditions of the valve tested consist in lower stiffness of the spring and lower tightness between the plate and t seat. Only a spring stiffness increase causes the valve lift to decrease. Lower spring stiffness leads to a drop in the mean peak-to-peak value. In the examined case − spring stiffness increase and related valve lift decrease − the decrease of mean peak-to-peak value turned out to be larger than the simultaneous increase caused by increased spring stiffness. Fractures in the valve plate cause a decrease in the mean peak-to-peak value. The causes may be as follows: decrease of the difference value of pressures on both sides of the valve and an increase of impact duration (due to lower plate stiffness). It seems that practically the wear of plate valves resulting in an essential increase of valve lift is unlikely. Therefore, it seems impossible that the vibration signal value will increase due to valve wear. In case of plate valves, one should expect that values of vibration measures will decrease depending on its technical condition. Additionally, these values depend on the measurement point: the signal weakens as the distance to a measuring point increases and if there are more indirect components in between.

References

[1] Bielawski, P., *Elementy diagnostyki drganiowej mechanizmów tłokowo-korbowych maszyn okrętowych*, Wyższa Szkoła Morska w Szczecinie, Szczecin 2002.

[2] Górski, Z., Perepeczko, A., *Okrętowe maszyny i urządzenia pomocnicze, tom I*, Trademar, Gdynia 1997.

[3] Rosenberg, Th., Schuhmann, R., *Überwachung von Kolbenverdichtern aus Sicht eines Betreibers*, Industriepumpen + Kompressoren, Heft 2/2010, Juni, S. 70–74.

[4] www.hoerbiger.com.

Journal of POLISH CIMAC
Faculty of Ocean Engineering & Ship Technology
GDAŃSK UNIVERSITY OF TECHNOLOGY

EXPOSURE TO VIBRATIONS GENERATED BY THE MOTOR VEHICLE

Rafał Burdzik, Piotr Czech, Łukasz Konieczny, Piotr Folęga

Silesian University of Technology
ul. Krasińskiego 8, 40-019 Katowice, Poland
tel.: +48 32 6034166, fax: +48 32 6034118
e-mail: rafal.burdzik@polsl.pl

Abstract

The article provides a discussion on the studies and analysis of exposure to vibrations generated by the motor vehicle. For the driving safety and comfort it is very important what kind and values of vibration are to car body. As the vibration source the motor-engine was chosen. The experiments were conducted on the car vehicle which was placed on the special test racks. It allows eliminate the road roughens impact on the suspension and in result to car body. The changes of the vibration signals from the motor-engine, floor panel and seat were observed and measured in 3 axes. These vibrations are producing a level of discomfort for driver..

Keywords: *engine vibration, exposure to vibration, vibration propagation*

1. Introduction

The vibrations are inseparable phenomena during operating and driving by all means of transport. Vehicles in motion are forced to vibration mainly by the road [20]. There are many of different vibration sources in vehicles as well. Some of them are main source of vibration during operating but without any movement. The motor engine should be considered as one of the most important vibration generator when the car doesn't drive. For the driving safety and comfort it is very important what kind and values of vibration are transfer to car body and driver. To improve the vibration isolation transferred to car body the identification of all sources of vibration and vibration material propagation should be taken into consideration. Thirty ears ago vehicles constructions were very heavy but than some policy started to demand to make the fuel consumption reduce. This started the evolution in material used in vehicles construction. Currently the car industry faces a crucial weight problem resulting from increasing customer demands in terms of safety and performance. Car bodies contribute 25% to the total weight of a car. Light weight metals are solution to decrease the body in weight. An increasing use of metals such as aluminium and magnesium in the automotive industry shows that there is still large scope for improvements [4,16,18]. It is very important to test new materials in many aspects. One of the more important is to guarantee the founded vibration damping level in terms of safety and comfort.

This paper take into account exposure to vibrations generated by the motor vehicle as the detrimental effect on the safety and comfort in mean of transport. The human response to vibration is depending on the values, frequencies and directions. The driver and passengers exposure to whole-body vibration of the vehicle can affect from short-term body discomfort and inefficient performance to longterm physiological damage.

2. Human perception of vibration in vehicles

Motor engine should be considered as the vibration generator as well. This kind of machine generate a disturbing force of one sort or another, but the frequency of the disturbing force should not be at, or near, a natural frequency of the structure otherwise resonance will occur, with the resulting high amplitudes of vibration and dynamic stresses, and noise and fatigue problems. Rotating machinery such as motors can generate disturbing forces at several different frequencies such as the rotating speed and blade passing frequency. Reciprocating machinery such as compressors and engines can rarely be perfectly balanced, and an exciting force is produced at the rotating speed and at harmonics. There are two basic types of structural vibration: steady-state vibration caused by continually running machines such as engines, air-conditioning plants and generators either within the structure or situated in a neighbouring structure, and transient vibration caused by a short-duration disturbance such as a lorry or train passing over an expansion joint in a road or over a bridge.

Ride comfort is extremely difficult to determine because of the variations in individual sensitivity to vibration. There are some research result published on effects of whole-body vibration and the ride comfort limits [6,9,10]. Some studies on heavy vehicles ride comfort mainly focus on road vehicles running on the ground [8,11]. There are some papers describing how vibration interferes with people's working efficiency, safety and health [1,14,15]. Therefore many researchers have concentrated their efforts on reducing the amount of vibration from vehicles. There are many reports describing the measurement of the transmissibility of the human body under vibration [7,12,13,17]. Some interesting researches were conducted for the low frequency discomfort for human analysed [19]. Ride vibrations are transmitted to the driver buttocks and back by the seat. The floor panel, pedal and steering wheel transmit additional vibrations to the feet and hands of the driver. These vibrations are producing a level of discomfort for driver.

Human perception of vibration is very good. It is a real challenge in structural design to ensure that the perception threshold level is not exceeded. Polish PN-91/N-01354 standard specifies methods for assessing exposure to vibrations of the overall impact on the human body. The parameter value can be used vibration dominant effective weighted vibration acceleration determined from the formula:

$$A_{w\max} = \max\left\{1.4 \cdot RMS(a_x), 1.4 \cdot RMS(a_y), RMS(a_z)\right\}, \tag{1}$$

where:
A_{wmax} - vibration dominant effective weighted vibration acceleration,
a_x – acceleration of vibration in X axis,
a_y – acceleration of vibration in Y axis,
a_z – acceleration of vibration in Z axis.

3. Research

Under the studies in question, active experiments were undertaken featuring measurements of vibration accelerations in a three directions in three selected points to analyse propagation of vibration generated by engine to driver feet and back.. It were recorded the vibration in three orthogonal axes (X,Y,Z). The purpose of the research was analysis of the car body vibration generated from motor engine. The experiments were conducted on the car vehicle which was placed on the special test racks. It allows eliminate the road roughens impact on the suspension and in result to car body. The paper presents some results of measurements vibration of motor engine, floor of the car under the driver foots and driver seat. It enables to analyse the way of vibration transfer from the source to driver. Ride vibrations are transmitted to the driver buttocks

and back by the seat. The floor panel transmit additional vibrations to the feet of the driver. These vibrations are producing a level of discomfort for driver.

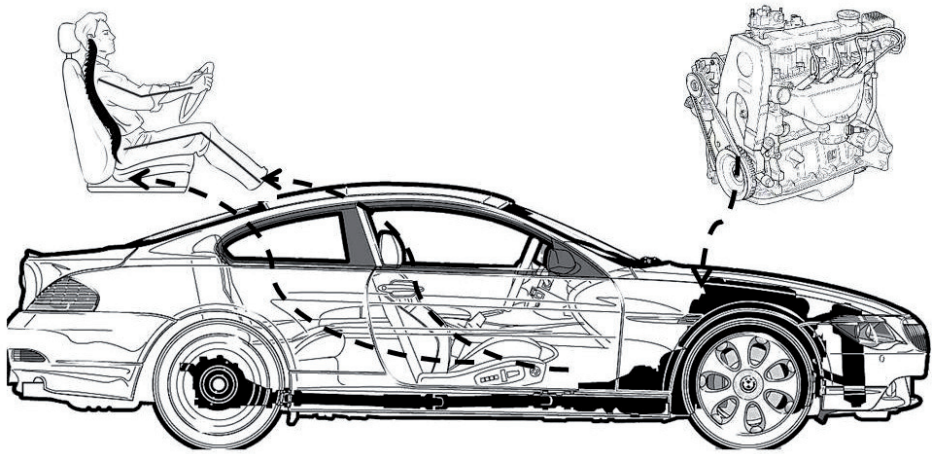

Fig. 1. Measurement of vibration of combustion engine in 3 directions

The established scope of research enables to observe changes of the vibration for chosen points on the vibration propagation way from engine. The three orthogonal axes were analysed separately. The comparison of the acceleration of vibration signals allows determine which directions of the vibration propagation is parent. The proposed methodology allows estimate influence of vibration generated by engine on human perception of vibration. The charts in this section illustrate time realization and spectrums of the vibration signals recorded during the experiments. The figures are grouped by the measurement points and contain vibrations in 3 axes.

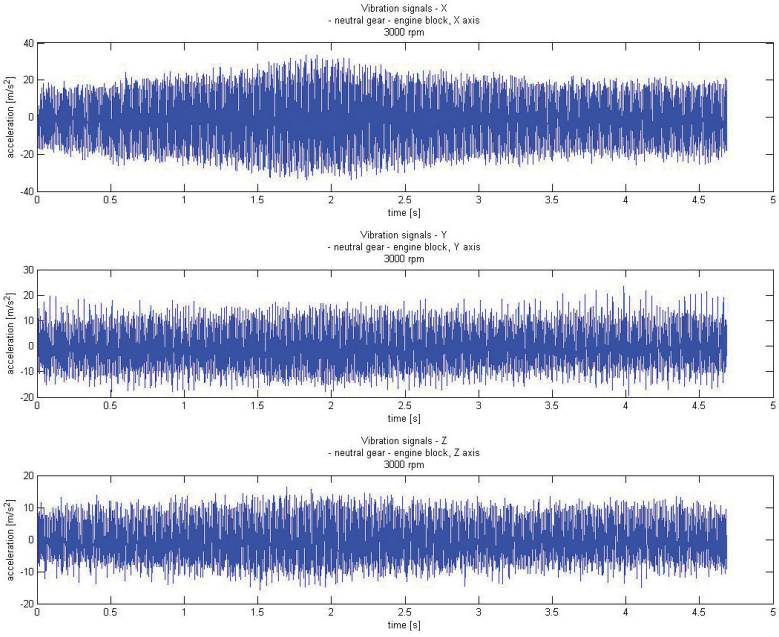

Fig. 2. Engine block vibration signal recorded in 3 axes

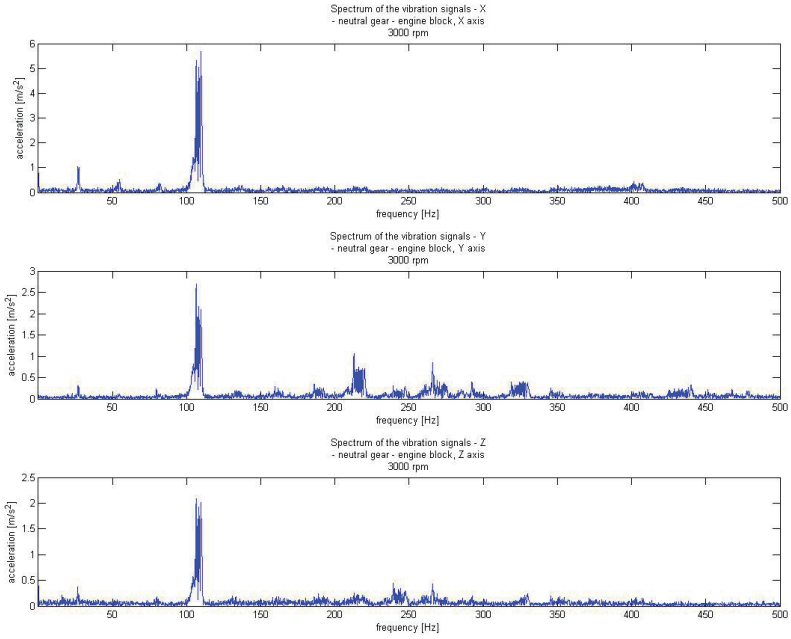

Fig. 3. Spectrums of the engine block vibration signal recorded in 3 axes

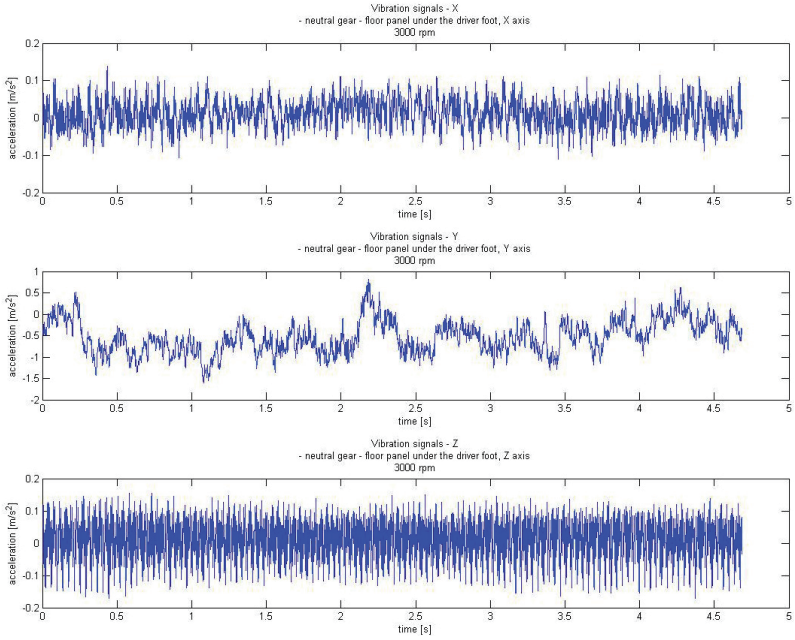

Fig. 4. Floor panel vibration signal recorded in 3 axes

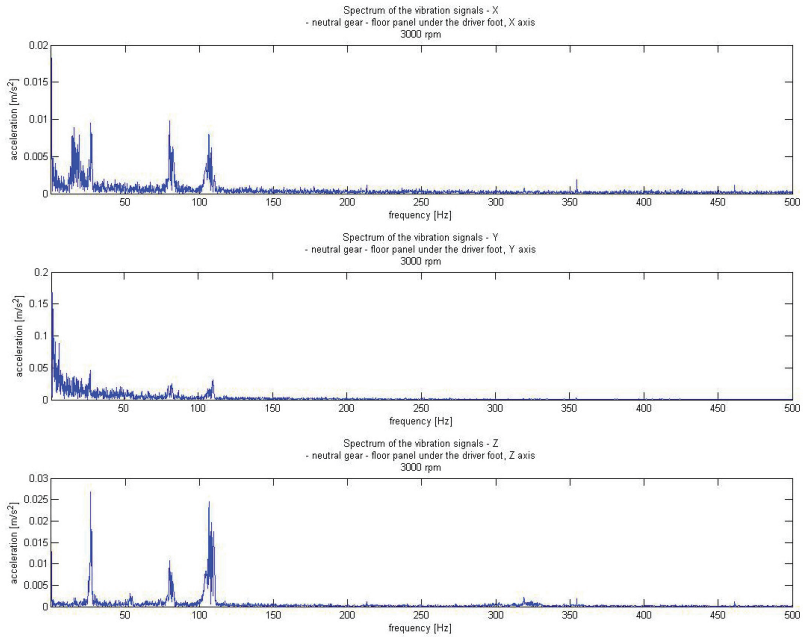

Fig. 5. Spectrums of the floor panel vibration signal recorded in 3 axes

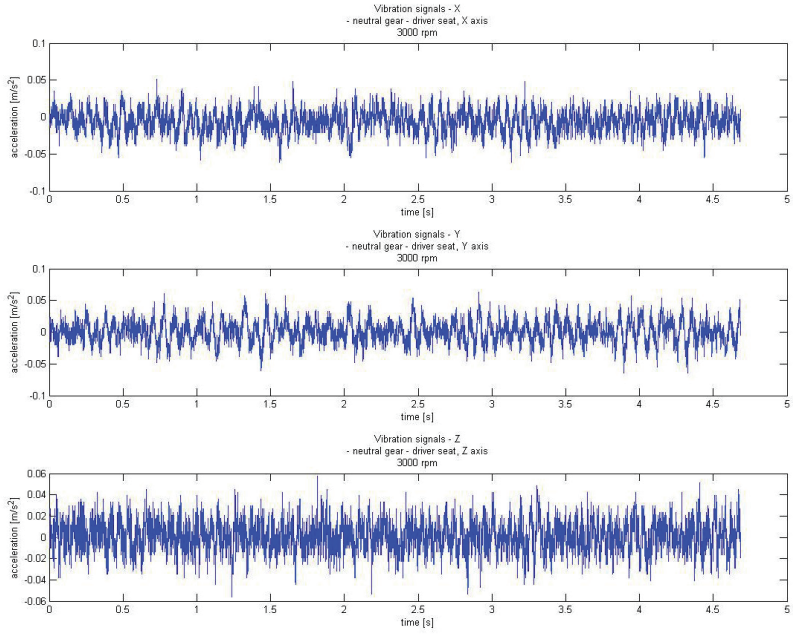

Fig. 6. Driver seat vibration signal recorded in 3 axes

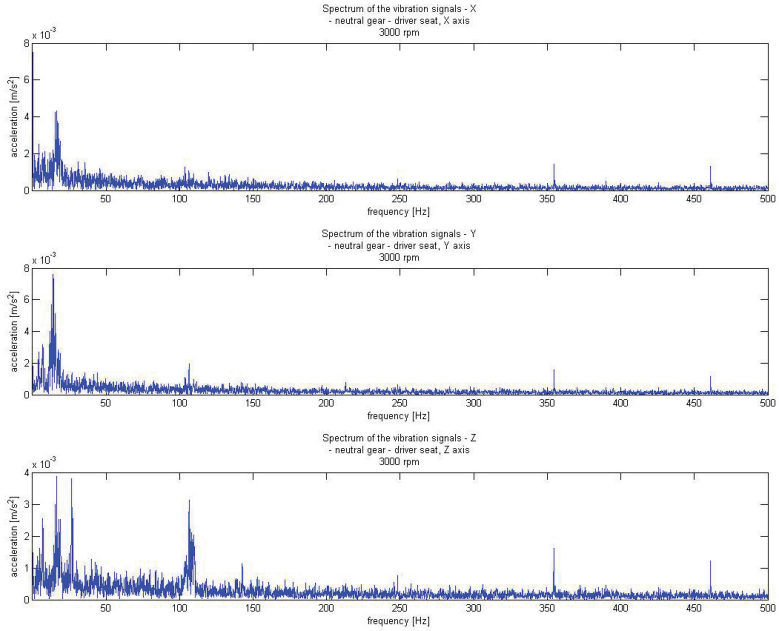

Fig. 7. Spectrums of the driver seat vibration signal recorded in 3 axes

To compare the energy of the vibration signal in orthogonal axes and energy loss during propagation of vibration the root mean square (RMS) was calculated. The results of RMS calculation have been depicted in Fig. 8.

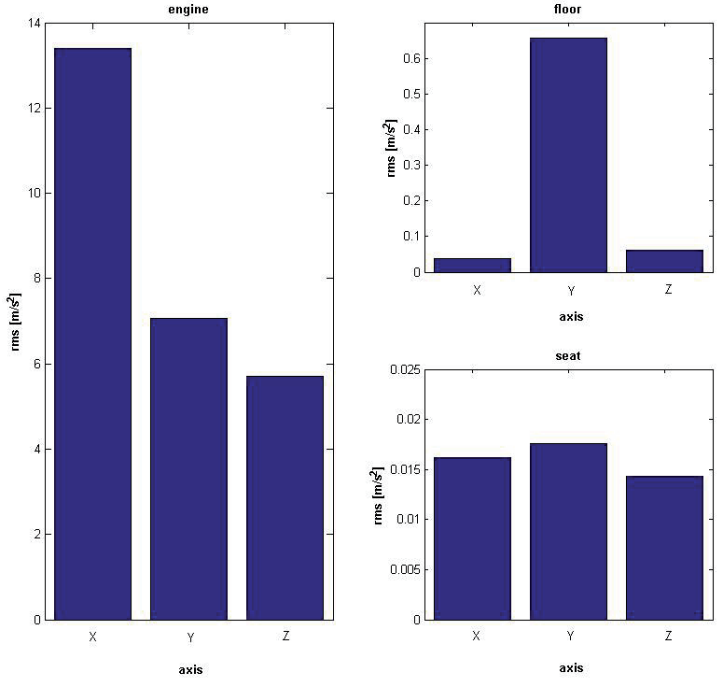

Fig. 8. The RMS values of the vibration in measured points and in 3 axes

This simple signal processing allows calculation of the vibration dominant effective weighted vibration acceleration. This estimator is used for assessing exposure to vibrations of the overall impact on the human body. The results have been depicted in Fig. 9.

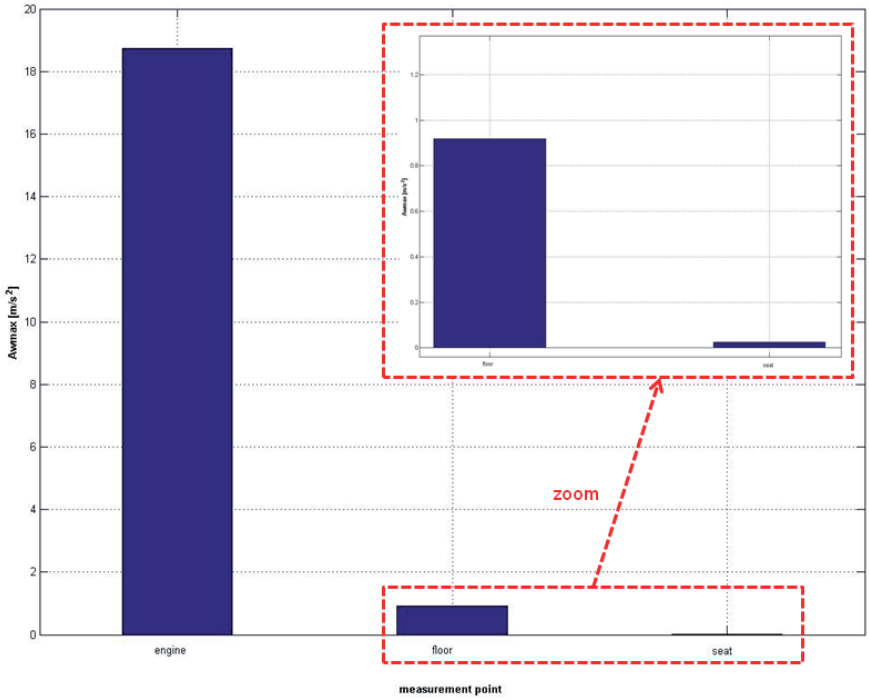

Fig. 9. A_{wmax} vibration dominant effective weighted vibration acceleration for the engine vibration propagation

4. Conclusion

The results of the conducted research allow detail analysing exposure to vibrations generated by the motor vehicle. As it has been presented in Fig. 2 and 3 the vibration of engine block are quasi stationary. The largest acceleration values can be observed for the longitudinal vibration (X axis). It can be effected by the engine mounting elements, which characteristics are mostly designed for vertical displacement preventing. Signals registered on floor panel and the seat have different dynamics structures. It can be observed domination of lower frequencies in the signal. Based on the results of the vibration dominant effective weighted vibration acceleration it can be assumed the vibration generated by the engine are strongly absorbed during the structural propagation and the human exposure to vibrations has small values.

References

[1] Bogert, A.J., *Analysis and simulation of mechanical loads on the human musculoskeletal system,* Exercise and Sport Sciences Reviews 22.

[2] Burdzik, R., *The research of vibration of vehicle floor panel*, Silesian University of Technology Scien-tific Papers, s. Transport 67, pp. 23-30, Gliwice: Silesian University of Technology Academic Press, 2010.

[3] Burdzik, R., Stanik, Z., Warczek J., *Method of assessing the impact of material properties on the propagation of vibrations excited with a single force impulse*, Archives of Materials and Metallurgy vol. 57 issue 2, pp. 409-416, 2012.
[4] Burdzik, R., Węgrzyn, T., *Effect of Mn and Mo on the quality of welding trucks steel supporting structures*, Journal of Achievements in Materials and Manufacturing Engineering JAMME, 43(1), pp. 276-279, 2010.
[5] Carle, D., Blount, G., *The suitability of aluminium as an alternative material for car bodies*, Materials and Design 20, 1999.
[6] Griffin, M.J., *Handbook of Human Vibration*, Academic Press Limited, London,1990.
[7] Griffin, M.J., *Vertical vibration of seated subject, effect of posture, vibration level, and frequency,* Aviation Space and Environmental Medicine 46 (3), 1975.
[8] Ibrahim, I.M., Crolla, D.A., Barton, D.C., *Effects of frame flexibility on the ride vibration of trucks*, Comput. Struct. 58, 1996.
[9] ISO *Guide for the evaluation of human exposure to whole-body vibration*, 2nd Edition, International Standard 2631-1978(E), International Organization for Standardization, 1978.
[10] ISO *Mechanical vibration and shock—evaluation of human exposure to whole-body vibration*, International Standard 2631-1:1997(E), International Organization for Standardization, 1997.
[11] Jiang, Z.Y., Streit, D.A., El-Gindy, M., *Heavy vehicle ride comfort*: *literature survey heavy vehicle systems*, Int. J. Vehicle. Des. 8 2001.
[12] Kubo, M., Terauchi, F., Aoki, H., Matsuoka, Y., *An investigation into a synthetic vibration model for humans: An investigation into a mechanical vibration human model constructed according to the relations between the physical, psychological and physiological reactions of humans exposed to vibration*, International Journal of Industrial Ergonomics 27, 2001.
[13] Matsumoto, Y., Griffin, M.J., *Dynamic response of the standing human body exposed to vertical vibration*, Journal of Sound and Vibration 212 (1), 1998.
[14] Mcleod, R.W., Griffin, M.J., *Mechanical vibration included interference with manual control performance,* Ergonomics 38, 1995.
[15] Qassem, W., Al-Nashash, H., Zabin, A., Othman, M., *ECG response of the human body subjected to vibration,* Journal of Medical Engineering & Technlogy 20 (1), 1996.
[16] Oleksiak, B., Siwiec, G., Blacha, A., Lipart, J., *Influence of iron on the surface tension of copper*, Archives of Materials Science and Engineering 44 (1), pp. 39-42, 2010.
[17] Randall, J.M., Mattehews, R.T., Stiles, M.A*., Resonance frequencies of standing humans,* Ergonomics 40 (9), 1997.
[18] Węgrzyn, T., Wieszała, R., *Significant alloy elements in welded steel structures of car body*, Archives of Materials and Metallurgy vol. 57 issue 1, pp. 45-52, 2012.
[19] Wyllie, I.H., Griffin, M.j., *Discomfort from sinusoidal oscillation in the pitch and fore-and-aft axes at frequencies between 0.2 and 1.6Hz,* Journal of Sound and Vibration 324, 2009.
[20] Xua, Y.L., Guo, W.H., *Effects of bridge motion and crosswind on ride comfort of road vehicles*, Journal of Wind Engineering and Industrial Aerodynamics 92, 2004.

GDAŃSK UNIVERSITY OF TECHNOLOGY

Journal of POLISH CIMAC

Faculty of Ocean Engineering & Ship Technology
GDAŃSK UNIVERSITY OF TECHNOLOGY

ASSESSMENT OF ENGINE OPERATION WITH THE USE OF AN OPERATION INDICATOR BASED ON TEST BENCH RESULTS OF A ROBIN-SUBARU EX17 ENGINE

Piotr Bzura
Jacek Rudnicki

Gdansk University of Technology
ul. Narutowicza 11/12, 80-952 Gdansk, Poland
tel. +48583472573
e-mail: pbzura@pg.gda.pl, jacekrud@pg.gda.pl

Rafał Grzeszczyk

ODIUT Automex Sp.z o.o.
ul. Marynarki Polskiej 55d, 80-557 Gdansk, Poland

Abstract

Paper presents results of an experimental verification of the method of quantitative evaluation of engine operation, presented in the literature, exemplified by a low-power internal combustion piston engine. In accordance with such interpretation, engine operation may be presented as a physical quantity defined as operation indicator. The paper presents results of preliminary tests, processed in that aspect, carried out on an engine test bench. The results have been used as a classifying measure of the engine reliability state.

Key words*: operation, internal combustion piston engine, reliability*

1. Introduction

Rational operation of technical devices and systems requires right operational decisions to be taken. The decisions are based on various premises and of a significant importance among them are reliability characteristics of the operated object.

The reliability analysis is a complex procedure of processing the empirical results gathered in the operational practice supplemented with analytical considerations, which procedure requires, apart from other elements, having access to comprehensive information on the current technical and power state of the object in question.

For identifying and predicting the technical states a suitable diagnostic system must be used. Without such a system it is impossible to acquire the information necessary for controlling the operation process in general and predicting the reliability level in particular.

Due to obvious technical and economic reasons, not all the possible technical states can be diagnosed even in the case of very simple technical objects.

As the process of changes of technical state is stochastic, continuous in terms of the states and time, it is necessary to subdivide that infinite set of states into a finite number of subsets (classes), clearly and permanently identifiable by means of the functioning diagnostic system. In

terms of reliability, selecting from the set of all possible technical states the subsets of significant states is connected with the need of defining precisely the broadly understood failure. For the task reliability (associated with the performed task) of complex technical objects, as are the devices and functional subsystems of a marine power plant, it is useful and practical to distinguish at least two groups of failures understood as:

- events causing inadmissible deviations of the system (device) operation parameters from the critical values – major failures causing unfitness for performing any task whatever;
- events causing only deterioration of the operating qualities – minor failures causing in effect higher cost of performing the task or a need of modifying it.

By adopting such subdivision criteria – capability of an object of carrying out the required functions connected with the objectives defined by the operating system in given conditions – a simple and practically useful for the operation process control set **S** of classes – technical states can be distinguished:

a) **State s_1** – subset of technical states of full task fitness. An object in that state is capable of performing all the tasks it has been prepared for in the design and manufacturing phase and the values of its operation (power, economic, ergonomic etc.) parameters are kept within the admissible range.
b) **State s_2 –** state of partial unfitness (partial fitness) for task execution. Including e.g. an engine to that class of states should occur in the case of:
   - incapability of fulfilling all the required ship design parameters, e.g. the specified speed or sailing range,
   - incapability of maintaining the manufacturer-guaranteed power and economic indicators of the operational process effectiveness, e.g. unit fuel consumption.
c) **State s_3** – state of full task incapability which makes it impossible to use the object in accordance with its intended purpose. This subset includes all the states characterised by very significant destruction (extensive failure) of the object.

In the case of transport power systems, the internal combustion piston engines take particular place. The universality of their use, impact on the system safety and ecological properties and also the connected operational costs make the knowledge of their current technical state particularly important from the point of view of timely reaction to any irregularities.

Among many indicators allowing to include that technical state in a synthetic way to one of the above defined classes, it seems sensible to consider the engine operation in such a valuating manner that the operation can be determined simultaneously by energy and time.

Operation within a [0, t] time range can then be interpreted as a physical quantity – hereinafter called operation indicator (D) – determined by a product of the energy $E = f(t)$ variable in time and the time, which may be generally expressed by the following relation [1, 4]:

$$D = \int_0^t E(\tau) d\tau \tag{1}$$

In the case of general analysis of the compression-ignition engine operation it may be assumed that the energy generated by combustion of fuel in the cylinders produces the engine torque. An effect of transmission of the torque from engine to receiver is the work L_e, which in this case may be determined from the expression:

$$L_e = M_o \cdot 2\pi n \cdot \mathrm{t} \tag{2}$$

where:

L_e – useful work,
M_o – mean torque,
n – engine rotational speed.

From relations (1) and (2), the engine operation indicator may be determined by the formula:

$$D = 2\pi \int_0^t M_0 \, n \, t \, dt \tag{3}$$

By introducing to further considerations the following notions:

- required operation – D_W necessary for carrying out the intended task (e.g. a transportation task – sea transport of cargo within a determined time – which means maintaining the determined average ship speed, i.e. average power developed by the ship main propulsion engine(s)),
- possible operation – D_M which the engine in a given technical state and in given functioning conditions is capable of performing,

and by verifying the relation [4]:

$$D_M \geq D_W \tag{4}$$

a criterion can be obtained of evaluation of the fitness for use, e.g. in accordance with principles presented in [4].

Further in this paper an experimental verification is presented of the above mentioned possibility of using the operation indicator as a general classifier of engine state, based on the test bench investigation of a low-power compression-ignition Robin-Subaru EX17 engine.

2. Engine diagnostic tests

The investigation of a Robin-Subaru EX17 engine was carried out on a laboratory test bench (Fig.1). This is a single-cylinder four-stroke carburettor engine fuelled with lead-free petrol, splash-lubricated with the SAE 30 CastelGarden oil.

Table 1. Basic characteristics of the Robin-Subaru EX17 engine

Rated power	2.6 kW
Cylinder diameter	67 mm
Nominal rotational speed	3000 revs/min
Engine displacement	169 cm^3
Compression ratio	85

The engine power was determined by means of an electric rotational brake with a control system allowing to measure the engine torque M [Nm].

The rotational speed was measured with an inductive gauge cooperating with a toothed wheel, where the consecutive teeth are the shaft position indicators.

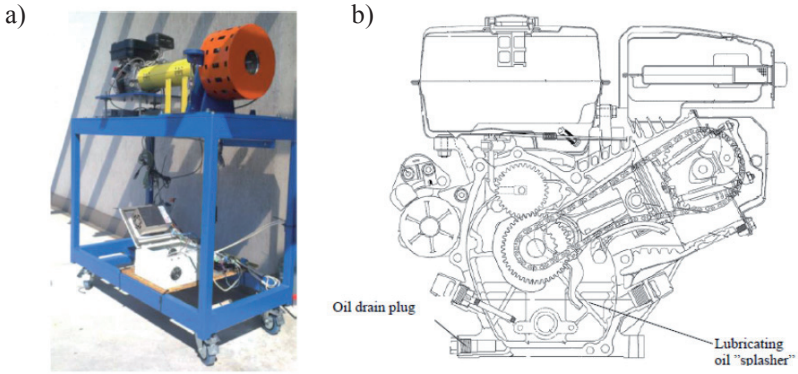

Fig. 1. View of the Robin-Subaru EX17 engine test stand (a) and the engine cross-section (b)

The investigation was performed in the form of a simple active experiment and was aimed at verification of the operation time of engine in three different fitness states, operating on 100 cm^3 of the 95 Lotos lead-free petrol with 720 kg/m^3 density and with the same loads. The following state classes were distinguished:

State 1 – state of full fitness.

State 2 – state of partial fitness – damaged lubrication oil splasher (Fig. 2).

State 3 – state of partial fitness – dirty air filter (Fig. 2).

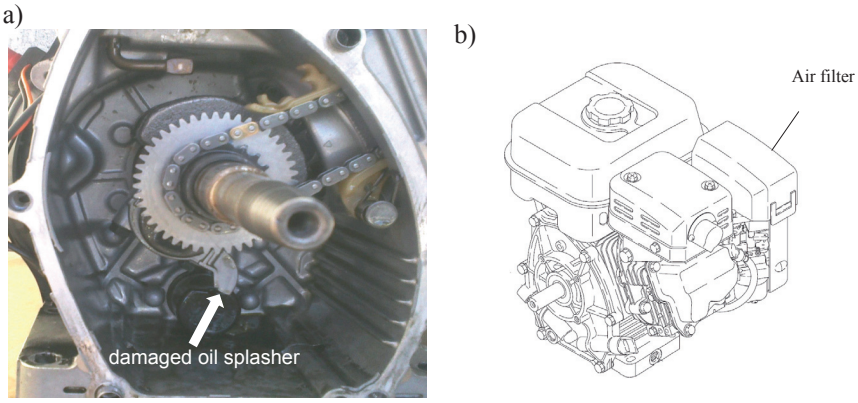

Fig. 2. Damaged oil splasher (a) and location of the air filter (b)

3. Investigation results and their analysis

The test was carried out for three values of the engine braking torque: 2.5 Nm, 5 Nm and 7.5 Nm, the engine operation time t_{OP} on 100 cm^3 of fuel was measured for each of those loads. Each measurement was repeated five times. Examples of the measurement results are presented in Fig. 3 and 4.

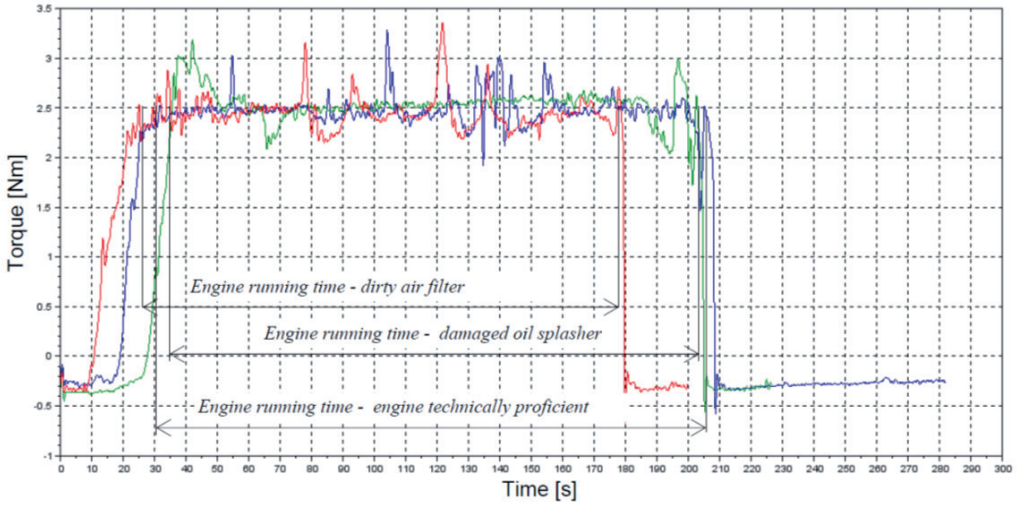

Fig. 3. Engine running time with braking torque value 2.5Nm

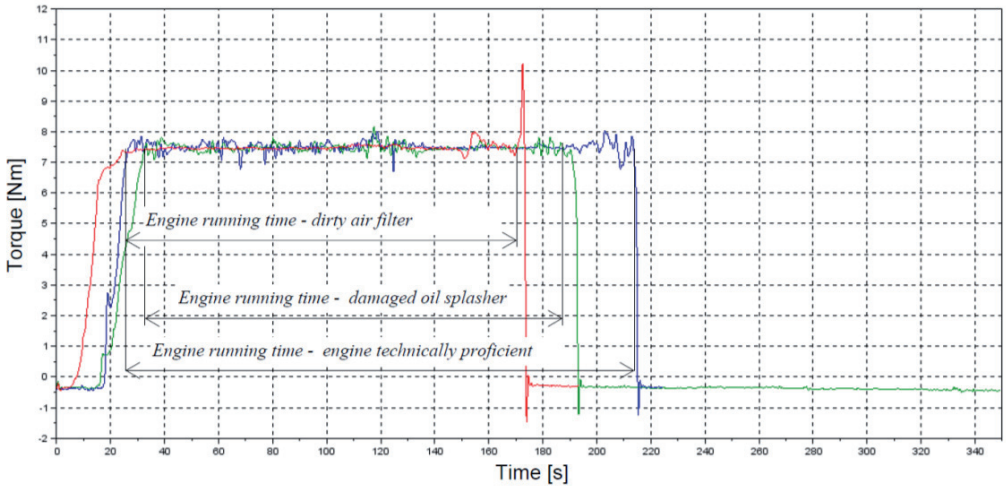

Fig. 4. Engine running time with braking torque value 7.5Nm

The analysed engine operating conditions made it possible to determine:

- numbers of the performed engine operation cycles within the t_{OP} time for different states of fitness and different loads [2,3] (Table 1),

Table 1: Comparison of the numbers of engine operation cycles

Engine state	Number of engine cycles with load M=2.5Nm	Number of engine cycles with load M=5 Nm	Number of engine cycles with load M=7.5Nm
State 1	323434	366504	297609
State 2	294742	296688	232500
State 3	172500	227050	207000

- values of work performed by the engine in the period (0, t_{OP}) of its operation in accordance with expression (2),

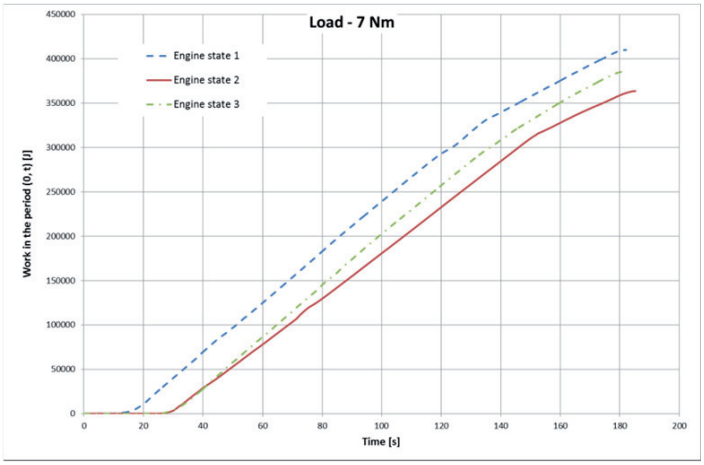

Fig. 5. Values of work performed by the engine in the period (0, t_{OP}) of its operation with a 7.5 Nm torque load

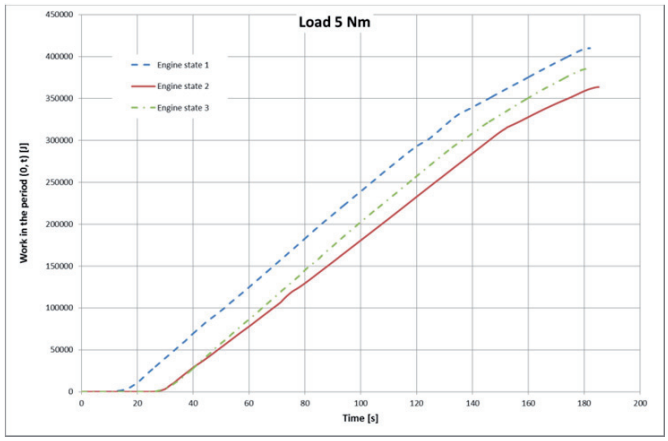

Fig. 6. *Values of work performed by the engine in the period (0, t_{OP}) of its operation with a 5 Nm torque load*

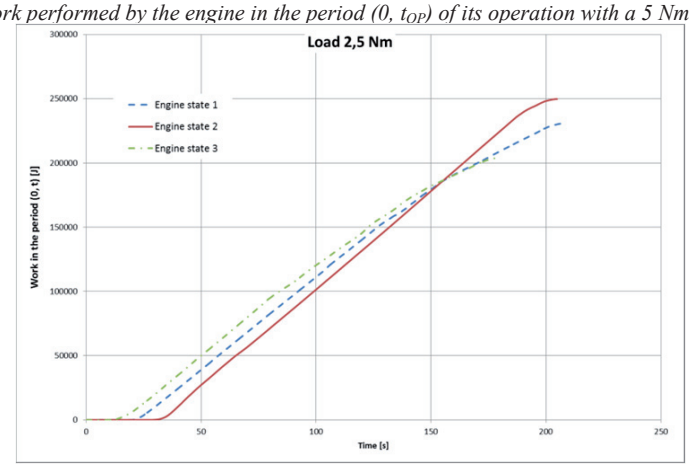

Fig. 7. *Values of work performed by the engine in the period (0, t_{OP}) of its operation with a 2.5 Nm torque load*

- values of the engine operation indicators in the period (0, t_{OP}) of its operation in accordance with expression (3).

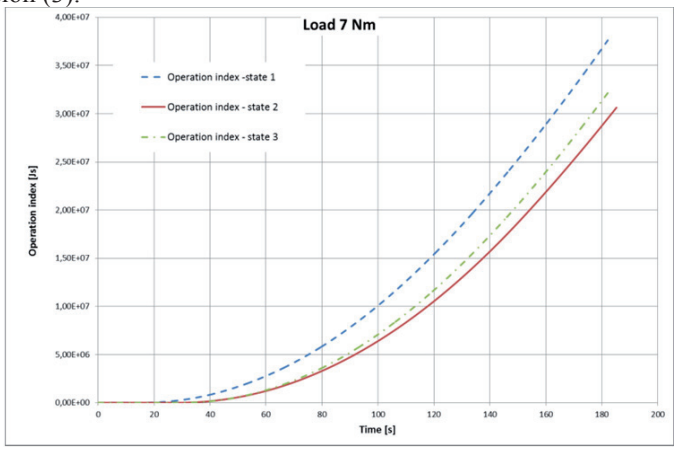

Fig. 8. *Values of the engine operation indicator in the period (0, t_{OP}) of its operation with a 7.5 Nm torque load*

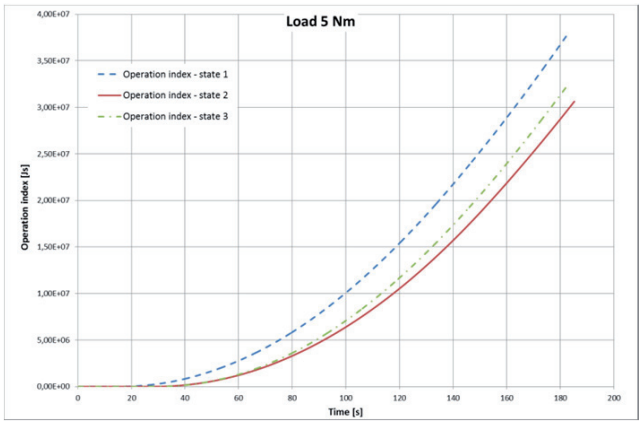

Fig. 9. *Values of the engine operation indicator in the period (0, t_{OP}) of its operation with a 5 Nm torque load*

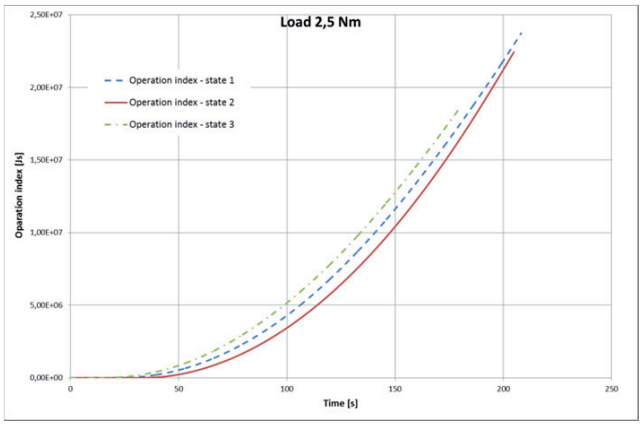

Fig. 10. *Values of the engine operation indicator in the period (0, t_{OP}) of its operation with a 2.5 Nm torque load*

Analysis of the results presented in figures 5 to 10 and in Table 1 allows to formulate the following conclusions:

a) engine operating in the state of full fitness is characterised by the longest operation time and the greatest number of performed work cycles with a given braking torque;
b) assessment of the engine fitness by the value of work performed in the period of its operation (figures 5 to 7) may lead to erroneous conclusions, because, as it can be seen in Fig. 7, work performed by the engine in a partial fitness state (in this case state 2) reached a higher value than in the full fitness state (state 1);
c) using the engine operation indicator as a classifier of the engine reliability state always leads to correct conclusions, because for the full fitness state it takes the highest values regardless of the load.

4. Final remarks and conclusions

Presented interpretation of engine operation makes it possible to formulate a preliminary assessment of the engine degree of fitness.

The presented method is, in the opinion of the Authors, a valuable complement to the so far applied methods of describing the reliability aspects of a so important element of most drive systems as an internal combustion piston engine. The basic advantageous feature of the method is

connecting the evaluation of power with the time of task execution, which is very important particularly in the case of carrying out long-lasting transportation tasks.

An additional advantage is its universality and therefore applicability to the reliability analysis of any power device or subsystem.

References

[1] Girtler J., *Metoda oceny działania maszyn z zastosowaniem diagnostyki technicznej*, Wojskowa Akademia Techniczna, Wydział Elektroniki, Warszawa 2013

[2] Jędrzejowski J., *Obliczanie tłokowego silnika spalinowego*, Wydawnictwo Naukowo-Techniczne, Warszawa 1988

[3] Niewiarowski K., *Tłokowe silniki spalinowe*, Wydawnictwo Naukowo-Techniczne, Warszawa 1983.

[4] Rudnicki J., *Energy-time method for assessment of main diesel engine operation,* Journal of KONES Powertrain and Transport. - Vol. 14, nr 3 (2007), s. 519-526

GDAŃSK UNIVERSITY OF TECHNOLOGY

Journal of POLISH CIMAC

Faculty of Ocean Engineering & Ship Technology
GDAŃSK UNIVERSITY OF TECHNOLOGY

APPLICATION OF THE THEORY OF SEMI-MARKOV PROCESSES TO DETERMINE A LIMITING DISTRIBUTION OF THE PROCESS OF CHANGES OF ABILITY AND INABILITY STATES OF FUEL SUPPLY SYSTEMS IN HEAVY FUEL DIESEL ENGINES

Jerzy Girtler
Technical University of Gdańsk
Faculty of Ocean Engineering and Ship Technology
Department of Marine and Land Power Plants
tel. (+48 58) 347-24-30; fax (+48 58) 347-19-81
e-mail: jgirtl@pg.gda.pl

Keywords: *heavy fuel oil, semi-Markov process, diesel engine, fuel supply system*

Abstract

The paper presents applicability of the theory of semi-Markov processes to determine a limiting distribution of the process of changes of technical states of fuel systems for marine engines running on heavy fuel oils. The proposed study of this process includes the components of such fuel systems like: 1 - injectors, 2 - high pressure hoses, 3 - injection pumps, 4 - low pressure hoses, 5 – fine filters, 6 - coarse filters, 7 – fuel-feed pump, 8 – fuel heater and 9 – viscosistat with a viscometer. A semi-Markov state transition model consisting of ten states has been developed for such systems. Application of technical diagnostics has been pointed to be necessary to investigate the state transition process for the systems. The conclusions presented furthermore in the paper provide advantages which (according to the author) are of the most importance in the design and operation phases of fuel systems in marine diesel engines that run on heavy fuel oils.

1. Introduction

During operation of internal combustion piston engines, the fuel combustion process which proceeds in marine diesel engines is particularly important. This process should run in a way that provides as low fuel consumption as possible. It is difficult to reach such a combustion process in internal combustion engines running on heavy fuel oils. This is due to the need of heating the fuel to a high temperature to be able to produce in the engine working spaces a fuel-air mixture having a proper micro- and macro-structure. Heating the fuel is indispensable to reduce the viscosity of heavy fuel oils which should range from 15 ÷ 25cSt (for low speed engines), and 12÷16cSt (for medium speed engines) [11, 12]. Such a structure can be gained when the engine power supply system (engine fuel system) for heavy fuel oil finds itself in a state of full ability (s_0). This means that all components of the system must stay in ability states. Such components include [11, 12, 14]: 1 - injectors, 2 - high pressure hoses 3 - injection pump, 4 - low pressure hoses, 5 - fine filters, 6 - coarse filters, 7 – fuel-feed pump, 8 – fuel heater and 9 – viscosistat with a viscometer [11, 12]. Failure of any of the components in the engine fuel system makes the component disable. This causes a failure and inability state of the entire fuel system. Therefore, the users of marine heavy fuel engines are interested in what the probability is that at any moment in a long time of operation (theoretically $t \to \infty$) the engine fuel system is in the state of ability (s_0) or states of inability ($\bar{s}_0 : s_1, s_2, ..., s_9$).

2. General identification of state changes for marine diesel engines

The state of ability (s_0) of each fuel system in marine internal combustion engine is found (as mentioned in the introduction) when all components in the system stay in ability states. If any of the components gets a failure, the fuel system must be considered to be damaged and, therefore, in state of inability ($\bar{s}_0$). A failure of the i-th (any) of the components in this system is fixed by the engine user during performance of a maintenance service. As a result of this action the faulty component is renovated and in consequence stays no longer in the inability state $s_i \in S^*$ (i = 1, 2, 3,…., 9), instead of this, it takes a condition that provides an ability state s_0 to the entire fuel system. Thus, a marine engine fuel system in the phase of operation can take one of the states from the set:

$$S = \{s_0, s_1, s_2, \ldots, s_9\} \tag{1}$$

with the following interpretation:

- s_0 – ability state of a fuel system,
- (s_i, i = 1, 2, 3,…., 9) – inability state of a system due to a failure of, respectively: injectors (s_1), high pressure hoses (s_2), injection pumps (s_3), low pressure hoses (s_4), fine filters (s_6), coarse filter (s_6), fuel-feed pumps (s_7), fuel heater (s_8) and viscosistat including a viscometer (s_9), i.e., that $S^* \subset S$.

Therefore, the process of occurring states $s_i \in S$ (i = 0, 1, 2, 3,…., 9) in sequence can be observed. The operational practice shows that the unconditional duration T_i of any state s_i, and T_{ij} of the state s_i, provided that the state s_j is the next one, are random variables [2, 3, 7, 8]. Furthermore, it is obvious that the system can stay in these states with a determined probability $P_{i,}$, while a transition from the state s_i to s_j proceeds with the probability p_{ij} [3, 8, 10, 13].

It can be assumed that a fuel system in a new engine is in the ability state (s_0). The same state of it can be found after its renovation made during performance of an appropriate maintenance service [3, 7, 12]. Due to the fact that the time of renovation performance is a random variable, the occurrence of the state s_0 is a random event. The system may stay in this state for the time period T_0 with the probability P_0. The time period T_0 is a random variable, because the value of the time results from the occurrence of a failure in the system, which is a random event. A state of inability of the fuel system occurs as a result of its failure. This state is a consequence of occurrence of disability of any component within the system. Thus, for this system there can be distinguished the following inability states: $s_i \in S$ (i = 1, 2, 3,…., 9). When the cause of the inability is a failure of injectors, the state transition from s_0 to s_1 takes place after the time period T_{01} with the probability p_{01}. The occurrence of the state s_1 will cause a need to implement some service in order to renovate the system and regain its state s_0. The fuel system returns to the state s_{0v} after the time period T_{10} with the probability p_{10}. However, if the cause of the state of inability of the fuel system is a failure of high pressure hoses, the transition proceeds from the state s_0 to s_2. This transition takes place after the time period T_{02} with the probability p_{02}. In this case, the system can return to the state s_0 after the time period T_{20} with the probability p_{20}, provided that a proper service is performed. The same situation applies when the fuel system loses s_0 in the event of a failure of any of its other components. For each of the considered cases the conclusion can be made that the current state of a fuel system and the time period of its duration depend significantly (even exclusively) on the immediate previous state. This is obvious when the consideration includes the fuel system states occurring in sequence: $s_i \in S$ (i = 0, 1, 2, 3,…., 9). For example, if a fuel system is in the state s_0, with the time of its failure this state transits to one of the possible

states of $s_i \in S$ (i = 1, 2, 3,…., 9), depending on which of the components of the system is damaged. When the inability state of the fuel system is s_1, then after its renovation and return to the state s_0, just this state (s_0) and the time period of its duration will depend only on the state s_1, not on those states that were earlier, so the states of $s_i \in S$ (i = 2, 3,…., 9). Duration of the state s_0, after implemented service will in turn depend on how well the service restoring this state (s_0) was performed and also on how much the system will be loaded during operation [5, 6, 7, 12, 14]. The above considerations show that a semi-Markov model of a real process of changes of its states can be considered in case of fuel systems for marine diesel engines running on heavy fuel oils. Such a model is possible to be built because the process states can be determined in such a way that the duration of the state existing at the instant τ_n and the state obtainable at the instant τ_{n+1} do not depend stochastically on the states that occurred earlier or duration of these states. The theory of semi-Markov processes can be applied to build a semi-Markov model $\{W(t): t \geq 0\}$ of the real process of changes of technical states for the operation phase of propulsion systems. The characteristics for the model are [7, 8, 10, 12, 13]:

1) the Markov condition is satisfied so that in future the evolution of the process of changes of states of a fuel system during its operation phase, for which the semi-Markov model has been built, would depend only on its state at the given time, not on the system operation in the past, thus so that *the future of this system would not depend on the past but on the present,*
2) random variables T_i (denoting the duration of the state s_i, independently which state it will be followed by) and T_{ij} (denoting the duration of the state „s_i", on the condition that the state "s_j" will be the next one in the process) have other than exponential distributions.

Modeling, which allows to develop a semi-Markov model of the process of changes of fuel system states includes the outputs of the conducted analysis of the changes in these states [2, 5, 8, 12, 14]. The states have been recognized to be the most important in studying the real process of changes of technical states of fuel systems for marine diesel engines on heavy fuel oils.

The presented description of the changes of technical states for fuel systems is a result of the noticed fact that for these systems, just like for other functional systems in diesel engines, prediction of changes in their technical states can be made when the current states of the systems and the conditions under which they are expected to operate in future are known. This also applies to many other technical objects, for example such as gas turbine engines, reciprocating compressors, centrifugal pumps, etc. [2, 4, 7, 12, 14]. This fact which also indicates that changes of technical states of this kind of objects are not closely related to the time of their operation (work), is explained as a scientific hypothesis by the publications [2, 7]. With regard to the fuel systems investigated herein, this can be explained in a form of the following scientific hypothesis (***H***): ***the process of changes of technical states of any fuel system*** *(defined as a random function whose the argument is time and the values are random variables denoting the current technical states),* ***running under rational operation*** *(that is operation based on economic calculation)* ***is a process with asymptotically independent values, because any particular state of the process investigated at any instant*** τ_n ***(n = 0, 1, …, m;*** $\tau_0 < \tau_1 < \ldots < \tau_m$***), depends significantly on the immediate previous state, not on the states that occurred earlier or the periods of their duration.***

It should be noticed that the formulated hypothesis does not contain any such contradictions that might falsify it in the logical sense, still before testing. The consequences of this hypothesis are as follows [2, 7, 8]:

1) K_1 – probabilities (p_{ij}; $i \neq j$; $i,j \in N$) of the process transition, i.e. changes of fuel system states from any state „s_i", which the process (system) is in, to the next (any) state " s_j ", do not depend on the states which the process was earlier in,
2) K_2 – periods of unconditional duration of the particular states "s_i" of the process of changes of fuel system states are stochastically independent random variables (T_i; $i \in N$),
3) K_3 – periods of duration of each of the possible-to-occur states "s_i" of the process of changes of fuel system states, provided that the next state is one of the remaining process states "s_j", are stochastically independent random variables (T_{ij}; $i \neq j$; $i,j \in N$).

The presented consequences reveal the probabilistic law for the changes of technical states of any fuel system. They are not mutually contradictory, and their logic truth raises no doubts. Thus, the non-contradiction condition for the consequences is satisfied. This means that nothing stands in a way to make advantage of the mentioned consequences regarded jointly as one consequence (K) in order to test the hypothesis (H) empirically, so to make its verification if should be accepted or falsified. This verification consists in experimental testing of the truthfulness of the consequences $K_i \in K$, $i = 1, 2, 3$. A non deductive inference method called a reductive inference can be applied to verify this hypothesis.

3. Semi-Markov model of the process of changes of technical states of fuel systems for marine diesel engines

Application of a semi-Markov model of the process of changes of technical states of a fuel system for a heavy fuel engine allows to:

- take into account preventive maintenance required to restore the system which becomes completed upon completion of maintenance of particular system's components and
- investigate more than two reliability states of an engine fuel system as well as its components.

This allows to investigate a semi-Markov model of changes of technical states of fuel systems for marine internal combustion engines with a ten-element set S (1). This means that the limiting distribution of the process of changes of ability and inability states of heavy fuel supply systems for marine diesel engines, can be defined by using the model of the process of changes of the system states, developed in a form of a semi-Markov process $\{\{W(t): t \geq 0\}$ with a set of states $S = s_i$; $i = 0, 1, 2, ... ,9$. Interpretation of the states $s_i \in S(i = 0, 1, 2, ... ,9)$ in accordance with the description in equation (1) is as follows: s_0 – ability state of a fuel system, s_1 – inability state of a fuel system due to a failure of an injector (injectors), s_2 – inability state of a fuel system due a failure of a high pressure hose (hoses), s_3 – inability state of a fuel system due to a failure of an injection pump (injection pumps), s_4 – inability state of a fuel system due to a failure of a low pressure hose (hoses), s_5 – inability state of a fuel system due to a failure of fine fuel filters, s_6 – inability state of a fuel system due to a failure of coarse filters, s_7 – inability state of a fuel system due to a failure of a fuel-feed pump (fuel-feed pumps), s_8 – inability state of a fuel system due to a failure of a fuel heater, s_9 – inability state of a fuel system due to a failure of viscosistat or viscometer.

Graph of state transitions for the process $\{W(t): t \geq 0\}$ is shown in Fig. 1

Transitions of the states s_i ($i = 0, 1, 2, ..., 9$) occur in succeeding times t_n ($n \in N$),, where at the time $t_0 = 0$, the engine fuel system is in state s_0. The state s_0 lasts until a failure of any of the components of the engine fuel system. However, the states (s_i($i = 1, 2, ..., 9$) last until the damaged engine fuel system is restored.

The above considerations show that it can be assumed that the state of an engine fuel system at time t_{n+1} and the time period of duration of the state at a time t_n do not depend on states that occurred at times t_0, t_1, ..., t_{n-1} or time periods of their durations. Therefore, the process $\{W(t): t \geq 0\}$ is a discrete-state continuous-time semi-Markov process [2, 3, 4, 8, 10, 13].

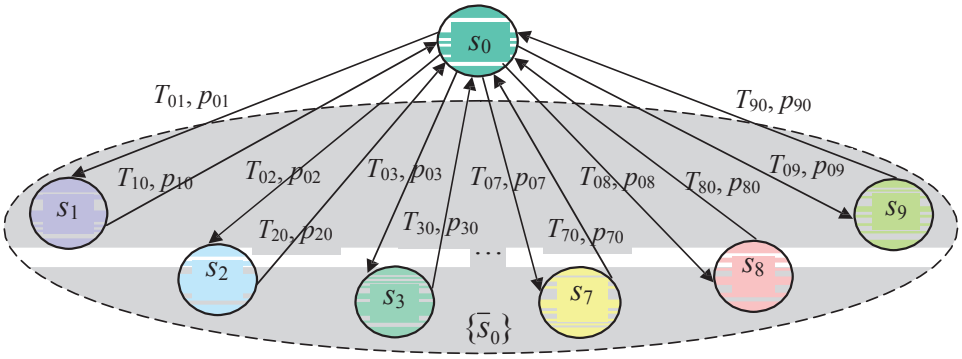

Fig. 1. Graph of state transitions for the process $\{W(t): t \geq 0\}$: s_0 – ability state of an engine fuel system, $\{\bar{s}_0\}$ – set of inability states of an engine fuel system: $\{\bar{s}_0\} = \{s_1, s_2, s_3, ..., s_9\}$, $s_i \in S (i = 1, 2, ... ,9)$ – states with the interpretations respectively: $s1$ – inability state of an engine fuel system due to a failure of an injector (injectors), $s2$ – inability state of an engine fuel system due a failure of a high pressure hose (hoses), $s3$ – inability state of an engine fuel system due to a failure of an injection pump (injection pumps), $s4$ – inability state of an engine fuel system due to a failure of a low pressure hose (hoses), $s5$ – inability state of an engine fuel system due to a failure of fine fuel filters, $s6$ – inability state of an engine fuel system due to a failure of coarse filters, $s7$ – inability state of an engine fuel system due to a failure of a fuel-feed pump (fuel-feed pumps), $s8$ – inability state of an engine fuel system due to a failure of a fuel heater, $s9$ – inability state of an engine fuel system due to a failure of viscosistat or viscometer, T_{ij} - time period of the process duration in the state s_i provided that the state s_j is the next one, p_{ij} – probability of staying the process in the state s_i, provided that the state s_j $(i, j = 0, 1, 2, ..., 9; i \neq j)$ is the next one.

An exemplary realization of the process $\{W(t): t \geq 0\}$, depicting occurrence of technical states of a fuel system in any heavy fuel engine when operated, is shown in Figure 2.

Obtaining (obviously in approximation) the values of the probabilities Pj (j = 0, 1, 2, 3) that make a limiting distribution of the process of changes of ability and inability states of a heavy fuel supply system for a marine diesel engine requires determination of the initial distribution of the process $\{W(t): t \geq 0\}$ and its matrix function.

The initial distribution of the process is:

$$P\{W(0) = s_i\} = \begin{cases} 1 & dla \quad i = 0 \\ 0 & dla \quad i = 1,\ 2,\ ...,\ 9 \end{cases} \tag{2}$$

and the matrix function has the form:

$$\mathbf{Q(t)} = \begin{bmatrix} 0 & Q_{01}(t) & Q_{02}(t) & Q_{03}(t) & Q_{04}(t) & Q_{05}(t) & Q_{06}(t) & Q_{07}(t) & Q_{08}(t) & Q_{09}(t) \\ Q_{10}(t) & 0 & 0 & 0 & 0 & 0 & 0 & 0 & 0 & 0 \\ Q_{20}(t) & 0 & 0 & 0 & 0 & 0 & 0 & 0 & 0 & 0 \\ Q_{30}(t) & 0 & 0 & 0 & 0 & 0 & 0 & 0 & 0 & 0 \\ Q_{40}(t) & 0 & 0 & 0 & 0 & 0 & 0 & 0 & 0 & 0 \\ Q_{50}(t) & 0 & 0 & 0 & 0 & 0 & 0 & 0 & 0 & 0 \\ Q_{60}(t) & 0 & 0 & 0 & 0 & 0 & 0 & 0 & 0 & 0 \\ Q_{70}(t) & & 0 & 0 & 0 & 0 & 0 & 0 & 0 & 0 \\ Q_{80}(t) & 0 & 0 & 0 & 0 & 0 & 0 & 0 & 0 & 0 \\ Q_{90}(t) & 0 & 0 & 0 & 0 & 0 & 0 & 0 & 0 & 0 \end{bmatrix} \quad (3)$$

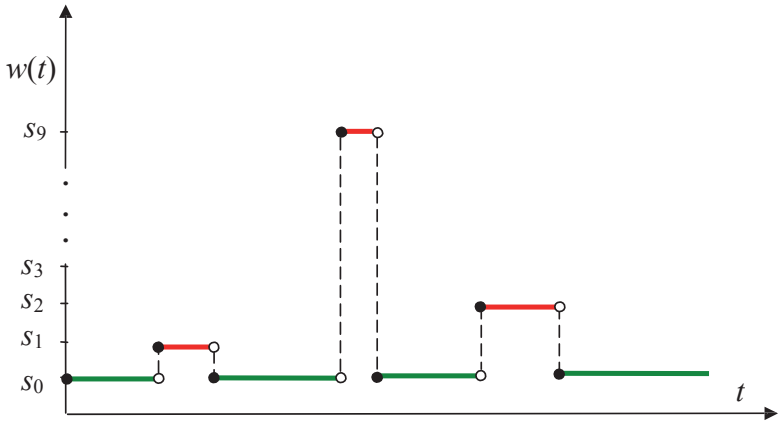

Fig. 2. An exemplary realization of the process {W(t): t ≥ 0} for the investigated fuel system components: s0 – ability state of the components and the system at the same time, si(i = 1, 2, 3, ... ,9) – states as described in Figure 1.

The matrix function **Q(*t*)** is a model of changes of technical states of a engine fuel system. Nonzero elements $Q_{ij}(t)$ of the matrix **Q(t)** depend on the distributions of random variables which are the time intervals of staying the process $\{W(t): t \geq 0\}$ in the states $s_i \in S(i = 0, 1,..., 9)$. The elements of the matrix function **Q(*t*)** are the probabilities of the process transitions from state s_i, to state s_j (s_i, $s_j \in S$) in time no longer than t, which are defined as follows [3, 8]:

$$Q_{ij}(t) = P\{W(\tau_{n+1}) = s_j,\ \tau_{n+1} - \tau_n < t | W(\tau_n) = s_i\} = p_{ij}F_{ij}(t) \quad (4)$$

where:

$p_{(ij)}$ – one-step transition probability of the homogeneous Markov chain;

whereas $p_{ij} = P\{Y(\tau_{n+1}) = s_j | Y(\tau_n) = s_i\} = \lim_{t\to\infty} Q_{ij}(t)$;

$F_{(ij)}(t)$ – distribution of the random variable $T_{(ij)}$ denoting the duration of the state s_i of the process $\{W(t): t \geq 0\}$, provided that the state s_j is the next one in the process.

The matrix **P** of transition probabilities of the embedded Markov chain to the process, as this results from the matrix function **Q(t)** (2), is composed of the elements which are [2, 7, 8]: $Q_{i0}(t) = p_{i0} = 1 (i = 1, 2, \ldots, 9)$ and $Q_{0j}(t) = p_{0j}$, because **Q(t)** is a stochastic matrix.

The process $\{W(t): t \geq 0\}$ is irreducible [1, 3, 4], and the random variables $T_{(ij)}$ take finite positive expected values. Therefore, its limiting distribution [7, 8]

$$P_j = \lim_{t\to\infty} P_{ij}(t) = \lim_{t\to\infty} P\{W(t) = s_j\},\ s_j \in S (j = 0, 1, \ldots, 4) \tag{5}$$

is of the following form [8]:

$$P_j = \frac{\pi_j \mathrm{E}(T_j)}{\sum_{l=0}^{9} \pi_l \mathrm{E}(T_l)} \tag{6}$$

The probabilities $\pi_j (j = 0, 1, 2, \ldots, 9)$ in the formula (6) are limiting probabilities of the embedded Markov chain to the process $\{W(t): t \geq 0\}$. However, $\mathrm{E}(T_j)$ and $\mathrm{E}(T_k)$ are expected values of the random variables of T_j and T_k respectively, which are the time periods of staying the system in states: s_j and s_k respectively, regardless of which state will be next.

To determine the limiting distribution (6) it is required to solve the system of equations that comprise the said limiting probabilities $\pi_j (j = 0, 1, \ldots, 9)$ of the embedded Markov chain and the matrix **P** of the probabilities of transition from the state s_i to s_j,. Such a system takes the following form:

$$\left.\begin{array}{l} [\pi_0, \pi_1, \pi_2, \pi_3, \pi_4, \pi_5, \pi_6, \pi_7, \pi_8, \pi_9] = [\pi_0\ \ \pi_1, \pi_2, \pi_3, \pi_4, \pi_5, \pi_6, \pi_7, \pi_8, \pi_9] \cdot \mathbf{P} \\ \sum_{k=1}^{4} \pi_k = 1 \end{array}\right\} \tag{7}$$

As a result of solving the system of equations (7), by using the formula (6), the following relationships can be obtained:

$$\left.\begin{array}{l} P_0 = \dfrac{\mathrm{E}(T_0)}{\mathrm{E}(T_0) + \sum_{l=0}^{9} p_{(0l)} \mathrm{E}(T_l)},\ P_1 = \dfrac{p_{(01)} \mathrm{E}(T_1)}{\mathrm{E}(T_0) + \sum_{l=0}^{9} p_{(0k)} \mathrm{E}(T_l)},\ P_2 = \dfrac{p_{(02)} \mathrm{E}(T_2)}{\mathrm{E}(T_0) + \sum_{l=0}^{9} p_{(0l)} \mathrm{E}(T_l)}, \\ P_3 = \dfrac{p_{(03)} \mathrm{E}(T_3)}{\mathrm{E}(T_0) + \sum_{l=0}^{9} p_{(0l)} \mathrm{E}(T_l)},\ P_4 = \dfrac{p_{(04)} \mathrm{E}(T_4)}{\mathrm{E}(T_0) + \sum_{l=0}^{9} p_{(0l)} \mathrm{E}(T_l)},\ P_5 = \dfrac{p_{(05)} \mathrm{E}(T_5)}{\mathrm{E}(T_0) + \sum_{l=0}^{9} p_{(0l)} \mathrm{E}(T_l)}, \\ P_6 = \dfrac{p_{(06)} \mathrm{E}(T_6)}{\mathrm{E}(T_0) + \sum_{l=0}^{9} p_{(0l)} \mathrm{E}(T_l)},\ P_7 = \dfrac{p_{(07)} \mathrm{E}(T_7)}{\mathrm{E}(T_0) + \sum_{l=0}^{9} p_{(0l)} \mathrm{E}(T_l)},\ P_8 = \dfrac{p_{08} \mathrm{E}(T_8)}{\mathrm{E}(T_0) + \sum_{l=0}^{9} p_{(0l)} \mathrm{E}(T_l)}, \\ P_9 = \dfrac{p_{09} \mathrm{E}(T_9)}{\mathrm{E}(T_0) + \sum_{l=0}^{9} p_{(0k)} \mathrm{E}(T_l)} \end{array}\right\} \tag{8}$$

P_0 is a limiting probability that the engine fuel system stays in the state s_0 (ability state) in a longer period (time interval) of operation (in theory at $t \to \infty$). Thus, this probability defines a coefficient of technical availability of the system for operation. However, $P_j (j = 1, 2,..., 9)$ are limiting probabilities of existence of the states $s_j \in S$ of the systems at $t \to \infty$, thus they are the probabilities that its components (and simultaneously the entire system, due to its serial reliability construction) are in states of inability.

Obtaining the probabilities $P_j (j = 0, 1, 2, \ldots, 9)$ which make a limiting distribution of the process of changes of ability and inability states of fuel supply systems for marine heavy fuel diesel engines requires, as it follows from (6) and (8) formulas, an estimation of the values of the probabilities p_{ij} and expected values $E(T_j)$. Obtainment of the values (obviously, in approximation) is expensive and labor consuming. This is due to the fact that collection of necessary information to estimate p_{ij} and $E(T_j)$ requires long-term empirical research using appropriate diagnosing systems (*SDG*) for engine fuel systems [1, 12, 15, 16, 17].

Estimation of the probabilities p_{ij} and expected values $E(T_j)$ is possible after getting realizations $w(t)$ of the process $\{W(t): t \geq 0\}$ in sufficiently long time period of investigation, thus for $t \in [0, t_b]$, whereas the time of the process investigation is: $t_b >> 0$. Then, it is possible to determine the numbers of: $n_{ij} (i,j = 0, 1, 2, 3; i \neq j)$, transitions of the process $\{W(t): t \geq 0\}$ from state s_i to s_j in sufficiently long time and to define the values of the estimator $\hat{P}_{ij}$ of the unknown probability p_{ij}. The estimator of the transition probability p_{ij} with the highest reliability is the statistics [7, 8]:

$$\hat{I}_{ij} = \frac{N_{ij}}{\sum_j N_{ij}}, \quad i \neq j; \quad i, j = 0,\ 1,\ 2,\ 3, \tag{9}$$

whose the value $\hat{p}_{ij} = \frac{n_{ij}}{\sum_j n_{ij}}$ is an estimation of the unknown transition probability p_{ij}.

The $w(t)$ course of the process $W(t)$ can also give the realizations $t_j^{(m)}$, $m = 1, 2, ..., n_{ij}$ of the random variables T_j. Application of a point estimation allows for ease calculation of $E(T_j)$ as an arithmetic mean value of $t_j^{(m)}$. Acquisition of the necessary information in order to calculate the probabilities requires employing adequate diagnosing systems (*SDG*) for the mentioned fuel systems which in this case become diagnosed systems (*SDN*) [5, 7].

The presented description of changes of states of a fuel system in a heavy fuel diesel engine can be obviously developed when taking into account the states of partial ability of such an engine system.

4. Final remarks and conclusions

Application of the aforesaid processes in the practice requires to satisfy the two following conditions:

- to collect the mathematical statistics that are necessary to determine the probabilities p_{ij} and the expected values T_{ij},
- to develop a semi-Markov model of changes of technical states of an engine fuel system with a small number of its states and simple (in the mathematical sense) matrix function **Q(t)**.

Application of a semi-Markov process as a model of changes of the specified states of an engine fuel system at a defined time (given moment), instead of a Markov process, results from that it should not be expected that the random variable $T_{(ij)}$ denoting the time period of duration of the state s_i on the condition that the state s_j is the next one and the random variable T_i denoting the time period of duration of the state $s_i (i = 1, 2, 3, \ldots, 9)$ of an engine fuel system, independently of which state will be next, have arbitrary distributions included in the set $R_+ = [0, +\infty)$. Employing a Markov process for this case would be justified if the assumption could be made that the random variables $T_{(ij)}$ and T_i have exponential distributions.

The presented model can be of considerable practical importance because of ease in determining the estimators of the transition probabilities p_{ij} which are the elements of the matrix **P** (9) and ease in estimating the expected values $E(T_j)$. However, the considerations should take into account the fact that a point estimation of the expected value $E(T_j)$ does not enable to define the estimation accuracy. Such accuracy is possible by the interval estimation, where a confidence interval $[t_{dj}, t_{gj}]$ with random endpoints is determined that contains with a certain probability (confidence level) β, the unknown expected value $E(T_j)$.

References

1. Cempel C., Natke H., G., Yao J.P.T.: Symptom reliability and hazard for systems conditio motoring. Mechanical Systems and Signal Processing. Vol. 14, No 3, 2000, pp.495-505.
2. Girtler J.: Girtler J.: Physical aspect of application and usefulness of semi-Markovian processes for modeling the processes occurring in operational phase of technical objects. Polish Maritime Research. No 3(41)/2004, vol. 11, pp. 25-30.
3. Girtler J.: Semi-Markovian models of the process of technical state changes of technical objects. Polish Maritime Research No 4(42)/ 2004, vol. 11, pp. 3-7.
4. Girtler J.: Reliability model of two-shaft turbine combustion engine with heat regenerator. Journal of KONES Powertrain and Transport, Vol. 132, No. 4, 2006, pp.15-22.
5. Girtler J.: Problemy oszacowania trwałości i niezawodności silników o zapłonie samoczynnym z zastosowaniem teorii procesów semimarkowskich i diagnostyki. Combustion Engines (Silniki Spalinowe), nr 3, 2013, s. 1-9[pdf].
6. Girtler J.: A method for evaluating the performance of a marine piston internal combustion engine used as the main engine on a ship during its voyage in different sailing conditions. Polish Maritime Research, Vol. 17 No. 4, 2010, s. 31-38
7. Girtler J.: *Diagnostyka jako warunek sterowania eksploatacją okrętowych silników spalinowych*. Studia Nr 28, WSM, Szczeci 1997.
8. Grabski F.: Teoria semi-markowskich procesów eksploatacji obiektów technicznych. Zeszyty Naukowe AMW, nr 75A, Gdynia 1982.
9. Korczewski Z.: Entropy function application In the selection process of diagnostic parameter of marine diesel and gas turbine engines. Polish Maritime Research. Vol. 17, No 2(65), 2010, pp.29-35.
10. Limnios N., Oprisan G.: Semi-Markov Processes and Reliability. Boston, Birkhauser 2001.
11. Piotrowski I. Witkowski K.: Okrętowe silniki spalinowe. Wyd. TRADEMAR, Gdynia 1996.
12. Piotrkowski I., Witkowski K.: Eksploatacja okrętowych silników spalinowych. AM, Gdynia 2002.

13. Сильвестров Д. С.: Полумарковские процессы с дискретным множеством состояний. Издательство „Советское Радио”. Москва, 1980.
14. Wojnowski W.: Okrętowe siłownie spalinowe. Cz. I. Wyd. AMW, Gdynia 1998.
15. *Inżynieria diagnostyki maszyn*. Praca zbiorowa po redakcją B. Żółtowskiego i C. Cempla. PTDT. Wyd. ITE, Warszawa, Bydgoszcz, Radom 2004.
16. MAN B&W Diesel A/S: CoCoS Maintenance, Designed for Maintenance Excellence, Kopenhaga 2005.
17. Wartsila Corporation: Service News from Wartsila Corporation 2 2002/1 2003, CBM for two stroke engines, Kaidara Software, Wartsila Corporation Helsinki, marzec 2003.

GDAŃSK UNIVERSITY OF TECHNOLOGY

Journal of POLISH CIMAC

Faculty of Ocean Engineering & Ship Technology
GDAŃSK UNIVERSITY OF TECHNOLOGY

THE MODELLING OF ACCUMULATION AND DISSIPATION OF ENERGY IN MECHANICAL DRIVE SYSTEM

Andrzej Kaczmarski

Gdansk University of Technology
Faculty of Ocean Engineering and Ship Technology
G. Narutowicza 11/12, 80-233 Gdansk, Poland
phone: +48 58 347 24 30, email: andrew925@wp.pl

Abstract

This paper presents a modelling of accumulation and dissipation energy in simple drive system. The simple drive system is presented by laboratory stand designed for calculate fatigue life of material for bending and rotation tests pieces. The laboratory stand was prepared to diagnosis of fatigue life of material by use energetic methods. This idea was submitted as utility model to Polish Patent Office. This laboratory stand gives ability to research a influence of change of fatigue life for energetic symptoms (like: temperature of material, vibration, Acoustic Emission, rotary speed, electrical energy). This paper presents influence of change of fatigue life for rotary speed. The rotary speed is value describing effect of accumulation and dissipation energy in drive system (in material). A difference between energy taken from power supply and consumed for giving rotary speed is used for fatigue of material. This simple theory is presented and modelling in this paper. The next paper (in this book) describes results of research that could verify this theory.

Keywords*: modelling, accumulation and dissipation of energy, mechanical drive systems*

1. Introduction

The necessary of diagnostic of machines is obvious consequence which is result of their maintenance. This concerns especially important and expensive machines. For many engineers and scientists a very difficult problem is how to calculate or predict the future life of mechanical elements that works by high cyclic load. We know that fatigue life is very complicated problem and it is difficult to precise calculation. We know too that the fatigue life is effect of accumulation of energy in material. The difficult problem is how to calculate this energy. We don't have to do this (at work of machines) but we can observe symptoms that are effect of accumulation energy. For example a growth of temperature is a value defining a increase of internal energy in material. We know that the growth of temperature depends on kind of material (elastic-plastic or plastic-brittle) and this is symptom describing the future fatigue life for this mechanical element.

The fatigue of material at work of mechanical elements could be described by many symptoms and parameters. Their are effect of change of properties of material. The cyclic load makes hardening or weakening of material that influences on rigidity. This makes that the bearings could be less loaded (the lesser deflection of shaft in place of support) and less energy is wasted there. The change of rigidity influences on change of vibration of mechanical drive system. For example a stable work after hardening of material (after 20 hours of work) makes stability of vibration

amplitude. This symptom is useful to diagnostic of technical state all machines or engines.

The change of properties of material influences on rotary speed. In used laboratory state the change of rotary speed is visible diagnostic symptom describing accumulation of energy in material. This accumulation of energy describes fatigue life of steel test piece. The observation of multi symptoms by use temperature, deflection, vibration, electrical energy: current and voltage, Acoustic Emission and rotary speed gives information about effects of accumulation energy in material. This same allows to estimate a fatigue life.

The multi symptoms research allow to make physical and mathematical model. It is necessary to verification results and could allow to predict fatigue life.

2. The purpose of test stand building

Every mechanical drive system owns a efficiency. The main stream of energy is passed to any working equipments. The part of energy is lost in mechanical elements (bearings, shafts, gear wheels, oil) which pass energy from source (electrical motor or engine) to working equipments. This small part of lost energy is used to change properties of material. The bearing and tooth of gear wheels are cyclic deformed. A oil is plastic deformed under cyclic loading of shaft neck. These all cyclic changes make growth of temperature and change material's properties. These results are effect of dissipation energy in material and dissipation energy in mechanical system (growth of vibrations).

Any delivered energy makes a change of situation of body (substance). This principle concerns to every situation: huge machines that are described like closed system and every elements (inside of substances). When it is considered to separate elements the dissipation of energy makes change of material's properties. Overflow of limit of this dissipation energy in material makes complete wear or crack of material. Present research should show how can describe technical state of working elements by use theory about dissipation energy in material. This problem is difficult to solve but it will give good information about calculate of reliability of mechanical structures.

The used laboratory stand is prepared to research fatigue life of bending and rotary elements working by cyclic loading. This laboratory stand is patterned on well-known fatigue machines - Schenck [4] but now it is used to calculate and diagnose of material by use energetic methods. The improvement of laboratory stand and new patterns was described in utility model [the number of application W.121416].

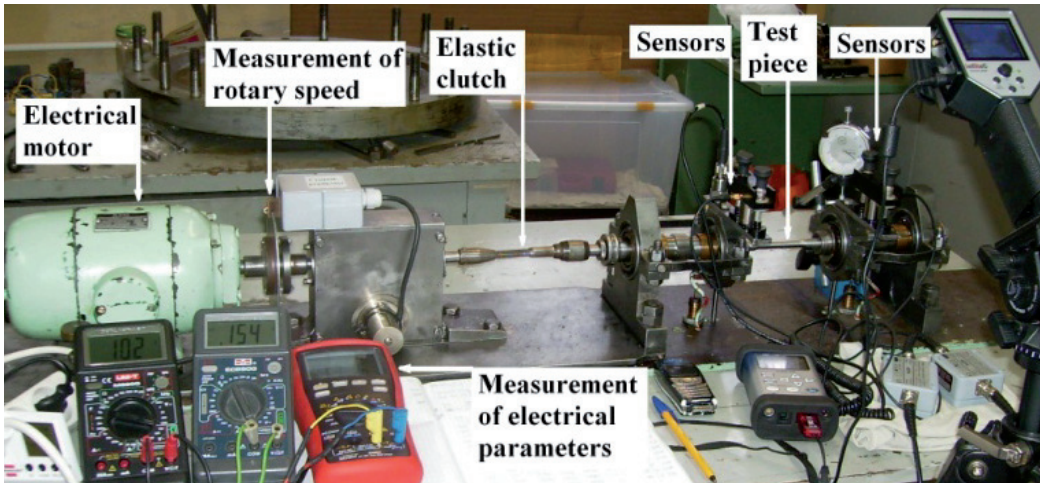

Fig. 1. The laboratory stand

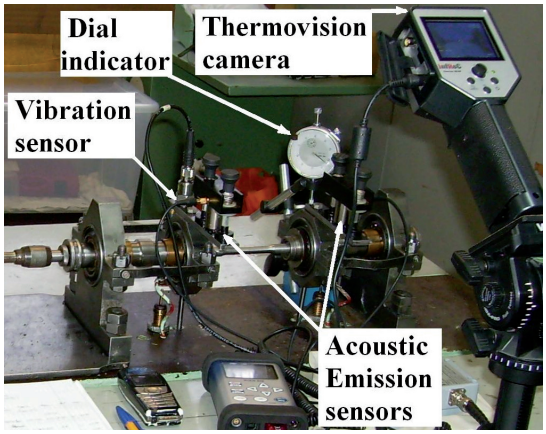

Fig. 2. The laboratory stand – place of sensor's installation

The principle of laboratory stand is possibility of observation of energetic symptoms for bending of rotary test piece. The main principle of laboratory stand is cause that all stream of energy is used in mechanical rotary system. The energy had been taken from electrically source could be used for two causes: giving kinetic energy to rotary elements or accumulation energy in material (what makes his fatigue). This allows to know better symptoms describing change of properties of material at cyclic loaded work. The main formula describing behaviour of drive model is relationship:

$$J\frac{d\omega}{dt} = M_d - M_{res} \tag{1}$$

where:

J – moment of inertia [kg·m^2],
ω– angular velocity [rad/s],
t – time [s],
M_d – drive moment [Nm],
M_{res} – resistance moment [Nm].

The principle 1 describes a behaviour of drive system as change between drive moment M_d and resistance moment M_{res}. The drive moment is value of energy delivered to system. The resistance moment describes wasting of energy in mechanical system: accumulation energy in material (increase of internal energy) and dissipation energy in mechanical system (growth of kinetic energy – increase of rotary speed). A difference between M_d and M_{res} is used to give rotary speed. So a value and a change of the rotary speed can describe a part of energy that is not used to change material's properties. The resistance moment M_{res} can be described generally as sum of two moments:

$$M_{res} = M_f + M_{str} \tag{2}$$

where:

M_f – friction moment (in bearings only – the simple model) [Nm],
M_{str} – moment of change of material's structure [Nm].

The M_f is simple function of one physical quantity - loading (stresses in material) because it makes more loading of bearings and more friction and lost energy. The principle between M_f and loading is linear function and can be simple to modeling. In laboratory stand is not more important elements where might be lost of energy.

The moment of change of material's structure M_{str} is difficult problem. This is nonlinear function of many physical quantities:

- temperature;
- deflection;
- rotary speed;
- parameters of Acoustic Emission (energy, amplitude, number of events, duration of signal, RMS);
- vibrations.

The M_{str} is following function:

$$M_{str} = f(T, D, \omega, AE, V) \tag{3}$$

where:

M_f – temperature [K],
D – deflection [mm],
ω– angular velocity [rad/s],
AE – parameters of Acoustic Emission,
V – RMS of vibrations.

3. The physical model of transformation of energy in mechanical drive system

Three values are necessary to modeling of behavior of drive system: input, output and disruptions. The input energy is measured by using electrical parameters:

- current (measured on rotor);
- voltage (measured on rotor);
- electrical input energy (energy delivered from power supply);

The drive moment M_d is calculated as electromagnetic moment [5]. This principle does not contain a efficiency of rotor's system (decrease a voltage in carbon brush and in rotor's winding) but this efficiency is high and might have solid number what helps by modeling. The main principle is shown below:

$$M_d = \frac{U \cdot I}{\omega} \tag{4}$$

where:

U – voltage (on electrical terminal of rotor) [V],
I – current (on electrical terminal of rotor) [A],
ω – angular velocity [rad/s].

The output values was specified before M_{str} = f(T, D, ω, AE, V) and present it is not necessary precise model describing M_{str} (moment of change of material's structure). The future research can help to make this precise model. In this paper I can show a influence of fatigue life on change of the rotary speed ω, the temperature T and the drive moment M_d. The main view of all mechanical drive system (laboratory stand) is shown below [3]:

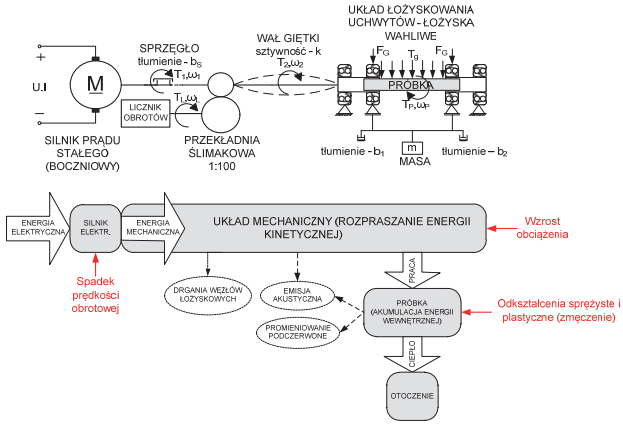

Fig. 3. The model of laboratory stand (simple mechanical drive system) [3]

The model on Fig. 3. shows a flow of energy in mechanical drive system. A increase of load makes change of diagnostic (energetic) parameters. A increase of load makes decrease of rotary speed and increase of temperature. The physical model is shown on Fig. 4. This presents relationships between mechanical elements (bearings, absorbers, test piece, electrical motor) and physical values that describe accumulation and dissipation energy in mechanical drive system. The main principle of physical model is relationship 1. The other relationships are less taken into consideration but that are going to model in relationship 3. The disruptions value is the load. The load is made by weight hanging under laboratory stand. This makes constant bending stresses on all length of test piece. The electrical motor makes that the bending stresses has changeable progress (sinusoidal progress). At normal work of machines a change of load is value which makes change of behaviour of system (for example as load is increasing as rotary speed is decreasing). The description of laboratory stand was presented in earlier articles of Author [1, 2].

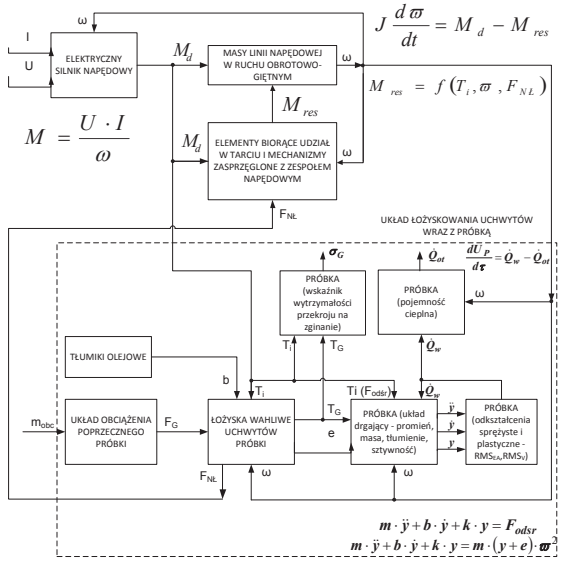

Fig. 4. Physical model of simple mechanical drive system and relationships between physical values [3]

4. The example of test's results

The experiment was made for five test pieces. The conditions of work were constant. The material of test pieces used in this experiment is designed for mechanical drive elements (shafts or gear wheels). The test pieces were made from one round bar that makes smaller spread of results what is obvious for fatigue wear. The parameters of starting work and kind of material are shown in Table 1:

Tab. 1. Parameters of test

number of test piece	outside temperature	loading	starting rotary speed	material
	[K]	[MPa]	[r/min]	C45+C
1,2,3,4,5	296	297 ≈0,35Rm	4000	Rm = 830 MPa (round bar)

The test's results corroborate a simple theory described in point 3. The progress and change of energy and rotary speed is depended on fatigue life. Results of five test pieces are not representative population for one test but are a part of bigger research. This test was planned by use earlier test (15 test pieces) [2]. A experiment and the laboratory stand were improved (the measured values and period of measurement). The behaviour of material under changeable loading is known but in present test are more values describing accumulation and dissipation of energy.

The results of test show a change of behaviour of drive system depending on fatigue life (number of cycles until crack). The results confirm the simple theory described in point 3: as a fatigue life is higher as rotary speed R(N) is higher and energy from power supply P(N), drive moment $M_d(N)$ and temperature T(N) are lesser.

The behaviour of mechanical drive system and accumulation of energy can describe follow: energy delivered to drive system is not waste in material but makes higher rotary speed – the energy is not accumulated in material and does not make changes in material (elastic-plastic deformations and increase of temperature). The temperature is a value describing the internal energy. For cyclic loading the internal energy is describing as a range of hysteresis lop between stresses and deformations. This statement was described by Szala and Boroński [6] and Kaleta [7]. In this test the internal energy is value describing fatigue life and reliability of mechanical drive systems.

The behaviour of mechanical system and principle 1 is shown on Fig. 5. The Fig 5 makes some questions:

- why does the rotary speed increase when conditions of work are this same?
- why does the drive moment M_d decrease?
- why does the resistance moment M_{res} decrease?

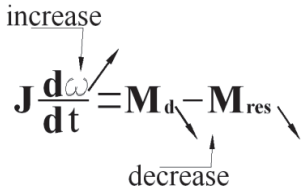

Fig. 5. Behaviour of mechanical drive system

The answers might be contained in progress of measured values. These characteristics show change of rotary speed, power supply, drive moment, temperature and current of rotor as function of fatigue life. These all characteristics are parameters describing a change of stream of energy at work of mechanical drive system. The main results of test are shown in table 2:

Tab. 2. Results of test

Test piece	**number of cycles until crack**	**temperature at moment of crack**	**rotary speed** (ending, stable)	**power supply** (ending, stable)	**drive moment** (ending, stable)
	[-]	[K]	[r/min]	[W]	[Nm]
1	$162x10^3$	313,3	3740	324	0,247
2	$140x10^3$	315,0	3400	345	0.258
3	$263x10^3$	308,8	4030	315	0,243
4	$274x10^3$	309,4	4700	300	0,230
5	$218x10^3$	312,1	3850	325	0,270

The current of rotor has a direct relationship with drive moment. For electrical motor (permanent current) the drive moment has follow relationship [5]:

$$M_d = c \cdot \phi \cdot I \tag{5}$$

where:

c – constant factor depending on construction of electrical motor [-],
ø – magnetic flux [Wb],
I – current (on electrical terminal of rotor) [A].

This relationship shows that drive moment (indirectly energy delivered to drive system) can be described by using the current of rotor only (magnetic flux is depended on induction current and is permanent). A calculation of drive moment M_d by using principle 5 is difficult but a trend of characteristic is kept.

5. Conclusion

The results of test confirm theory of accumulation energy in mechanical drive system. The energy which is not lost in material is used to make increase of kinetic energy (increase of rotary speed). This shows that rotary speed is value which can be used to describing fatigue life and reliability of drive systems.

The figure 7 shows interesting progress of power supply. The energetic theory of fatigue wear could be described as a energy delivered to material. The endings of progress of power supply show Wöhler's characteristic.

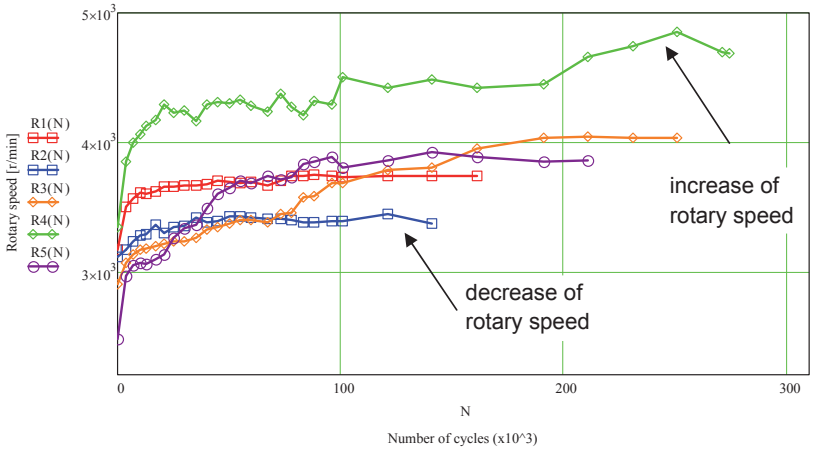
5×10^3
4×10^3
3×10^3
Rotary speed [r/min]
R1(N)
R2(N)
R3(N)
R4(N)
R5(N)
increase of
rotary speed
decrease of
rotary speed
0
100
200
300
N
Number of cycles (x10^3)

a)

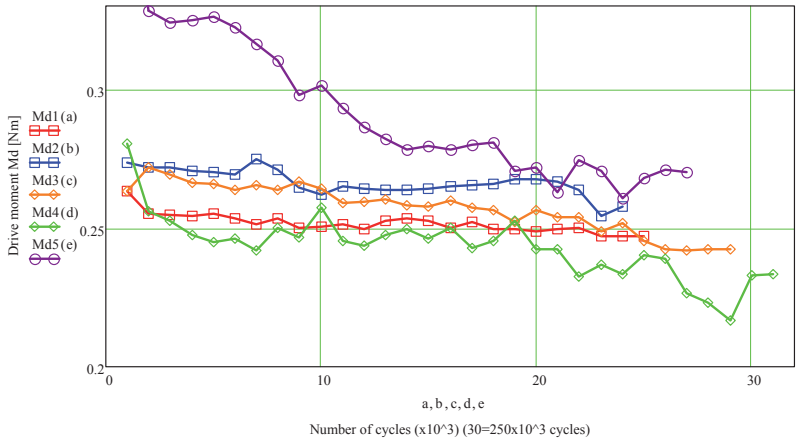
0.3
0.25
0.2
Drive moment Md [Nm]
Md1(a)
Md2(b)
Md3(c)
Md4(d)
Md5(e)
0
10
20
30
a, b, c, d, e
Number of cycles (x10^3) (30=250x10^3 cycles)

b)

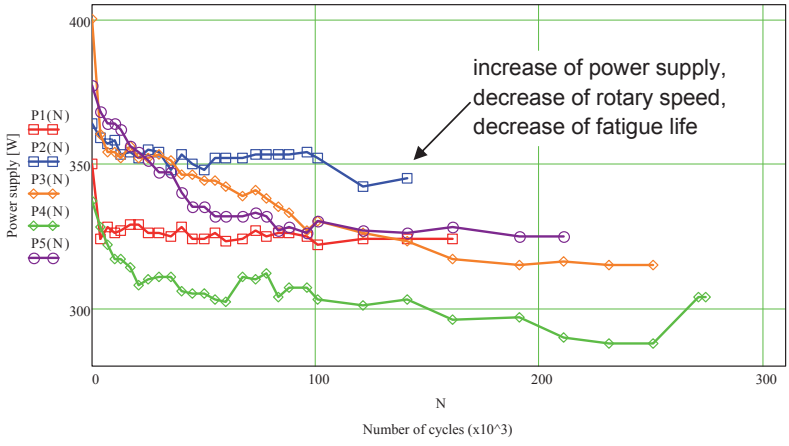
400
350
300
Power supply [W]
P1(N)
P2(N)
P3(N)
P4(N)
P5(N)
increase of power supply,
decrease of rotary speed,
decrease of fatigue life
0
100
200
300
N
Number of cycles (x10^3)

c)

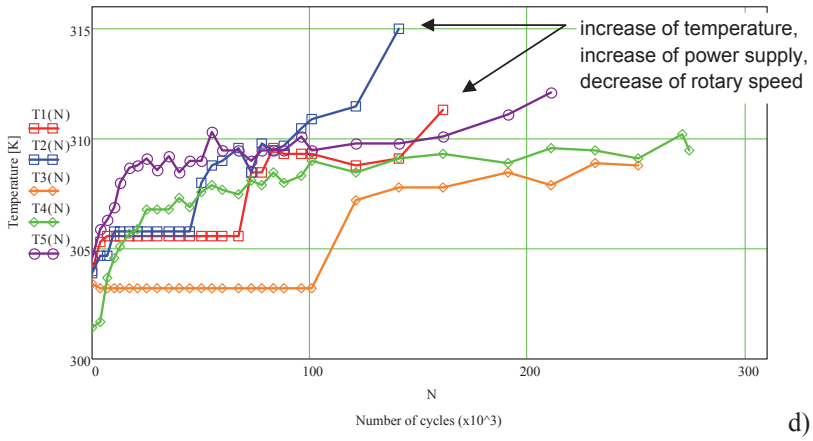

d)

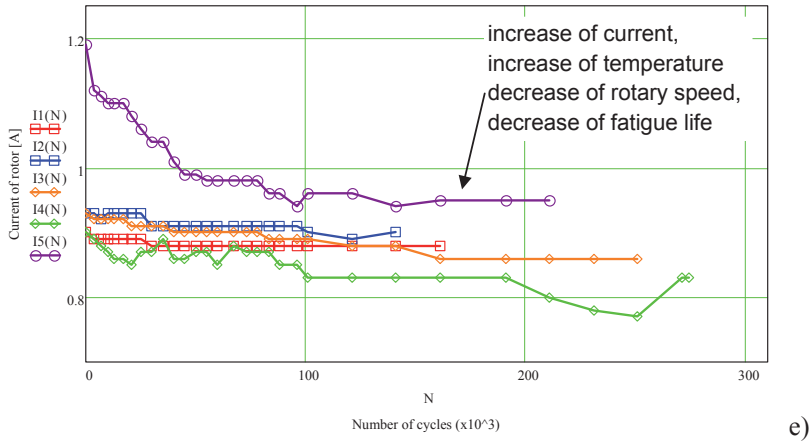

e)

Fig. 6. Change of physical values in depending on fatigue life (number of cycles N): a) rotary speed R(N), b) drive moment M_d, c) power supply P(N), d) temperature T(N), e) current of rotor I(N)

The results show following conclusions:

- the change of rotary speed is depending on fatigue life,
- the temperature is a value describing internal energy accumulated in material and is depending on fatigue life,
- the drive moment and the power supply are value describing energy delivered to mechanical drive system and are depending on fatigue life.

At this test were used other diagnostic parameters: vibrations and Acoustic Emission (AE). These parameters confirm energetic methods using by diagnostics of mechanical elements and fatigue wear.

This test allows to predict a behaviour of diagnostic parameters in the next part of experiment. Thanks to this test is making now a method of research of the future experiment and a statistical analysis.

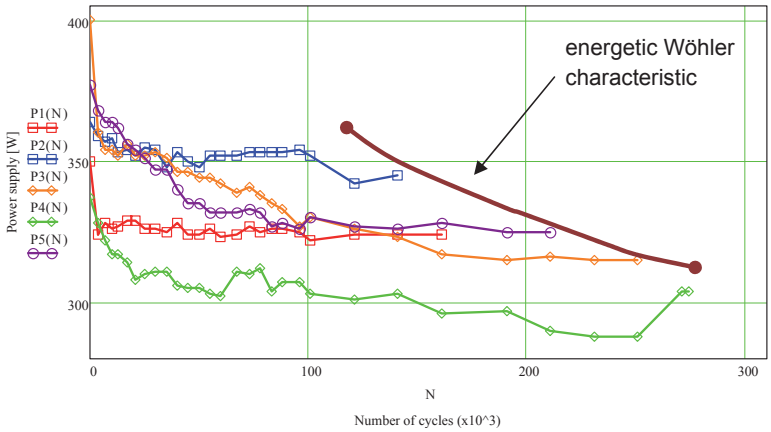

Fig. 7. Wöhler characteristic as function of power supply (delivered energy)

This test allows to predict a behaviour of diagnostic parameters in the next part of experiment. Thanks to this test is making now a method of research of the future experiment and a statistical analysis.

The next tests will be doing for higher and smaller loading that allow to observe the parameters of drive system (especially a rotary speed) depending on delivered power and a influence on fatigue life of material. This all results will be necessary to elaborate a statistical analysis for a whole experiment. This allows elaborate characteristic of behaviour of drive system and make mathematical model of accumulation and dissipation of energy in this system.

References

[1] Kaczmarski A.: *Application of laboratory stand for multi-symptoms tests for high cyclic fatigue of constructional material, Journal of POLISH CIMAC*, Vol. 7, No. 3, Gdańsk 2012.
[2] Kaczmarski A.: *Stanowisko laboratoryjne do badania wytrzymałości zmęczeniowej materiałów konstrukcyjnych na podstawie energetycznych procesów resztkowych. Współczesne technologie i konwersja energii*, Wydawnictwo Politechniki Gdańskiej, Gdańsk 2012.
[3] Korczewski Z.: *The conception of energetic investigations of the multisymptom fatigue of the simple mechanical systems' constructional materials. Journal of POLISH CIMAC*, Vol. 7, No. 1, Gdańsk 2012.
[4] Kocańda S.: *Badanie własności mechanicznych metali*, WNT, Warszawa 1954.
[5] Plamitzer A.: *Maszyny elektryczne*, WNT, Warszawa 1982.
[6] Szala J., Boroński D.: *Ocena stanu zmęczenia materiału w diagnostyce maszyn i urządzeń,* Wydawnictwo Naukowe Instytutu Technologii Eksploatacji – PIB, Radom 2008.
[7] Kaleta J.: *Metody doświadczalne w zmęczeniu materiałów i konstrukcji. Badania podstawowe. Zbiór monografii pod redakcją Józefa Szali,* WU ATR w Bydgoszczy, Bydgoszcz 2000.

Journal of POLISH CIMAC
Faculty of Ocean Engineering & Ship Technology
GDAŃSK UNIVERSITY OF TECHNOLOGY

THE MODEL OF THE EXHAUST GAS DUCT FLOW OF THE MARINE 4-STROKE DIESEL ENGINE

Jerzy Kowalski

Gdynia Maritime University
Department of Engineering Sciences
Morska Street 81-87, 81-225 Gdynia, Poland
tel.: +48 58 6901434, fax: +48 58 6901399
e-mail: jerzy95@am.gdynia.pl

Abstract

The manuscript presents the model of the exhaust gas flow through the exhaust gas duct of the marine 4-stroke engine. Presented model are computational fluid dynamic model based on dimensions and the construction of the real exhaust gas duct. The measurement parameters from real object are used to the model validation. The simulation of the exhaust gas duct throttling by rotational throttling plate was done. Obtained calculation results allow to determination of the exhaust gas mass flow for the simulated flow characteristics. The model of turbulence flow was taken into account. The gravity forces and the heat transfer phenomena were neglected. Obtained calculation results are qualitatively consistent with results obtained from literature. The analyze of the velocity distribution in the exhaust gas duct allows to conclusion that the changes of the angular position of the throttling plate causes significant disturbances in the exhaust gas flow. The result of this is the decrease of the exhaust gas flow. Additional purpose of the manuscript was approximation of the obtained results of the exhaust gas flow for different angular positions of the throttling plate. Obtained polynomial function may be useful tool to modeling the combustion process in the engine cylinders for the different flow characteristics of the exhaust gas duct. The calculation results allow to determination the mass flow of the exhaust gas with mean error equal 11%.

Keywords: *marine diesel engine, exhaust gas composition, toxic emission, CFD model, exhausts gas duct throttling*

1. Introduction

4-stroke diesel engines are commonly used sources of the mechanical energy in the land and the marine applications. Unfortunately they are the sources of the gaseous toxic compounds also. Mentioned compounds are products of the hydrocarbon fuels in air. According to regulations of the Annex VI to MARPOL Convention [11] all marine engines with nominal power output above 130kW must apply the nitric oxides emission limits. Emission must be calculated according to regulations from "Technical code on control of emission of nitrogen oxides from marine diesel engines" [12] and the ISO-8178 standard regulations [3]. According to European Commission regulation [2] the diesel engines operated in the on-road vehicles must apply the emission limits of carbon oxides, hydrocarbons and solid particles.

Delimitation of the toxic gaseous compounds emission requires direct measurements of the fractions of the mentioned compounds in the exhaust gas during the engine operation with specified loads. Quantity of the emission of the toxic compounds requires the calculation of the mass flow of the exhaust gas. Three methods are acceptable:

- direct measurement of the exhaust gas flow,

– measurement of the fuel consumption and the air flow to the engine and calculation of the exhaust gas flow,
– measurement of the fuel consumption and calculation of the exhaust gas flow according to carbons balance method [3].

Direct measurement of the exhaust gas flow in the case of large, marine diesel engines is very difficult and not precise. Therefore, often applied method is calculation of the exhaust gas flow by carbons balance method. Disadvantage of this method is the calculation error caused by "a priori" assumed the chemical composition of the fuel.

The diesel engines operations causes deterioration of its technical state. Effect of this are the changes in the organization of the combustion process in the engine cylinders and changes in the emission of the toxic compounds. The solid particles emission causes particles deposition on the surfaces of the exhaust gas duct. In [5] author presents the results of the laboratory research about influence of the exhaust gas duct throttling on the composition of the exhaust gas. According to these results the throttling of the exhaust gas duct causes significant changes of the carbon oxide emission. Obtained results allow to only qualitatively analyzing. The reason of this lack of possibility of the determination of influence of the exhaust gas duct throttling on the exhaust gas flow. According to this the 3D model of the exhaust gas flow was prepared. The method applied in proposed model is Computational Fluid Dynamic (CFD).

2. Laboratory research

The chosen object of research is 3-cylinder, four-stroke, turbocharged, laboratory engine. The engine is loaded by a generator, electrically connected to the water resistance. During tests the engine was fuelled by diesel oil and operated at a constant speed, equal to 750rpm. The engine load and speed, parameters of the turbocharger, systems of cooling, fuelling, lubricating, and air exchange were measured. Pressure, temperature and humidity of air were recorded by laboratory equipment also. All mentioned results were recorded with a sampling time of 1 second. The scheme of the laboratory stand is presented in [4] and the engine parameters are presented in Tab.1.

Tab. 1. The laboratory engine parameters

Parameter	Value	Unit
Max. electric power	250	kW
Rotational speed	750	rpm
Cylinder number	3	–
Cylinder diameter	250	mm
Stroke	300	mm
Compression ratio	12,7	–

The experimental study consists of 3 stages of 3 observations with simulations of different malfunctions of the exhaust gas duct. During each start of the observation, the engine was loaded to maximum load equal 250kW, and, after stabilizing the temperature of the exhaust gas behind the turbine, the engine operating parameters were recorded for 3 to 5 minutes. After this, the load of the engine was decreased by 10kW and, after stabilizing the temperature of the exhaust gas behind the turbine, the engine operating parameters were recorded again. The observation was continued with loads up to 50kW. The engine did not work with a load of 190kW due to resonance vibrations.

Stages of experiment were set as follows:
– the first stage during the operation of the engine assumed as "working properly",

– the second stage during the operation of the engine with the throttling of the cross section area of the exhaust gas duct by changing the barrier angle mounted in the exhaust gas duct behind the turbine by 21 degrees,
– the third stage during the operation of the engine with the throttling of the cross section area of the exhaust gas duct by changing the barrier angle mounted in the exhaust gas duct behind the turbine by 71 degrees.

The exhaust gas duct throttling simulation consisted of changing the angle of the throttling barrier mounted in the exhaust gas duct behind the turbine. Scheme of the exhaust gas duct and the prepared 3D model are presented in Fig.1.

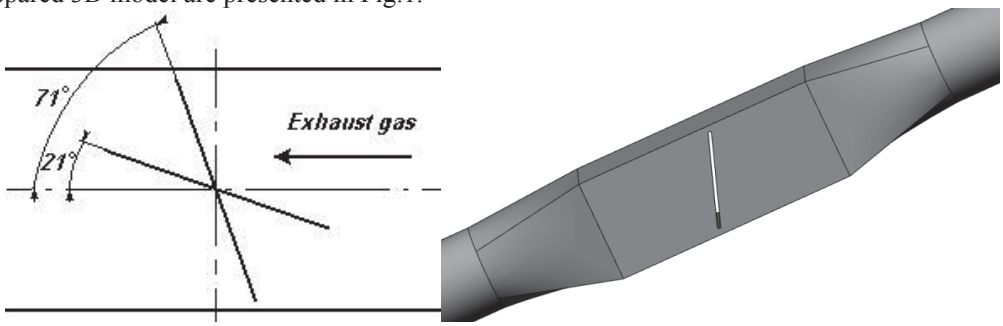

Fig.1. Scheme of the exhaust gas duct and the 3D model

3. CFD model

Obtained laboratory research results and the geometric dimensions of the exhaust gas duct allow preparing the exhaust gas flow model behind the turbine. Throttling of the exhaust gas duct by the rotating plate causes the decrease of the cross section area of the exhaust gas duct and the changes in the flow characteristic, resulting the changes of the duct geometry. The result of this is intensity of turbulence phenomena in the exhaust gas flow.

According to the mentioned purpose the modelling of the exhaust gas flow through the exhaust gas duct was conducted. Chosen method of modelling was Computational Fluid Dynamic (CFD) method.

The used software to CFD conduction was AVL Fire. The exhaust gas duct construction was transferred and meshed to the pre-processor of the AVL Fire package. The cubic mesh with the minimum dimension equal 2,5 mm was chosen. The area of the rotating plate was re-meshed to the minimum dimension equal 1mm. The large dimensions of the exhaust gas duct and its axis symmetric construction, only the axis-symmetric half of the exhaust gas duct was modelled. The momentum and the continuity equations with k-zet-f model of turbulence [10], [14] were performed. The energy balance equations, the heat transfer phenomena and the gravity forces were neglected.

The boundary conditions were selected as follows:

– the exhaust gas duct inlet with the ambient temperature and the ambient pressure of the exhaust gas behind turbine,
– the exhaust gas duct outlet with the ambient temperature of the exhaust gas behind the turbine and the environment pressure,
– the axis-symmetry in the axis-symmetry surface.

The maximum number of iterations was set on 3000 and the convergence criteria of the normalized residuals were set. The calculated result, as an extrapolate values of the cross section area of the exhaust gas duct outlet, is mass flow of the exhaust gas.

Obtain the correct results of the calculation depends on specify the quantity of the Prandtl number and the density of the exhaust gas [6], [9]. The exhaust gas is mixture of the gaseous

combustion products, the water steam and not combusted in the engine cylinders air. The results of the exhaust gas analyze, obtained from [5] allows to specify the exhaust gas composition.

Basis on the NIST Chemistry Book [11], about the parameters of the gaseous compounds of the exhaust gas in the obtained temperature and pressure ranges, the calculations of the Prandtl number and the density of the exhaust gas were conducted.

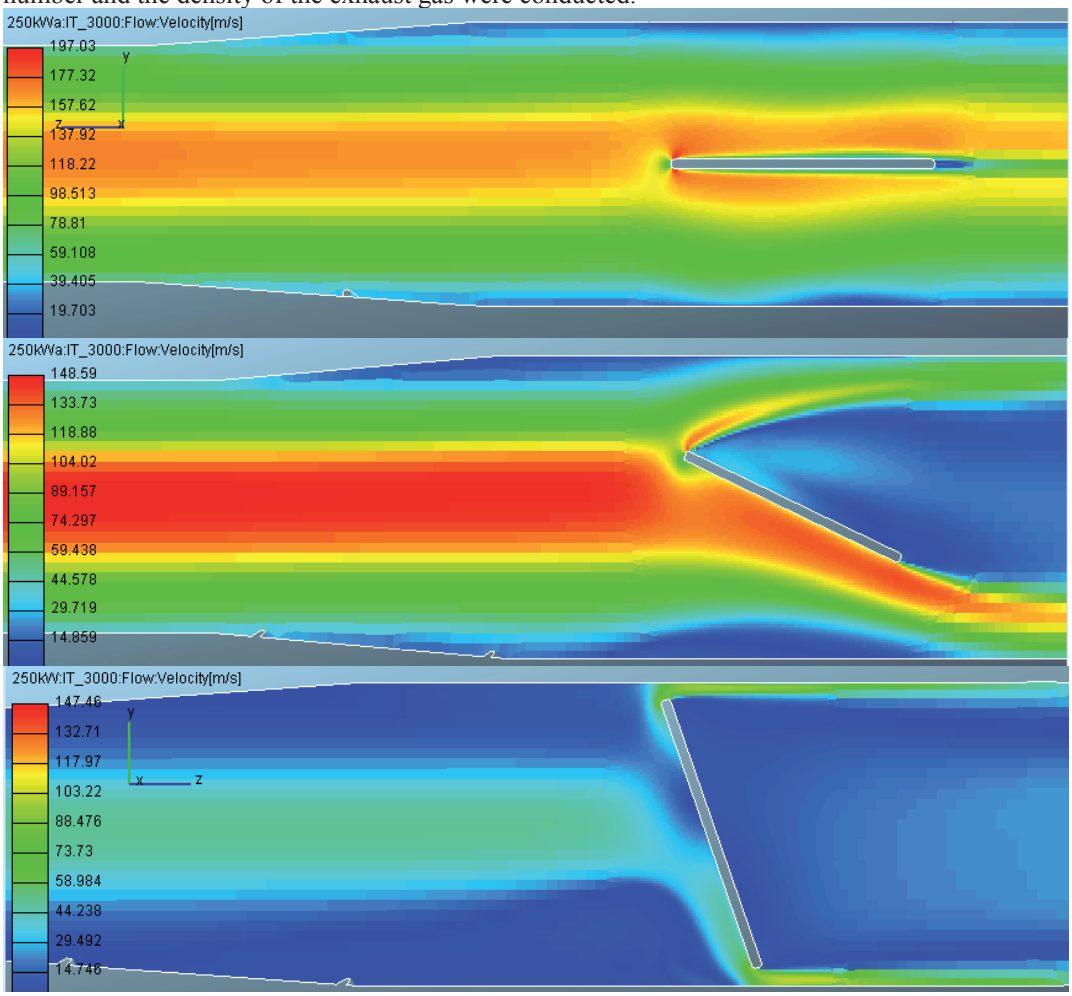

Fig.2. Velocity in the exhaust gas duct for 250kW the engine load

Mentioned calculations were conducted according to the weighted average by the following formula:

$$\mathrm{Pr} = \sum_{i=n}^{i=1} \mathrm{Pr}_i \cdot U_i \,, \tag{1}$$

were:

Pr_i – the Prandtl number for the i-th gaseous compound,

U_i – the fraction of the i-th gaseous compound in the exhaust gas.

The density of the exhaust gas was calculated accordingly to the (1) formula.

4. Results and discussion

Mentioned actions allow to obtain the mass flow of the exhaust gas through the exhaust gas duct of the laboratory engine. The calculations for all considered loads of the engine and all angle positions of the throttling plate presented in [5] are done.

On the Fig.2 the example of calculation results in the form of exhaust gas flow velocity for the engine load equal 250kW and different positions of the throttling plate are presented. Mentioned results are qualitatively representative for all considered loads of the engine. According to presented results horizontal position of the throttling plate disturbs the exhaust gas flow only a small degree. The flow is laminar. Only flow near the duct walls causes the changes on the flow direction. The 21° angle rotation of the throttling plate causes disturbance of the exhaust gas flow. It should be noted that the maximum velocity of the exhaust gas flow in the central point of the cross section decreases by 10%. Further increase of the exhaust gas duct throttling decreases the mass flow of the exhaust gas. The maximum velocity in this condition decreases by 50%. Presented results are qualitatively similar to presented in [1], [8], [13].

Fig.3 presents the results of calculations of the exhaust gas mass flow and measured parameters of the exhaust gas behind the turbine. According to presented results increase of the exhaust gas duct throttling causes the decrease of the mass flow of the exhaust gas.

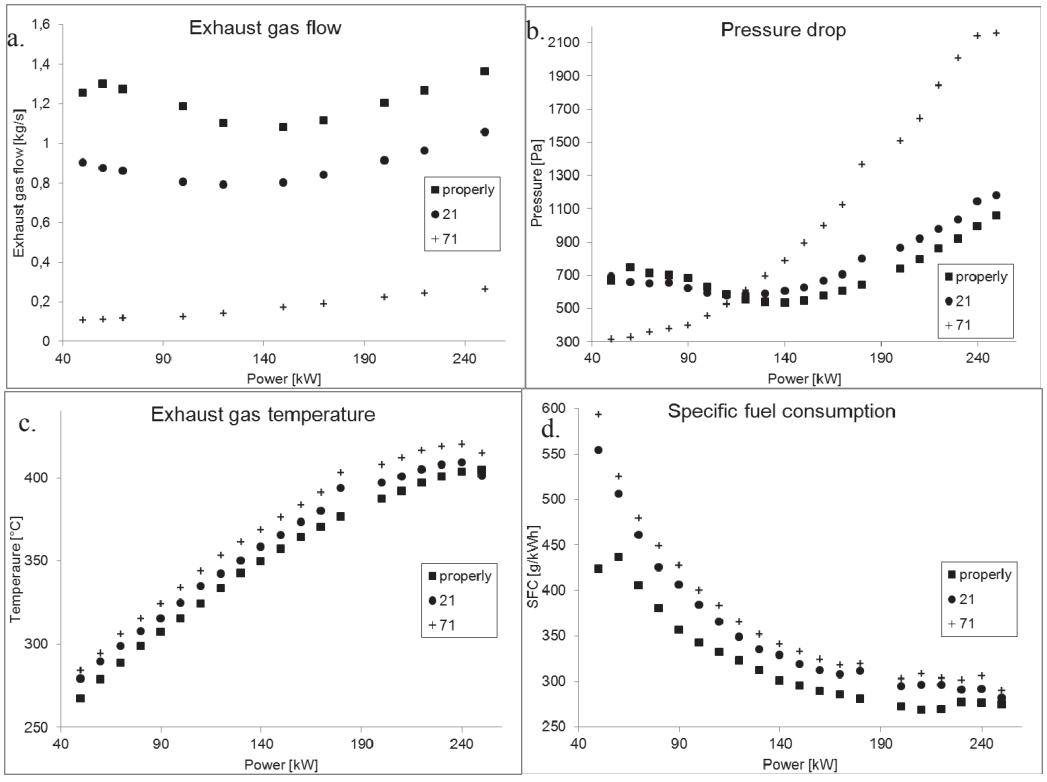

Fig.3. Measured and calculated parameters of the exhaust gas duct

Throttling of the exhaust gas duct decreases the pressure of the exhaust gas behind the turbine and increases its temperature behind the cylinders. Fig.3b and Fig.3c shows changes of the exhaust gas pressure and temperature behind the turbine. According to the presented results, the

temperature of the exhaust gas behind turbocharger increases with the increase of both exhaust duct throttling and the load of the engine. The exhaust duct throttling causes abnormalities in the combustion process. Abnormalities of combustion process cause a growth of the fuel consumption. Fig.3d shows specific fuel consumption measured for all considered states of the engine. Throttling of the exhaust gas duct by changing the barrier angle by 21deg. causes average increase of the fuel consumption by 3,7%, and 8,2% for changing the barrier angle by 71deg respectively.

The decrease of the differences of the exhaust gas pressure in the exhaust gas duct causes decrease of the turbocharger performance. The quantity of air delivered to the engine decreases. Simultaneously with this phenomena, the quantity of delivered fuel increases. The effect of this is combustion of the richer mixtures in the cylinders.

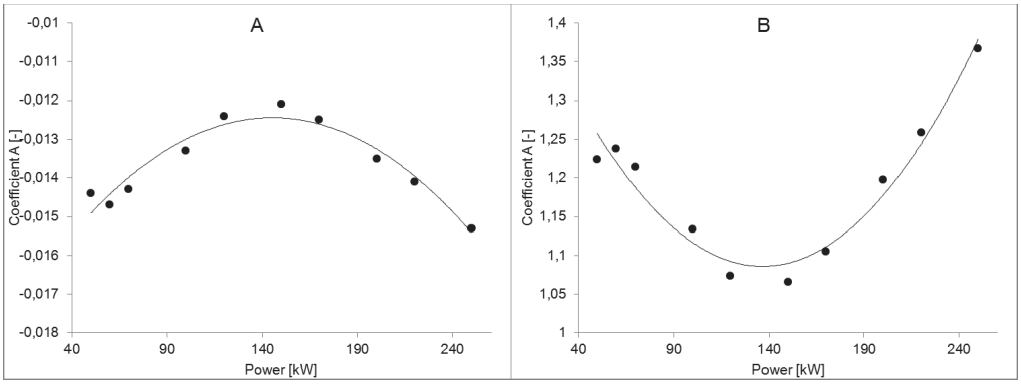

Fig.4. Approximation coefficients for exhaust gas duct flow

The second goal of this research was approximation of the mass flow through the exhaust gas duct in accordance to different position of the throttling plate. Mentioned approximation may be useful tool to modelling the combustion processes in the engine cylinders in the different than laboratory conditions.

Fig.3 presents the linear dependence between the exhaust gas mass flow and the angular position of the throttling plate of the engine in the constant rotational speed. According to this the approximation of this dependence is the linear function as follows:

$$q = A \cdot An + B, \tag{2}$$

where:

q – the mass flow in [kg/s],
An – the angle position of the throttling plate [°],
A, B – coefficients of the linear function.

Change of the engine output power causes changing the values of the mentioned coefficients "A" and "B". Fig.4 presents the changes of the coefficients values in function of the engine power. The black dots presented the measured points. According to presented results the values of both "A" and "B" coefficients may to be approximated by a second order polynomial, according to the following formulas:

$$A = a1 \cdot P^2 + a2 \cdot P + a3, \tag{3}$$

$$B = b1 \cdot P^2 + b2 \cdot P + b3, \tag{4}$$

where:

P – the power output of the laboratory engine [kW],
a1 ÷ a3, b1 ÷ b3 – the coefficients of the second order polynomials [-].

Presented analyse allows to select the values of values of coefficients from "a1" to "b3" for the considered laboratory stand. Mentioned values are presented in Table 2. The results of calculation the "A" and "B" coefficients with use of values from the Tab.2 are presented in Fig.4 by continuous line.

Tab.2. The coefficients values of the approximation function

Coefficient	a1	a2	a3	b1	b2	b3
Value [-]	-3E-07	8E-05	0,0182	2E-05	0,0062	1,5124

Presented results allow calculating the quantity of the exhaust gas mass flow for different values of the exhaust gas duct throttling in the range from the 0 to the 71° of the angular position of the throttling plate area without direct measurement. The maximum error of obtained approximation compared to measured values not excided 11%.

5. Conclusions

The main purpose of the presented manuscript is determination of the flow characteristic of the exhaust gas duct of the marine 4-stroke diesel engine. The simulation of the exhaust gas duct throttling by rotational throttling plate was done. The 3-dimensional flow model witch use of CFD method is applied. Obtained calculation results allow to determination of the exhaust gas mass flow for the simulated flow characteristics. The model of turbulence flow was taken into account. The gravity forces and the heat transfer phenomena were neglected. Obtained calculation results are qualitatively consistent with results obtained from literature. The analyze of the velocity distribution in the exhaust gas duct allows to conclusion that the changes of the angular position of the throttling plate causes significant disturbances in the exhaust gas flow. This causes the eddies creation and back flows. The result of this is the decrease of the exhaust gas flow.

Additional purpose of the manuscript was approximation of the obtained results of the exhaust gas flow for different angular positions of the throttling plate. Obtained polynomial function may be useful tool to modeling the combustion process in the engine cylinders for the different flow characteristics of the exhaust gas duct. The calculation results allow to determination the mass flow of the exhaust gas with mean error equal 11%. The author's assessment is that obtained accuracy is not enough to use in the modeling practice. Therefore, further work is required in this area. May find the following a parametric assessment of the exhaust gas flow phenomena.

Acknowledgments

The project was supported by the National Science Centre in Poland, granted on the basis of decision No. DEC-2011/01/D/ST8/07142

The project was supported by AVL Company according to University Partnership Program and license of AVL Fire software

References

[1] Canbazoglua S., Bozkirb O.: *Analysis of pressure distribution of turbulent asymmetric flow in a flat duct symmetric sudden expansion with small aspect ratio*, Fluid Dynamics Research, Vol. 35, pp. 341 – 355, 2004.

[2] Dyrektywa UE nr 692/2008 w sprawie homologacji typu pojazdów silnikowych w odniesieniu do emisji zanieczyszczeń pochodzących z lekkich pojazdów pasażerskich i użytkowych Euro 5 i Euro 6.
[3] ISO 8178 - *Reciprocating internal combustion engines*.
[4] Kowalski J., *Laboratory study on influence of air duct throttling on exhaust gas composition in marine four-stroke diesel engine.* Journal of Kones, Vol. 19. No 1, pp. 191 – 198, Warsaw 2012.
[5] Kowalski J., *Laboratory study on influence of the exhaust duct throttling on exhaust gas composition in marine four-stroke diesel engine*, Journal of Polish CIMAC, Vol. 7, No 1. pp. 109 – 115. Gdańsk 2012.
[6] Kuo K.k., *Principles of combustion,* Willey & Sons Inc., New Jersey 2005.
[7] Linstrom P.J., *NIST Standard Reference Database,* National Institute of Standards and Technology, 2013.
[8] Macchion O., Lior N., Rizzi A., *Computational study of velocity distribution and pressure drop for designing some gas quench chamber and furnace ducts*, Journal of Materials Processing Technology, Vol. 155–156, pp. 1727 – 1733, 2004.
[9] Poinsot T., Veynante D., *Theoretical and numerical combustion,* Edwards 2005.
[10] Popovac, M., Hanjalic, K., *Compound Wall Treatment for RANS Computation of Complex Turbulent Flows and Heat Transfer*, Flow Turbulence and Combustion, Vol. 78, pp. 177 – 202, 2007.
[11] *Revised Marpol Annex VI. Regulations for the Prevention of Air Pollution from Ships*. Resolution MEPC.176(58). International Maritime Organization. 2008.
[12] *Technical Code on Control of Emission of Nitrogen Oxides from Marine Diesel Engines*. Resolution MEPC.177(58). International Maritime Organization. 2008.
[13] Wang L.-B., Tao W.-Q., Wang Q.-W., Wong T. T., *Experimental study of developing turbulent flow and heat transfer in ribbed convergent/divergent square duct*, International Journal of Heat and Fluid Flow, Vol. 22, pp. 603 – 613, 2001.
[14] Zienkiewicz O.C., Taylor R.L., *The finite element method, Vol.3 Fluid Dynamics*, Butterworth-Heinemann, Oxford 2005.

GDAŃSK UNIVERSITY OF TECHNOLOGY

Journal of POLISH CIMAC

Faculty of Ocean Engineering & Ship Technology
GDAŃSK UNIVERSITY OF TECHNOLOGY

MEASUREMENT OF AUTOMOTIVE VEHICLES POWER IN REAL ROAD CONDITIONS

Ewa Kuliś*, Tomasz Kałaczyński, Marcin Łukasiewicz, Andrzej Sadowski, Joanna Wilczarska, Bogdan Żółtowski

University of Technology and Life Sciences in Bydgoszcz
ul. Prof. S. Kaliskiego 7, 85-789 Bydgoszcz, Poland
tel.: +48 52 3408226, fax: +48 52 3408271
e-mail: ekukla@utp.edu.pl*

Abstract

A portable engine test bench makes it possible to measure power and torque, acceleration of given speed, breaking distance, and distortions of the speedometer reading. The operation principle of a portable test bench is similar to that of a stationary load test bench with the only difference that the vehicle testing takes place in real road conditions, not in simulated ones, on the rollers of a stationary engine test bench.

In this work, the operation principle of the portable engine test bench, the measurement method and exemplary results that have been obtained from carried out experimental test have been presented which provides the basis for further measurements of the vehicle operation real parameters in real not laboratory conditions.

Keywords: *measurement of engine power, portable engine test bench*

1. Introduction

In their service instructions, car producers provide some engine parameters. This information is of great significance for the user, especially for the potential buyer of a given vehicle. From this data customers can draw fargoing conclusions.

These parameters include:

- engine capacity
- torque
- power

As it is commonly known, the engine power means work of pressure of gases acting on the piston bottom, performed in a time unit. For multi cylinder engines it is the sum of the power of cylinders that make up the power unit.

The driver is interested in useful power. This is power which can be transmitted to a receiver in any conditions of the engine operation [1, 3].

Rated power of an engine is guaranteed by the producer of the power unit for given conditions of operation. For passenger car engines the rated power equals maximal power, i.e. such that the engine can provide under constant load over a given time without the fear of exceeding mechanical allowable load or overheating. The maximal value of power is given in most of service instructions and technical data specifications for passenger cars. Both power and torque are variable in the function of the engine rotational speed.

A portable engine test bench makes it possible to measure power and torque, acceleration of any speed, breaking distance and distortions of the speedometer reading. The operation principle of the engine test bench is similar to a stationary load engine test bench with the difference that the measurement is performed in real conditions on the road not in conditions simulated on rollers.

A portable engine test bench has many advantages [2]:

- accuracy – with the assumption that the parameters are appropriate, measurement error is smaller than 1%.
- the car is tested in its natural conditions, on the road – there is no problem with improper air supply, which makes the measurement accuracy higher than in a test house on a chassis test bench,
- frequency of drawing data onto a chart: 60 times per a wheel revolution. Power and torque is provided with accuracy up to 0.1 KM and 0.1Nm. and the revolutions for which these parameters are obtained with accuracy of 1 revolution. .
- program for control of the engine test bench enables manual entering of transmission values – it allows to eliminate errors which occur due to wrong calculations by programs for control of engine test bench transmissions.
- program for control of the engine test bench has many interesting functions: ability ot compare up to 4 charts simultaneously, clear results in the form of tables and charts, full control of printouts etc.
- correction of measurements according to DIN70020 ensures that neither the air temperature nor pressure affects fluctuations of power measurements.
- there is a possibility to test a car with four wheel drive.

Fig. 1. Image of portable engine test bench

2. Operation principle of portable engine test bench

Like in a load engine test bench: the car, being in a given gear, is accelerated within an established range, then it is switched into the neutral and the rolling resistance is measured- with the difference that the sensor reading 60 impulses per one wheel revolution is fixed on the car, not at the rollers of a stationary test bench.

Due to such an operation principle the device is characterized by high accuracy. For the purpose of high measurement accuracy it is necessary to be familiar with the vehicle weight, gear box ratio (it can be determined on the road), size of tires. It is also necessary to enter the air temperature and atmospheric pressure to make the given result recalculated with DIN norm obligatory in Europe.

Since changes of atmospheric pressure, air humidity or its temperature affect the measured values – they are normalized and the obtained measurement results are converted into values corrected with normal parameters (according to DIN 70020 – 25C°and 1000 HPa (does not account for humidity) and a special correction factor –power is estimated to change by 1% for temperature change by 5-6 degrees) engines tested according to American norm SAE do not have some accessories: air filter, alternator/ generator, fuel pump, clutch, radiator fan and exhaust system – therefore, the results according to SAE norm are higher by nearly 15-20 %.

3. Description of the experiment

The tests were performed with the use of Honda Accord VI from 2000 with engine 1.8 16V (136KM). Preparation for tests involved screwing a measuring disc and its revolution sensors to the vehicle wheel, connection of a cable for reading of the ignition system impulses (fig. 2)- measurement is performed in normal riding conditions and the results are transmitted to a portable computer which shows particular results of measurements.(fig. 3).

In order to achieve proper results, such data as temperature, air pressure, size of tires, ratio of the power transmission system – were given.

Fig.2. Manner of fixing a measurement disc with the sensor

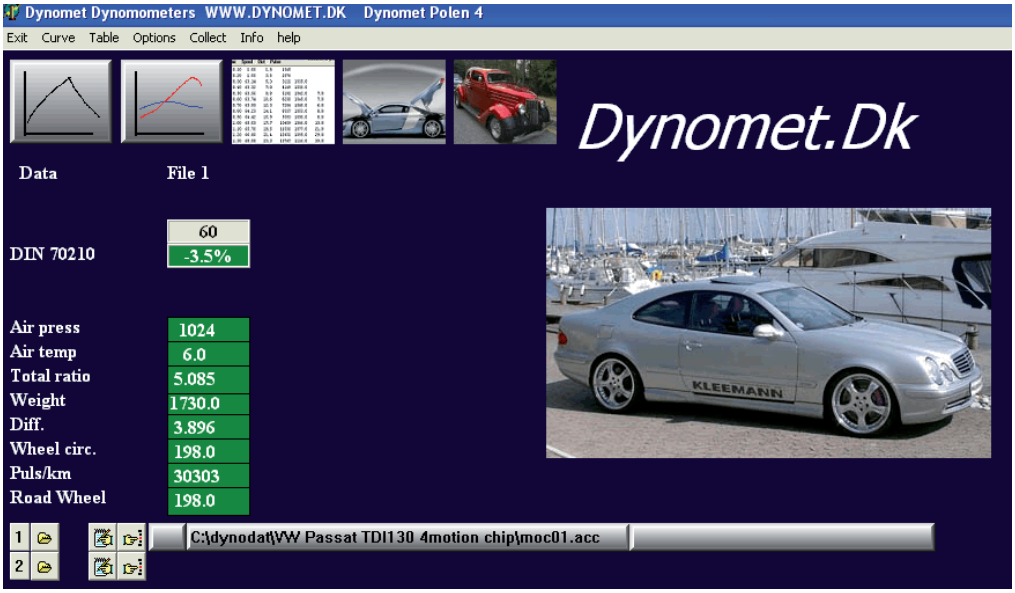

Fig. 3. Image of Dynomet dk program window

The measurements have proved that (fig.4) although the vehicle is 12 years old its power in real conditions does not differ from the power indicated by the producer.

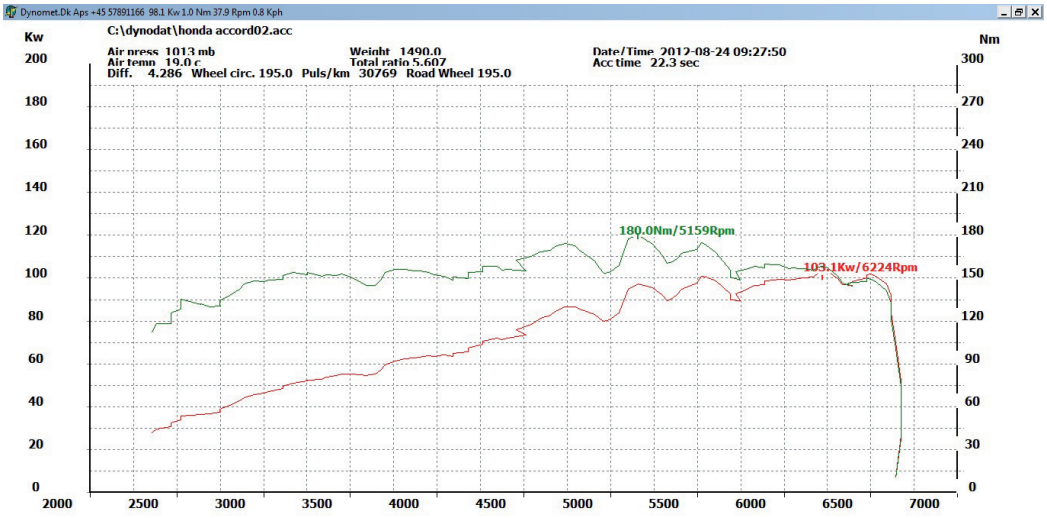

Fig. 4. Exemplary chart from the tested vehicle power measurement

During testing it was possible to observe the vehicle actual speed (fig.5)

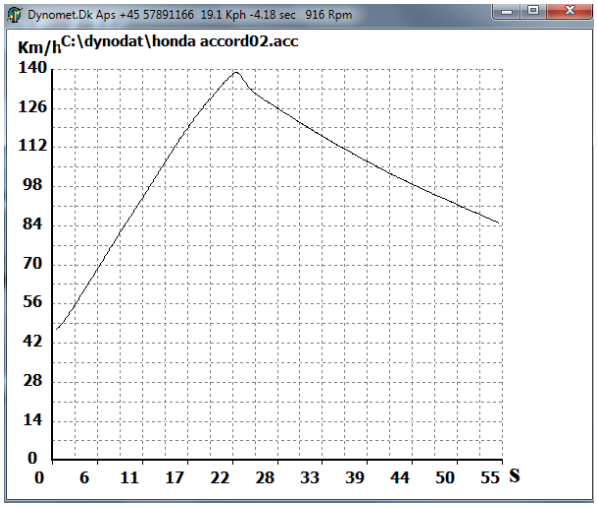

Fig. 5. Chart of speed shows how the vehicle actual speed changes in te function of time.

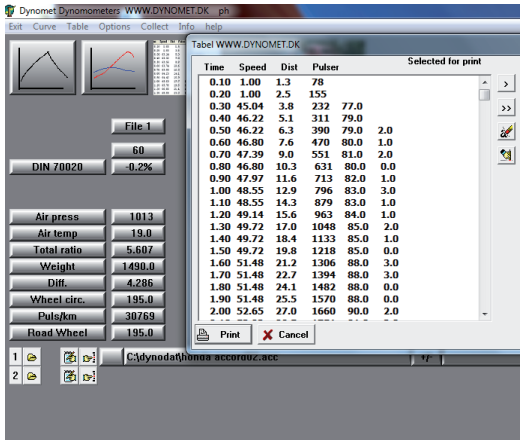

Fig. 6. Measurement table

In the above presented table 3 the first columns are: Time = (s) – Speed (km/h) and Distance Dist – distance covered (m).

5 Summary

A device of this type can provide data on the car acceleration, its elasticity in particular gears within assigned values, power and torque in the function the engine revolutions and even the braking force. Accuracy of the power measurement on the wheels is increased by the value of air resistance – significant for high speeds, and it allows to establish what actual power is actually available and what is the maximal power that can be reached by the vehicle [4]. Undoubtedly, a disadvantage of such a device is approximate power of the engine (calculated by means of special algorithms which are designed to calculate approximate value of losses in the power transmission system). Moreover, when there is a sensor fixed on the wheel the measurement must be performed precisely along a straight line so that the wheel will not travel a distance different than the one that has been assumed.

This study aimed to carry out a preliminary measurement verification test, the development of reliable methods for measuring and obtaining data for further verification.

While further research should be carried out verification of the above mentioned studies and research carried out by stationary dynamometer. Only the results of these studies will help to understand the real differences arising from the use of the vehicle in real time.

References

[1] Cempel, C., Tomaszewski, F., *Diagnostyka maszyn*, MCNEMT, Radom, 1992.
[2] Niziński, S., Michalski, R., *Diagnostyka obiektów technicznych*, ITE, Radom 2002.
[3] Żółtowski, B., *Badania dynamiki maszyn*, Akademia Techniczno-Rolnicza w Bydgoszczy, Bydgoszcz 2002
[4] Żółtowski, B., *Podstawy diagnozowania maszyn*, Uniwersytet Technologiczno-Przyrodniczy w Bydgoszczy, Bydgoszcz 2000

The work was carried out under the project „**Techniki wirtualne w badaniach stanu, zagrożeń bezpieczeństwa i środowiska eksploatowanych maszyn”**.
Project number: **WND-POIG.01.03.01-00-212/09**

GDAŃSK UNIVERSITY OF TECHNOLOGY

Journal of POLISH CIMAC

Faculty of Ocean Engineering & Ship Technology
GDAŃSK UNIVERSITY OF TECHNOLOGY

VARIABILITY OF COMPRESSION RING PRESSURE AGAINST THE DEFORMED CYLINDER WALL DURING ENGINE OPERATION

Wojciech Serdecki

Institute of Combustion Engines and Transport
Poznań University of Technology
3, Piotrowo St., 60-965 Poznań
tel.+48 665 2243, fax: +48
e-mail: wojciech.serdecki@put.poznan.pl

Abstract

Problems connected with the circumferential distribution of compression ring pressure against the deformed cylinder wall during engine run were presented in this paper. In particular, division of the resultant force pressing the ring against the wall into component connected with ring own elasticity and the one originated from gas pressure was carried out and the influence of each force at individual phases of engine run was evaluated as well. The relationship allowing calculation of the circumferential ring pressure was also established. The paper contains figures and drafts obtained in a course of exemplary calculations of compression ring pressure concerning a running bulldozer engine. These figures show the areas of cylinder wall where so called light slots can appear.

Conclusions resulting from the carried out simulation tests are discussed in Summary. The need for further investigations mentioned in presented study was shown as well.

Keywords*: combustion engine, piston ring, ring elastic pressure*

1. Introduction

As soon as new cylinder liner is being installed a considerable deformation can occur caused by an erroneous installation in cylinder block. These deformations can grow to considerable size (of a few dozen micrometers [2]) during engine operation when the liner is being exposed to the influence of changing loads. Examples of such effect are presented in Fig. 1.

The compression ring is being pressed to the cylinder wall with the radial forces that result from material own elasticity and gas pressure acting upon ring surfaces (see Fig. 2). While the elasticity force F_s remains roughly constant during engine run, the other force F_g changes itself. Investigations on the compression ring position in ring groove allow to conclude [1, 4] that the ring is pressed to the groove bottom side on the prevailing section of stroke which means that the acting gas pressure is almost the same as the pressure in combustion chamber (p_a). Only on short sections of ring path the ring loses its contact with the bottom side of groove which causes that the F_g force value depends above all on pressure p_b in space below the ring.

On the other hand the ring is separated from the cylinder wall with the F_f force resulting from the hydrodynamic pressure of oil film. The value of mean pressure is given by the equation [5]

$$p_s = p_a + (p_b - p_a) W_p + \frac{\eta \cdot u \cdot b_f}{h_m^2} W_u + \frac{\eta \cdot v \cdot b_f^2}{h_m^3} W_v , \quad (1)$$

where:

p_a, p_b – external pressures acting on the ring,
u, v – ring velocities, axial and radial respectively,
η – viscosity of lubricating oil,
h_m – oil film minimum thickness,
b_f – height of ring face covered with oil film,
W_i – load capacity coefficients, that allow to consider the effect of external pressures (p index), slide (u) and squeeze (v); their values depend on the profile of ring face.

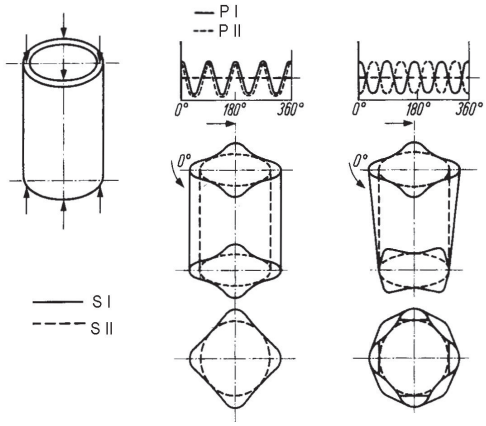

Fig. 1. Deformations of cylinder sinusoidally loaded along its circumference; P I and P II – load of upper and lower part of ring, respectively, S I and S II – form of bore before and after loading [3]

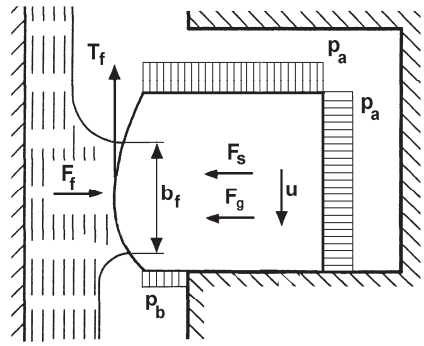

Fig. 2. Sketch of compression ring moving relatively to cylinder wall; p_a, p_b – external pressure, F_s – force of ring own elasticity, F_g – force equivalent to gas forces loading ring, F_f – reaction of oil layer, T_f – friction between ring and oil layer, u – ring speed, b_f – ring axial height covered with oil film

If the value of oil film pressure was not enough to balance the forces pressing the ring against the wall the film rupture would occur and the ring would collaborate with wall in conditions of mixed or even boundary lubrication. In case of incomplete contact of ring face and cylinder wall the circumferential slots can occur which lead to the gas blow-by. This can cause the drop in engine power and an excessive oil consumption (which in turn leads to the increase in exhaust emission). Another task performed by rings, namely the heat conduction from piston to cylinder deteriorates as well.

In his earlier papers author evaluated the ring pressure circumferential distribution against the deformed cylinder wall caused only by the ring own elasticity [7]. This pressure is additionally strengthened by the exhaust on the running engine which can lead to a different collaboration of these parts. Due to that the determination of combined effect of elasticity and gas force on pressure distribution and eventual definition of areas of ring and deformed wall contact was chosen as the goal of described tests.

In order to realize the given aim the model tests were performed in which an extremely unfavorable case was selected, i.e. the lack of continuous oil film over the cylinder wall to eliminate the disturbance factors. Though this assumption is merely of theoretical character

(engine operation in such conditions would lead to a quick failure of collaborating parts) the obtained results allow to estimate value of some parameters indeterminable with other methods. One can mention here the forces loading radially the ring indispensable for full contact of ring and arbitrarily deformed cylinder wall.

2. Ring to wall pressure from elastic and gas forces

It was proved in [8] that the ring circumferential pressure distribution $p_m(\varphi)$ over the deformed cylinder wall can be determined according to the formula:

$$p_m(\varphi) = \frac{E \cdot I}{h_p \cdot r_m^4}\left[K \cdot r_m - \left(z_a + z_b(\varphi) + 2 \cdot z_b''(\varphi) + z_b^{IV}(\varphi)\right)\right]. \tag{2}$$

where:

E – Young's modulus,
I – inertia moment of ring cross section,
r_m – radius of neutral layer of ring in cylinder,
h_p – ring axial height,
z_a – constant deformation of cylinder,
$z_b(\varphi)$ – deformation of cylinder wall, variable along the cylinder circumference (and its second and fourth derivative),
K – characteristic coefficient of ring given with the formula

$$K = \frac{p_m \cdot h_p \cdot r_m^3}{E \cdot I}. \tag{3}$$

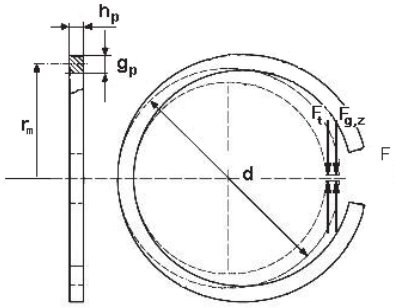

Fig. 3. Sketch of a ring with marked dimensions and position of tangential force F_t and resultant gas force $F_{g,z}$

The value of K coefficient calculated according to formula (3) is just a reflection of ring dimensions and its material properties. However, taking into account the aim of investigation a trial was undertaken to such define the K coefficient that it would describe not only its elasticity but also the effect of exhaust gases. Using the following formula

$$K = \frac{F_t \cdot r_m^2}{E \cdot I}, \tag{4}$$

that is another form of the formula (3) from [6], following relation has been obtained that allow to calculate a modified form of the K coefficient (because of its relation to crankshaft angle α further denoted as $K_z(\alpha)$):

$$K_z(\alpha) = \frac{\left(F_t + F_{g,z}(\alpha)\right) \cdot r_m^2}{E \cdot I} \qquad \text{or} \qquad K_z(\alpha) = K + \frac{p_g(\alpha) \cdot h_p \cdot r_m^3}{E \cdot I}, \tag{5}$$

where:

F_t – tangential force fixed in the plane of neutral axis at ring free gap,
$F_{g,z}(\alpha)$ – force fixed in the plane of neutral axis at ring free gap, equal to the gas force loading the ring,
$p_g(\alpha)$ – exhaust gas pressure loading the ring,
α – crankshaft angle.

Gas pressure loading the internal and working ring surface depends on the instantaneous pressure over (p_a) and below (p_b) the ring and on the position of ring in groove. For an initially adopted assumption about the lack of continuous oil film over the liner surface a linear drop in pressure along the ring face axial height was assumed. Due to that one can distinguish two cases for which the approximate value of gas pressure loading the ring is:

$$p_g(\alpha) = 0.5 \cdot \left(p_a(\alpha) - p_b(\alpha)\right), \tag{6a}$$

when the ring leans on the bottom side of groove and

$$p_g(\alpha) = 0.5 \cdot \left(p_b(\alpha) - p_a(\alpha)\right), \tag{6b}$$

when the ring leans on the upper side of groove.

When the pressure over and below the ring is equal, the resultant pressure is zero, which means that both characteristic parameters are the same, i.e. $K = K_z(\alpha)$.

3. Calculations of compression ring pressure on the deformed cylinder wall

The presented below example concerns a trial of computational definition of compression ring wall pressure distribution against the deformed cylinder of earth moving machine engine (DT 466 International Harvester). Technical data of this ring have been presented in Table 1.

Tab. 1. Technical data of exemplary IC engine compression rings

Quantity		Ring
cylinder diameter d	[m]	0.109
ring neutral radius r_m	[m]	0.0522
axial height h_p	[m]	0.003
radial thickness g_p	[m]	0.0046
Young modulus E	[Pa]	$112 \cdot 10^9$
mean pressure p_o	[MPa]	0.178
tangential force F_t	[N]	27.6
stiffness EI	[Nm^2]	2.65
parameter K	[–]	0.0286

According to the primary goal of this study the further presented results concern an evaluation of the effect of gas forces on ring contact with a deformed cylinder wall. However, these deformations were limited to the one case, namely a circumferential line like in Fig. 1 described with the formula

$$z_b = A_4 \cos(4\varphi + \delta_4), \tag{7}$$

where A_4 and δ_4 are amplitude and phase shift of the Fourier series fourth harmonic, respectively (see Fig. 4).

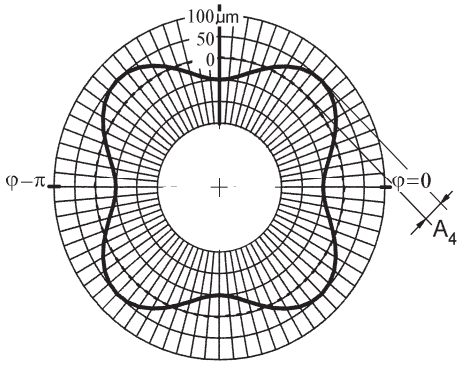

Fig. 4. Course of cylinder circumferential line for A_4 = 50 μm and $\delta_4 = \pi$

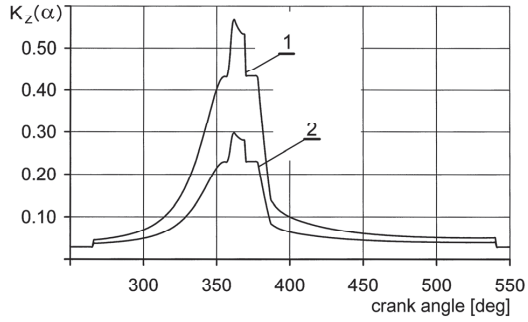

Fig. 5. Course of $K_z(\alpha)$ coefficient value vs. crank angle for full (1) and partial (2) engine load

According to the analysis presented in Chapter 1 it was assumed that the ring is pressed against the bottom side of groove during the stroke of compression and expansion. The ring position during other strokes has been regarded as less important for the analyzed example because of far lower gas pressure (the radial position of ring depends above all on the ring own elasticity).

Knowledge of engine constructional data as well as its operational conditions allowed to evaluate on the course of theoretical computations the pressure over and beneath the ring and eventually calculate the value of modified coefficient corresponding to the consecutive positions of piston (only a fraction of these variations were presented in Fig. 5). The calculations of gas forces were carried out for engine full and partial load.

Next, using Eqs. (2) and (7) the dependence (8) was defined that allows the calculation of ring wall pressure at an arbitrary point of cylinder circumference (φ) and for a chosen crankshaft angle (α).

$$p_m(\varphi) = \frac{E \cdot I}{h_p \cdot r_m^4}\left[K_z(\alpha) \cdot r_m - 225 \cdot A_4 \cdot \cos(4\varphi + \delta_4)\right]. \tag{8}$$

Exemplary results presented further were achieved for the fourth harmonic amplitude which equals 10, 20, 50 and 100 μm, respectively.

The lines seen in Fig. 6 and 8 show the places on cylinder wall where the ring pressure falls to zero for a given engine load and amplitude of cylinder wall deformation (because of ring symmetry only its section from 0 to π/2 was shown). It was assumed that pressure equal or lower than zero means no contact of ring and wall.

As it results from courses presented in Fig. 6 the area of ring face and cylinder wall contact increases along with the increase in ring wall pressure (caused by the increase of gases in combustion chamber). For example, during compression stroke for the cylinder deformation amplitude equal to 10 μm the elastic ring pressure alone does not secure such contact. As soon as the gas pressure reaches the required magnitude which relates to the crank angle 260 degrees the contact is full. For the amplitude A_4 equal to 20 μm the same effect is visible at 300 degrees CA while for 100 μm the full circumferential contact appears close to TDC. During expansion stroke

the areas of full and partial contact have different shape because of different angular distribution of gas pressure. Reference [7] provides dependences that allow to calculate the amplitude boundary value of any harmonic which secures a positive ring wall pressure. On that basis the courses were drawn which allow to define the value of amplitudes for the analyzed example.

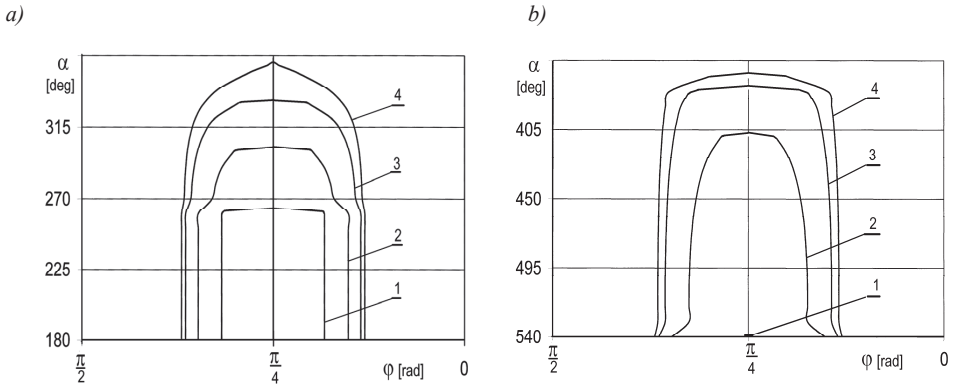

Fig. 6. Course of boundary lines of positive ring wall pressure for ring moving during stroke of compression (a) and expansion (b) for engine full load and selected values of cylinder deformation; A_4: 1 – 10 μm, 2 – 20 μm, 3 – 50 μm and 4 – 100 μm

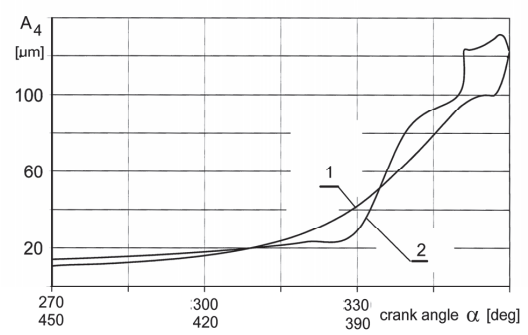

Fig. 7. Fourth harmonic amplitude value vs. crank angle for engine full load at: 1 – compression stroke, 2 –expansion stroke

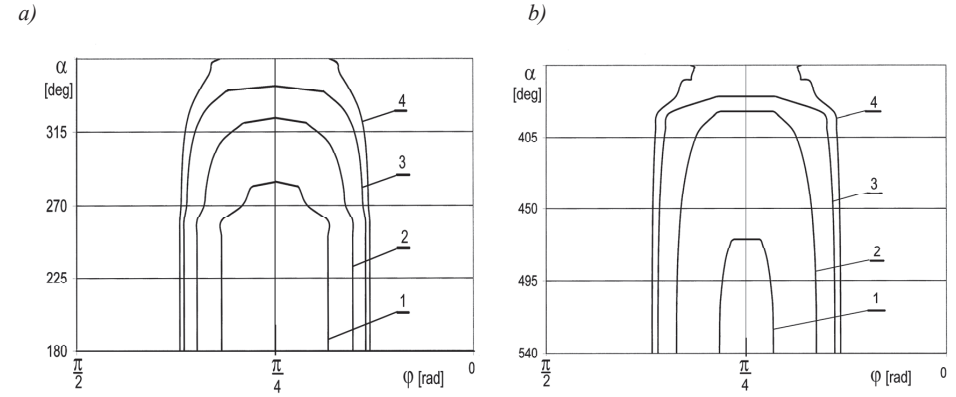

Fig. 8. Course of boundary lines of positive ring wall pressure for ring moving during stroke of compression (a) and expansion (b) for an engine partial load and selected values of cylinder deformation; A_4: 1 – 10 μm, 2 – 20 μm, 3 – 50 μm and 4 – 100 μm

Along with the decrease in engine load and reduction of gas forces the ring wall pressure also decreases which one can observe in the course of ring boundary pressure (Fig. 8). For example, for the amplitude of 100 μm and engine full load the ring touches the wall with its entire circumference close to the TDC. For the same amplitude of cylinder deformation and engine reduced load the light slot within a considerable angle of cylinder circumference emerges at the same area.

4. Summary and conclusions

Taking into consideration the results of theoretical studies and results of exemplary calculations following conclusions can be drawn:

- the ring wall pressure caused by gas forces exceeds several times the pressure from ring own elasticity at strokes of compression and expansion,
- the ring elastic pressure ensures the full wall contact only for minor deformations of cylinder wall (less than 10 μm for the analyzed example),
- for major deformation of cylinder wall ring pressure depends mainly on gas forces during strokes of compression and expansion close to the TDC in particular.

It is worth mentioning that the presented studies concern the case of no lubrication. When the presence of lubricating oil is taken into account, the minor slots are filled with oil and gas blow-by would not happen.

Another problem that should be the subject of eventual tests but was completely ignored in presented study is the analysis of stress in ring material during ring collaboration with deformed (worn) cylinder wall. Such tests should define the border values of cylinder deformations which would not lead to the ring failure.

References

[1] Abramek K., *Określenie wpływu nieszczelności przekroju tłok-pierścień-cylinder na wielkość strat ładunku.* Zeszyty Naukowe WSOWL , nr 4, 2010.

[2] Gruszka J., *Technologiczne kształtowanie cech funkcjonalnych warstwy powierzchniowej tulei cylindrowej*. Wydawnictwo PP, Poznań 2012.

[3] Kozaczewski W., *Konstrukcja grupy tłokowo-cylindrowej silników spalinowych*. WKŁ, Warszawa 2004.

[4] Mittler R., Mierbach A., Richardson D., *Understanding the Fundamentals of piston ring axial motion and twist and the effects on blow-by*. Proceedings of the Internal Combustion Engine Division ASME, ICES2009-76080.

[5] Serdecki W., *Badania współpracy elementów układu tłokowo-cylindrowego silnika spalinowego.* Wydawnictwo Politechniki Poznańskiej, Poznań 2002.

[6] Serdecki W., *Analysis of relations between the compression ring characteristic parameters*. Journal of POLISH CIMAC. Energetic aspects, Gdańsk 2011, Vol. 6, No. 2.

[7] Serdecki W., *Analysis of ring pressure distribution on a deformed cylinder face*. Journal of POLISH CIMAC. Energetic aspects, Gdańsk 2012, Vol. 7, No. 1.

[8] Serdecki W., Krzymień P., *An analysis of phenomena accompanying ring collaboration with worn cylinder surface.* W: Combustion Engines, No. 2/2013.

GDAŃSK UNIVERSITY OF TECHNOLOGY

Journal of POLISH CIMAC

Faculty of Ocean Engineering & Ship Technology
GDAŃSK UNIVERSITY OF TECHNOLOGY

EXPERIMENTAL STUDY OF THE DISJOINING PRESSURE IN THE CYLINDER OIL FILMS ON MARINE DIESEL ENGINE PISTON RINGS

Slobodianiuk D.I., Slobodianiuk I.M., Kolegaev M.A.

Odessa National Maritime Academy
8, Didrikhsona str., Odessa, 65029, Ukraine
tel.+380972484864
e-mail: Ioan2012@ukr.net

Abstract

The paper includes the results of the experimental study of the disjoining pressure in the thin oil films with anisotropic properties on the grey cast iron piston rings. It is shown that the disjoining pressure in the thin film, in a mode of self-regulation, can automatically balance the normal load between a pair "ring – cylinder liner". The received data is used to increase the reliability of marine diesel engines by preventing from sudden failures as the result of piston ring breakage.

Keywords: *isotherm, pressure, oil film, anisotropy, ellipsometry, cylinder-piston group, diesel*

1. Introduction

The organization of modern low speed diesel engines operating requires to improve the control of the friction processes of the mating parts of the cylinder-piston group (CPG) and to protect from the emergency situations. The breakage of forced piston rings of low speed diesel engines is the most common cause of functional failure. However, the cause of this phenomenon have not been studied properly yet.

According to the literary analysis modern ships monitor the condition and functions of the individual essential CPG parts, including piston rings [1,2,11]. But these systems are used in the case of high speed of piston movement at hydrodynamic lubrication with isotropic properties. The piston rings breakage, in particular, can occur during passing through scavenge ports as a result of lubrication breakdown [11]. Thus, there is a need to develop the methods of technical condition identification at low speeds, while the ring passes through scavenge ports, at that the lubrication regime is not hydrodynamic, and the film has anisotropic properties.

It is known that while the piston ring moves through the scavenge port of the cylinder liner the lubricant film drastically reduces, but the friction coefficient has a value $\mu = 0{,}12 \div 0{,}18$, that indicates the absence of dry friction [11]. There is the disjoining pressure in a thin boundary layer of cylinder oil, which increases rapidly as the film thickness reduces at low speeds of the piston ring, due to the structuring of lubricant molecules [4,7,8,9].

The theoretical research of a ring movement process through the scavenge ports, in a case when a film with anisotropic properties separates parts, is not possible without the experimental value of the disjoining pressure in this film [9].

Thus, the lack of the properties research of thin lubricant films with the anisotropic properties on cast iron surfaces, of which the ring as well as cylinder liner are manufactured of, is a

deterrent for the improvement of low speed diesel engine reliability by preventing from sudden rings breakage, therefore such studies are relevant.

The work objective is an experimental study of the disjoining pressure in thin oil films on the surface of the cast iron piston rings of low speed diesel vessels.

2. Study of the disjoining pressure isotherm in the cylinder oil films

This study was conducted using typical for the low speed diesel engine vessels cylinder oil ENERGOL CLO 50M, and the piston ring taken from the main engine MAN B & W 7S46MC-C.

The metallographic analysis showed that the ring consists of grey cast iron; the base has a ferritic-pearlitic structure. The hardness of the ring is HB2770. The surface was polished to a value R_a0,4÷0,6, which corresponds to the surface condition of the piston ring and edges of the cylinder liner in service.

The isotherms of disjoining pressure in a thin lubricant oil film on some steel surfaces, used in diesel engine manufacturing, was studied in the works [6.7]. The beginning of the film formation occurs at different thicknesses and pressures in the film. The film thickness and maximum disjoining pressure level depends on the chemical composition of the metal.

The disjoining pressure isotherms study was conducted on an experimental ellipsometrical plant [5], such scheme is presented below.

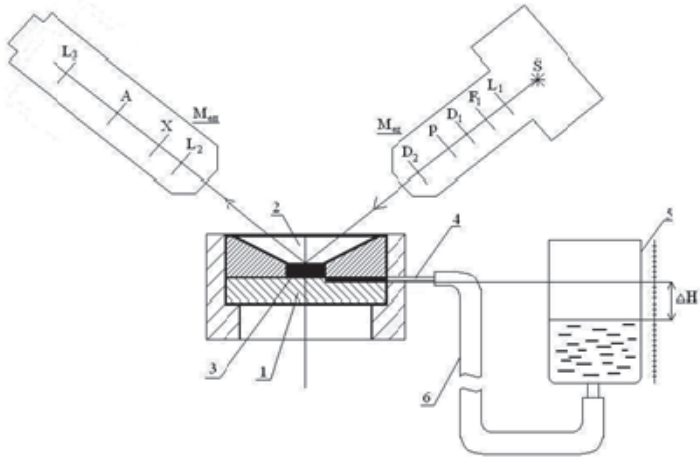

$M_{эм}$ - *ellipsometric microscope*

Fig 1. The installation scheme of the disjoining pressure isotherms study in thin oil films on metal surfaces. 1- cast iron sample;2- steel cone;3- oil film; 4-groove;5- pressure vessel;6- hose

The cell of the film was performed as follows: a steel cone with a hole of 1 mm diameter (2) was installed on the polished cast iron sample (1). The oil film (3) was formed in it and connected with the hose (6) to a pressure vessel (5), wherein there was the investigated cylinder oil.

On a Gibbs' theory there exist transition layers at boundary of any adjacent phase, whose properties differ from those of the bulk phase. In the case of interfacial layers overlapping the hydrostatic pressure in the thin layer is different from the pressure of the bulk phase the part of which is the film, ie, Pascal's law is not implemented in the thin film[10,11] . The additional pressure providing the thermodynamic equilibrium of the film was called the disjoining pressure. It can be both positive and negative. The dependence of $\Pi_{(h)}$ – the isotherm of disjoining pressure is the thermodynamic characteristic of the thin film of liquid.

To measure the disjoining pressure it is necessary to provide the mechanical equilibrium of the wetting film, by means of the external pressure. If the system is in thermodynamic

equilibrium, and the disjoining pressure is positive, then its value will be the low (negative) pressure produced in the conjugate bulk phase, by lowering the pressure vessel. Conversely, if the disjoining pressure is negative, its value will be excessive hydrostatic pressure. In both cases, the disjoining pressure $\Pi_{(h)}$ will be equal to the difference between the pressure P_1 on the film surface and the pressure P_0 in the bulk phase [4,5,10].

$$P = \rho g\,(H_0 - H_1), \tag{1}$$

where:
ρ -oil density,
H_0 - initial altitude of vessel lowering,
H_1 - final altitude of vessel lowering,
g- acceleration of gravity.

H_0 and H_1 values were determined using a micrometer device respectively, with accuracy $\Delta H = \pm 0{,}1$ mm, that caused the disjoining pressure error $\Delta P = \pm$ I Πa.

The experimental time to determine the equilibrium thickness for the wetting oil films with an opening of 1 mm diameter was 30 ÷ 40 minutes.

The position of the zero level H_0 in the pressure vessel, corresponding to the time of film formation from the bulk phase, was determined according to the interference lines condition. It was set for the point at which the movement of convergence and divergence of the interference pattern was stopped.

The film thickness h was measured using the ellipsometric microscope – $M_{эл}$. The methods of the ellipsometric thickness measurement of wetting nonpolar oil films on conductive metal surfaces was developed by the authors and described in detail in the work [7]. The ellipse of the reflected light polarization is described by the ellipsometric angles Ψ and Δ, where tg Ψ - is equal to the relative amplitudes change p- и S - a component, and Δ - the relative phase difference between them. The azimuth of analyzer A_0', A_0'' and polarizer P_0', P_0'' of light extinction were determined during the experiment.

The thickness of layer was calculated using Drude equation [4], which connected the experimental parameters Ψ and Δ and the optical characteristics of the reflected sample, defined with generalized Frenel coefficients R_p и R_s

$$tg\psi \cdot e^{i\Delta} = \frac{R_p}{R_s}\,, \tag{2}$$

where:
tg Ψ - relative amplitudes change,
Δ - phase shift between the P and S components that arises during reflection,
R_p, R_s - Fresnel generalized coefficients for the reflected light.

The equitation (2) has the following form for the presented case of a homogeneous isotropic layer [4]:

$$tg\psi \cdot e^{i\Delta} = \frac{R_{12p} + R_{23p}e^{-2i\delta}}{1 + R_{12p}R_{23p}e^{-2i\delta}} \cdot \frac{1 + R_{12s}R_{23s}e^{-2i\delta}}{R_{12s} + R_{23s}e^{-2i\delta}}\,, \tag{3}$$

Here $\delta = \frac{2\pi}{\lambda_0} n_2 d \sin\varphi_2$, where d is the required layer thickness, and R_{12p}, R_{12s}, R_{23p}, R_{23s} are defined accordingly:

$$R_{12p} = \frac{n_2 \cos\varphi_1 - \cos\varphi_2}{n_2 \cos\varphi_1 + \cos\varphi_2} \quad R_{23p} = \frac{n_3 \cos\varphi_2 - n_2 \cos\varphi_3}{n_3 \cos\varphi_2 + n_2 \cos\varphi_3}$$
$$R_{12s} = \frac{\cos\varphi_1 - n_2 \cos\varphi_2}{\cos\varphi_1 + n_2 \cos\varphi_2} \quad R_{23s} = \frac{n_2 \cos\varphi_2 - n_3 \cos\varphi_3}{n_2 \cos\varphi_2 + n_3 \cos\varphi_3}, \tag{4}$$

The task is complicated by the need to take into account the effects of the electromagnetic waves weakening in the metal substrate. In general case, the equation (3) is formulated for the inhomogeneous wave and can be solved by the introduction of complex refractive index, taking into account the damping effects. In the presented case $n_3 \Rightarrow N_3 = n_3 - i\kappa_3$ and n, k- are the coefficients of substrate refraction and absorption. The following values n = 3,9, k = 6.96. are for cast iron.

Thus, the equation (3) with (4), is a complex expression, and hence, the simultaneous equations is required to be solved to find the layer thickness:

$$Re\left(tg\psi \cdot e^{i\Delta} - \frac{\left(R_{12p} + R_{23p}e^{-2i\delta}\right)\left(1 + R_{12s}R_{23s}e^{-2i\delta}\right)}{\left(1 + R_{12p}R_{23p}e^{-2i\delta}\right)\left(R_{12s} + R_{23s}e^{-2i\delta}\right)} \right) = 0$$
$$Im\left(tg\psi \cdot e^{i\Delta} - \frac{\left(R_{12p} + R_{23p}e^{-2i\delta}\right)\left(1 + R_{12s}R_{23s}e^{-2i\delta}\right)}{\left(1 + R_{12p}R_{23p}e^{-2i\delta}\right)\left(R_{12s} + R_{23s}e^{-2i\delta}\right)} \right) = 0 \tag{5}$$

The experimental isotherm of disjoining pressure of the oil film on the cast iron surface with roughness (R_a0,4), obtained at a temperature of 295 º K is shown in Fig. 2. The isotherm is close to an exponential form that corresponds to the works [6].

$$P = \frac{A}{h^3}, \tag{6}$$

A - Hamaker constant

The isotherms in the oil films on cast iron corresponds to the area of positive values of the disjoining pressure Πs > 0. They are of the decreasing nature. From this it follows that the disjoining pressure in the thin films, in the mode of self-regulation, can automatically balance the normal load, between the pair "ring – cylinder sleeve". Each new value of pressure has new equilibrium thickness of the film.

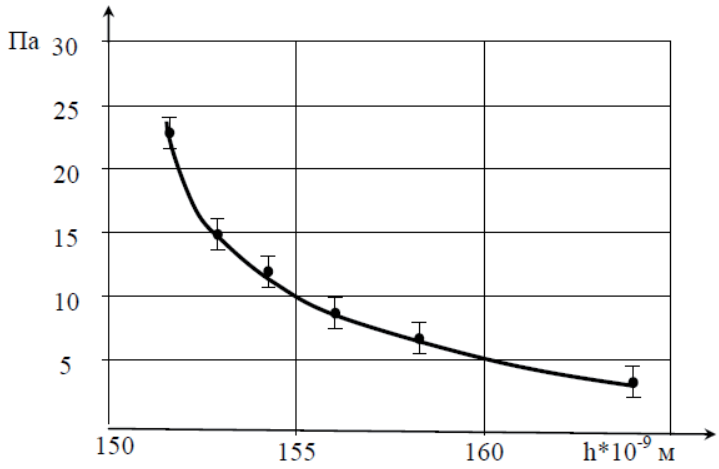

Fig. 2. The disjoining pressure change in a thin film of lubricant ENERGOL ClO 50M on the cast iron piston ring, depending on the film thickness

The maximum value of the disjoining pressure was determined from the graph constructed in the semi-logarithmic coordinates of dependence lnP (h) on the film thickness h. The maximum value of the disjoining pressures for the cast iron is equal to $\Pi_{(h)}$=140000Па .

The distinctive feature of the oil films with anisotropic properties on cast iron is the small amount of change in the film thickness from the beginning of its formation to the minimum at which the pressure in the film begins to increase sharply. For the films on the cast iron the thickness is 10 ÷ 12 nm. In comparison with the thickness of the films on steels (Fig. 3) [6,7] we can see that on steel 35 XMA,of which the piston heads and MAN B & W were manufactured, it is equal to 126 nm, which is an order of magnitude greater than that of cast iron.

The value of the disjoining pressure is the sum of the molecular component $\Pi m_{(h)}$, at low film thicknesses and structural $\Pi s_{(h)}$:

$$\Pi_{(h)} = \Pi m_{(h)} + \Pi s_{(h)}.$$

According to the obtained results the chemical composition of the substrate has a significant effect of on the change in the degree of orientation molecules order as the film thickness changes, that determines the amount of the structural constituent of the disjoining pressure $\Pi s_{(h)}$. Obviously, that such a difference in the obtained values of $\Pi_{(h)}$ can be explained by the different contributions of the molecular component of the disjoining pressure, which is essential for small film thicknesses. Previously, the effect of the molecular components on the disjoining pressure value was defined for polar liquid film on dielectrics [3,5].

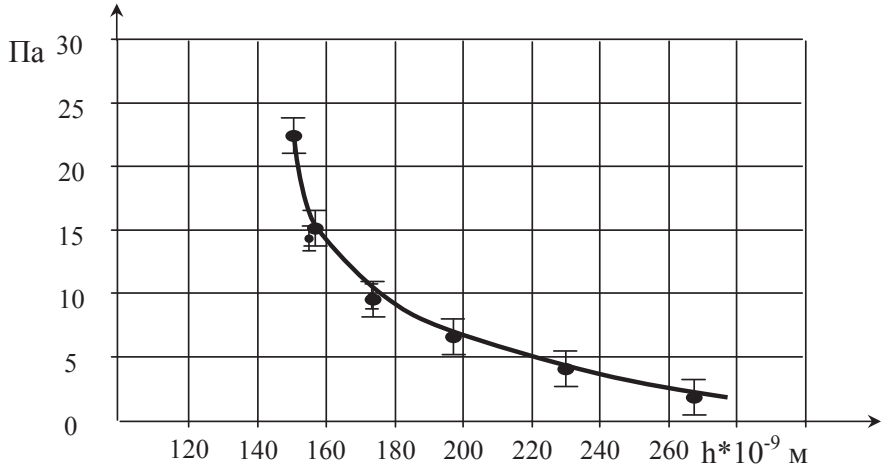

Fig.3. The dependence of the disjoining pressure in the oil film ENEKOL GLO 50M on its thickness on steel SH15

The analysis of the received values of disjoining pressure shows that the use of $\Pi s_{(h)}$ as the exponent is not always correct, and the real dependence of structural constituent on the film thickness is more complicated.

The analysis of the photomicrographs of the thin oil film on the surface of iron shows that the film is not flat by its nature. (Fig. 4)

The distribution of the interference lines demonstrates the formation of the film with the anisotropic properties in the center of the cell and the increase of the film area as it is growing thinner (Fig 4.b, c, d, e). An interference pattern is formed by the graphite inclusions (Fig.4f).

The control of lubricating film with anisotropic properties, determined by the disjoining pressure, make it possible to compensate the normal load on friction zone, therefore energy loss and the amount of conjugated surfaces deterioration can be reduced.

The obtained results enable to improve the identification methods of piston ring working capacity according to the lubricant state in order to prevent an emergency on board.

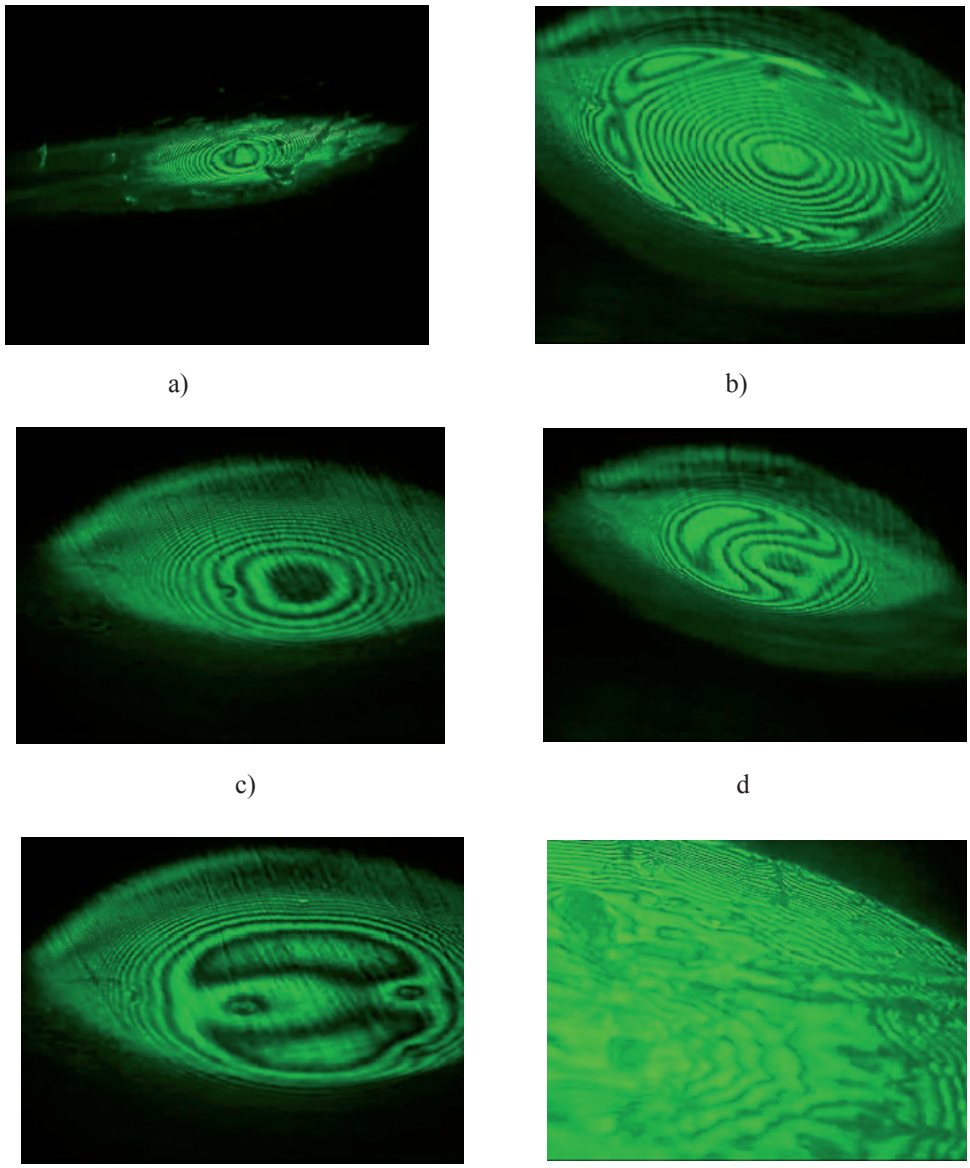

a) b)

c) d

e) f)

Fig. 4.The photomicrographs of the oil film on cast iron: formation (a), the minimum film thickness (f)

Conclusions

1. For the first time the isotherm of the disjoining pressure in the cylinder oil films on cast iron was experimentally obtained. It corresponds to the positive pressure region Π_s. There is force in a thin cylinder oil film directed to the opposite side of the ring pressure on the port of cylinder liner.
2. It is determined that the isotherm of disjoining pressure in the cylinder oil films on iron and steel surfaces are of the decreasing nature. It ensures the process of self-regulation of piston rings pressure on the cylinder liner. Each new pressure value has a

new equilibrium thickness. The process of self-regulation is automatic and it does not require the human intervention.

3. The comparison of the experimental isotherm of the disjoining pressure in the oil film on steel and iron surfaces have the following results:

- the film formation on steel and cast iron occur at different film pressure and thickness. The film formation on steel occurs at interval of 240 ÷ 280 nm, and with a much smaller thickness of 163 ÷ 165 nm on grey cast iron;
- the film thickness from the beginning of its formation and before the sharp pressure increase is 130 nm for steel. It is higher than on cast iron, that is only 10 ÷ 12 nm;
- the minimum film thickness on the iron surface where the disjoining pressure has a maximum value is in the range of 155-160 nm;
- the maximum disjoining pressure in the cylinder oil film was determined. It is equal to Π_s=0,14 МПа;

The further development of the piston rings movement process study, in the presence of thin oil films with the anisotropic properties, using the obtained data of the disjoining pressure on cast iron, will enable to improve the reliability of marine low speed diesel engines. Identification methods of piston rings technical condition and prevention from the sudden failures in the result of the piston rings damage will be developed.

References

[1] Hellingman, G.J. and Barrow, S., *"Shipboard investigations with Selected Fuels of Tomorrow*", Helsinki CIMAC 1981.

[2] Neate R.J. and Barrow S., *"SIPWA-A Shipowner's Point of View",* New Sulzer Diesel Ltd, December 1990.

[3] Горюк А.А., *Исследование структурной составляющей расклинивающего давления в смачивающих пленках нитробензола*. Дисс. канд. физ. мат наук, Одесса 1988.

[4] Дерягин Б.В., Чураев Н.В. *К вопросу об определении понятия расклинивающего давления* //Коллоид. Журн –Т.38.–№3.–С.438-448.Москва 1976.

[5] Дерягин Б.В., Чураев Н.В. *Смачивающие пленки* М.: Наука, –с. 157., Москва 1984.

[6] Дерягин Б.В., Поповский Ю.М. *Жидкокристаллическое состояние граничных слоев некоторых полярных жидкостей* //Коллоид.журн.–Т. 44. –№5.–С.863-870.,Москва1982.

[7] Слободянюк Д.И. *Совершенствование методики идентификации состояния поршневых колец МОД на основе экспериментального исследования частоты акустического сигнала*. Проблеми техніки –№3.–С. 68-75., Одесса 2012.

[8] Слободянюк Д. И., Ханмамедов С. А. *Экспериментальные изотермы расклинивающего давления в пленках цилиндрового масла и их применение для повышения надежности судового дизеля.* //Науково–виробничий журнал Проблеми техніки №2.2011.–С. 136–148., Одесса 2011.

[9] Слободянюк Д. И., Ханмамедов С.А., Шакун К.С. *Расчет частоты импульсов акустического сигнала от сопряжения «кольцо-втулка» ЦПГ МОД с учетом расклинивающего давления в тонких пленках смазки.*// Судовые энергетические установки: сб. науч. тр.– № 29. – ОНМА. – С. 58-67., Одесса 2011.

[10] Ханмамедов С.А., Слободянюк Д.И., Горюк А.А., Шакун К.С. *Изотермы расклинивающего давления в структурированной пленке цилиндрового масла* судового *дизеля.* //Науково–виробничий журнал Проблеми техніки –№1. –С: 90-102., Одеса 2011.

[11] Ханмамедов С.А.*Совершенствование функциональных свойств систем смазывания судовых энергетических установок.* Дисс. докт. техн. наук,– Николаев 1990.

GDAŃSK UNIVERSITY OF TECHNOLOGY

Journal of POLISH CIMAC

Faculty of Ocean Engineering & Ship Technology
GDAŃSK UNIVERSITY OF TECHNOLOGY

ANALYSIS OF THE EFFECT OF THE CHEMICAL COMPOSITION OF LOW CALORIFIC GASEOUS FUELS ON WORKLOAD CONCENTRATION IN AN ENGINE'S COMBUSTION CHAMBER

Sławomir WIERZBICKI

University of Warmia and Mazury in Olsztyn
ul. Słoneczna 46A, 10-710 Olsztyn, Poland
tel. +48 89 5245222, fax. +48 89 5245150
e-mail: slawekw@uwm.edu.pl

Abstract

Low calorific gaseous fuels are becoming increasingly used as alternative fuels for feeding power equipment of all kinds, including combustion engines. The increased interest in these fuels results, above all, from support for the development of this type of power engineering by governmental and international institutions, aiming to increase the renewable energy share in the overall energy balance. Fuels of this type are obtained by processing different kinds of biomass and natural raw materials and can also be recovered from natural processes occurring in nature. Due to the diverse technologies for obtaining these fuels, their chemical composition is variable, which significantly affects the efficiency of their use as fuels for combustion engines. When engines are fed with gaseous fuels, combustion chamber filling conditions change considerably due to the much higher gaseous fuel volume compared to liquid fuels, which significantly affects the engine's performance.

This paper presents the effect of individual combustible components contained in different low calorific gaseous fuels on changes in the degree of engine combustion chamber air filling and on the calorific value of the produced combustible air-gaseous fuel mixture.

Keywords: *environmental protection, low calorific gaseous fuels, calorific value, excess air coefficient, combustible mixture*

Introduction

Growing social awareness and concern for the environment and the increasingly stricter standards for reducing greenhouse gas and toxic compound atmospheric emission limits have prompted a search for new alternative energy sources [1, 6]. Another important factor causing an increased interest in renewable energy sources is the need to increase the share of energy produced from alternative energy sources as required by EU legislation. It is also worth stressing that the heightened interest in alternative fuels is favoured by shrinking resources of fossil fuels, particularly petroleum [4, 5, 6].

Low calorific gaseous fuels of different types are potential energy sources which can be obtained by processing different kinds of biological products and can also form spontaneously as a result of natural processes occurring, among others, in dumping sites, sewage treatment plants and animal farms [1, 4, 5].

The composition of such fuels is not constant and is closely dependent not only on the raw materials from which they are produced but also on the technology for their production and treatment. The combustible compounds making up fuels of this type include, above all, methane

(CH_4), carbon monoxide (CO) and hydrogen (H_2). The basic properties of the listed combustible components of gaseous fuels are presented in Table 1.

The percentage of individual components in gaseous fuels is not constant and, as has been mentioned, is conditioned by many factors. The main low calorific gaseous fuels most often used currently include [1, 2, 5, 7, 8, 9]:

- agricultural biogas – obtained by methane fermentation of plant raw materials or animal excrement;
- biogas from sewage treatment plants – gas recovered in sewage treatment plants in sewage and water treatment;
- landfill gases – forming by decomposition of organic substances contained in municipal waste after disposal;
- fossil gases – gases obtained in hard coal mine demethanization;
- synthesis gases (syngas) – obtained in gasification of solid fuels, petroleum refining residues, steam methane reforming or partial methane oxidation with oxygen.

Table 2 presents the percentages of individual combustible components in the most common low calorific gaseous fuels.

Table 1. Basic properties of combustible components of low calorific gaseous fuels

Gas	Calorific value [MJ/m^3]	Standard density [kg/m^3]	Air demand [m^3/m^3]	Self-ignition temperature [K]
Hydrogen (H_2)	10,78	0,0899	2,38	807
Carbon monoxide (CO)	12,6	1,25	2,38	881
Methane (CH_4)	35,89	0,717	9,54	923
Ethane (C_2H_6)	63,77	1,34	16,7	793
Propane (C_3H_8)	91,28	1,97	23,8	783
Butane (C_4H_{10})	122,6	2,33	31	692

Table 2. Volumetric content of individual components in gaseous fuels [2, 4, 6, 8]

Gaseous fuel	H_2 [%]	CO [%]	CH_4 [%]	CO_2 [%]	N_2 [%]	O_2 [%]
Agricultural biogas	-	-	45-75	25-55	0-5	0-3
Biogas from sewage treatment plants	-	-	57-62	33-38	3-8	0-1
Landfill gas	0-15	-	37-67	24-40	10-25	0-45
Mine gases	-	-	40-80	8-15	20-40	0-10
Synthesis gases	3-0-70	0-60	0-10	5-30	0-2	-

Because of the quite large differences possible in the chemical composition of such gaseous fuels, the combustion conditions for such fuel in the engine change significantly, which causes significant changes in the obtainable engine power, the amount of heat carried away by the engine's cooling system and heat carried away by exhaust gas.

Characteristic parameters of the fuel-air mixture

The power obtained from a combustion engine depends primarily on the calorific value and the amount of fuel burnt in the combustion chamber. The amount of burnable fuel is conditioned by the amount of oxygen available in the engine chamber, which is necessary for burning combustible components contained in the fuel. The vast majority of the oxygen supplied to the engine's combustion chamber comes from the air and only a small part of oxygen can be supplied with fuel (for oxygen-containing fuels).

Therefore, the power obtainable by the engine is limited by the amount of air (oxygen) induced into the combustion chamber needed for complete fuel combustion. For liquid fuels, the theoretical amount of induced oxygen results from its content in the air and the maximum combustion chamber volume. In this case, the volume of supplied liquid fuel is minute and can be ignored practically without error. In reality, the induced fresh air volume depends on the engine filling efficiency, which is most affected by the structure of ducts feeding fresh load to the combustion chamber, the efficiency of cleaning exhaust gas residues from the previous work cycle of the combustion chamber, engine speed as well as the temperature in the combustion chamber during the suction stroke. In real combustion engines, cylinder filling efficiency ranges from 0.7–0.85 and decreases with rising engine speed, due to shortening suction stroke length.

While for liquid fuels the volume of fuel fed to the combustion chamber can be ignored, for gaseous fuels, containing not only combustible compounds but also substantial percentages of non-combustible compounds such as carbon dioxide (CO_2) and nitrogen (N_2), the volume of fuel fed to the engine chamber is considerable (except for solutions with gas injection directly into the combustion chamber). Therefore, this significantly reduces the volume of air induced into the combustion chamber for fuel combustion which, in turn, changes the engine performance.

As mentioned before, low calorific gaseous fuels contain three basic combustible components: methane (CH_4), hydrogen (H_2) and carbon monoxide (CO). Assuming that the whole amount of fed fuel is burnt, the occurring combustion reactions for these compounds can be written as:

$$CH_4 + 2O_2 = CO_2 + 2H_2O \tag{1}$$

$$2H_2 + O_2 = 2H_2O \tag{2}$$

$$2CO + O_2 = 2CO_2 \tag{3}$$

Considering that 21% of oxygen is in the air by volume, it can be stated that the theoretical amount of air needed for the combustion of a fuel which is a mixture of these three gases is:

$$L_t = \frac{1}{0{,}21}\left[0{,}5\left(H_2 + CO\right) + 2CH_4\right] \text{ [m}^3\text{ air / m}^3\text{ gaseous fuel]} \tag{4}$$

For gaseous fuels containing oxygen, this amount of oxygen should be taken into account, therefore, the above formula assumes the form:

$$L_t = \frac{1}{0{,}21}\left[0{,}5\left(H_2 + CO\right) + 2CH_4 - O_2\right] \text{ [m}^3\text{ air / m}^3\text{ gaseous fuel]} \tag{5}$$

To determine the volume of air induced into the combustion chamber with the air-gas mixture, the degree of combustion chamber air filling γ_{air} can be defined. With the assumption that the cylinder filling efficiency is $\eta_v = 1$, the exhaust gas removal from the combustion chamber is complete and an air-gas mixture has formed outside the combustion chamber, this ratio can be written as:

$$\gamma_{air} = \frac{V_{air}}{V_{ch}} = \frac{V_{ch} - V_{fuel}}{V_{ch}} \tag{6}$$

where:
V_{air} – air volume in the air-gas mixture;
V_{ch} – combustion chamber volume;
V_{fuel} – gaseous fuel volume.

Effect of gaseous fuel composition on the degree of combustion chamber air filling and the calorific value of the mixture

The variable composition of gaseous fuels significantly affects both the degree of combustion chamber air filling and the calorific value of the produced combustible mixture. Fig. 1 presents changes in the degree of engine combustion chamber air filling for basic combustible components of gaseous fuels as a function of the excess air coefficient λ. The presented changes clearly show that for feeding with gaseous fuels the volume of induced air is much lower than when the engine is fed with liquid fuels. For a stoichiometric mixture (λ = 1), the volume of air induced into the combustion chamber is 10% lower for feeding with methane and 30% lower for feeding with hydrogen or carbon monoxide. Fig. 2 presents changes in the calorific value of the combustible mixture produced from individual gaseous fuel components depending on λ. For comparison, this figure also contains changes in the calorific value of propane (C_3H_8) and butane (C_4H_{10}), the main LPG components.

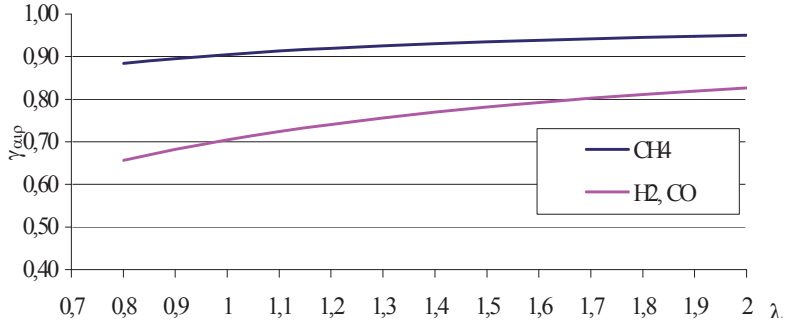

Fig. 1. Degree of combustion chamber air filling for feeding with CH_4, H_2 and CO as a function of λ

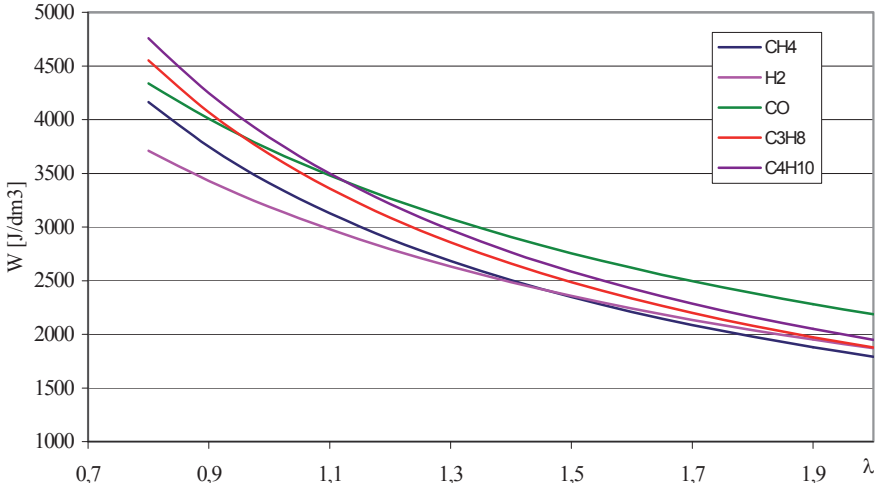

Fig. 2. Change in the calorific value of the air-gas mixture depending on λ for different gaseous fuel components

Fig. 3 presents changes in the degree of combustion chamber air filling γ_{air} and changes in the

calorific value of the air-gaseous fuel mixture containing only biogas (e.g. methane) depending on the percentage of CH_4 in fuel with the excess air coefficient $\lambda = 1$. It can be concluded based on changes in combustion chamber air filling that a rise in the percentage of methane in fuel significantly affects the use of the combustion chamber. For fuels with a ca. 40% methane content the degree of engine combustion chamber volume use is only 65%.

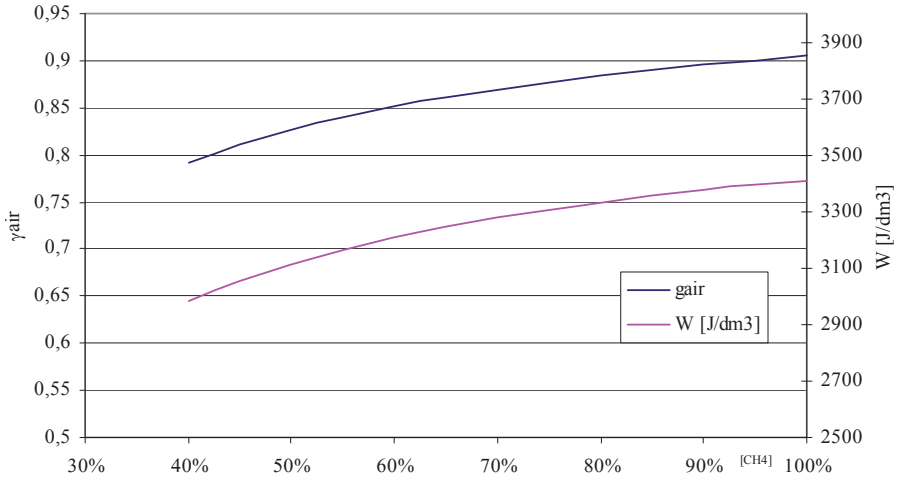

Fig. 3. Change in the degree of combustion chamber air filling and the calorific value of the air-gaseous fuel mixture for fuels with different methane percentages for $\lambda = 1$

Fig. 4 presents changes in the degree of combustion chamber air filling γ_{air} with $\lambda = 1$ for gaseous fuels containing two combustible components, e.g. landfill gases. Fig. 5 presents changes in the calorific value of the air-landfill gas combustible mixture for different concentrations of individual combustible components depending on the excess air coefficient λ.

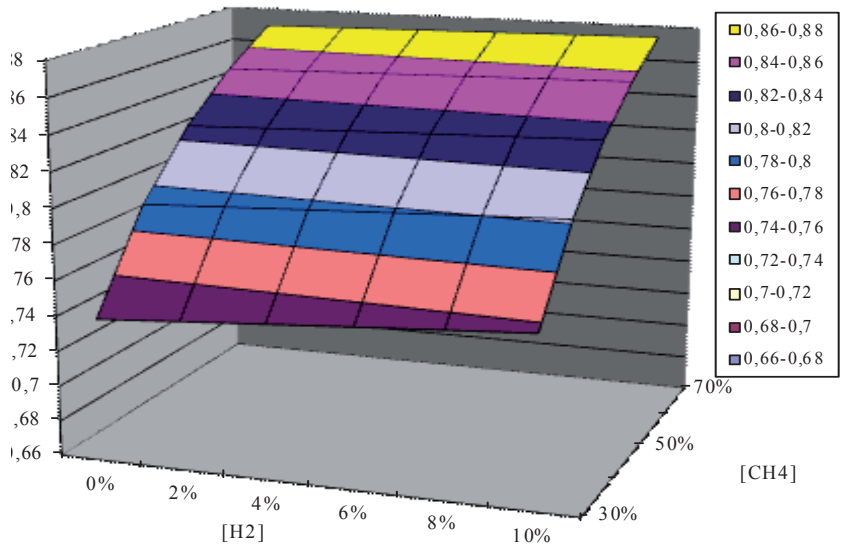

Fig. 4. Change in the degree of combustion chamber air filling for the air-combustible gas mixture with different CH_4 and H_2 percentages for $\lambda = 1$

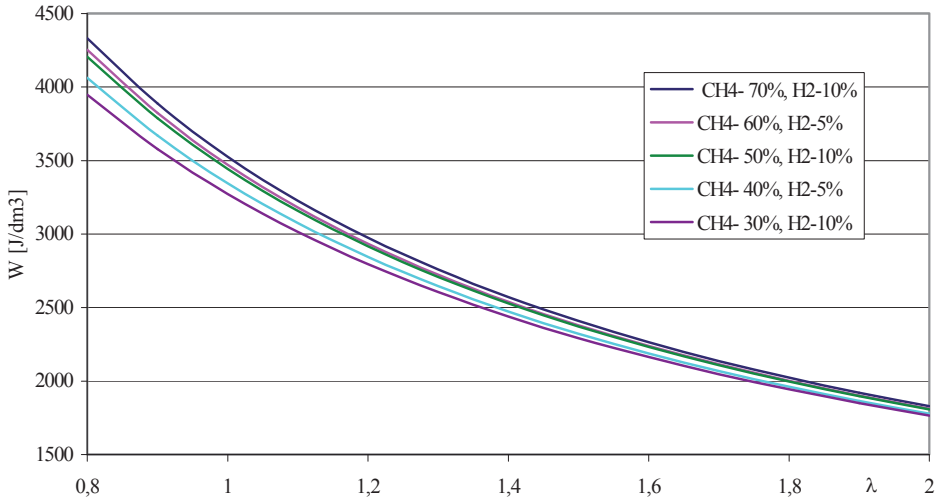

Fig. 5. Change in the calorific value of the air-landfill gas mixture depending on λ for different percentages of combustible components

For the combustion of synthesis gases, obtained by gasification of biomaterials (e.g. biomass, wood), coal gasification or steam methane reforming, oxygen contained in this fuel should also be taken into account. In fuels of this type, the oxygen volume fraction can reach even 20%, which significantly changes fuel combustion conditions. Fig. 6 presents changes in the combustion chamber air filling ratio for selected synthesis gases [3] and Fig. 7 presents changes in the calorific value of the air-synthesis gas mixture depending on the pure oxygen content in this fuel for $\lambda = 1$. The presented changes show that oxygen contained in fuel considerably increases the value of heat obtainable from the combustion of a specific portion of the produced air-gaseous fuel mixture.

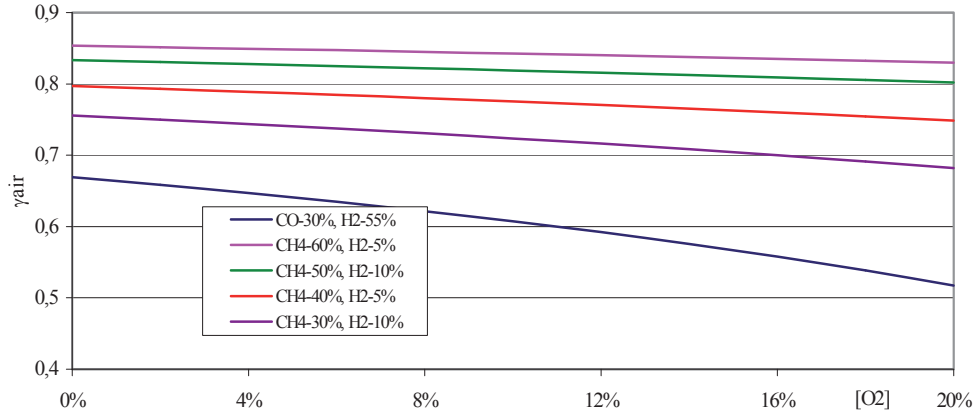

Fig. 6. Effect of the oxygen content in the synthesis gas on the value of the combustion chamber air filling ratio maintaining λ = 1

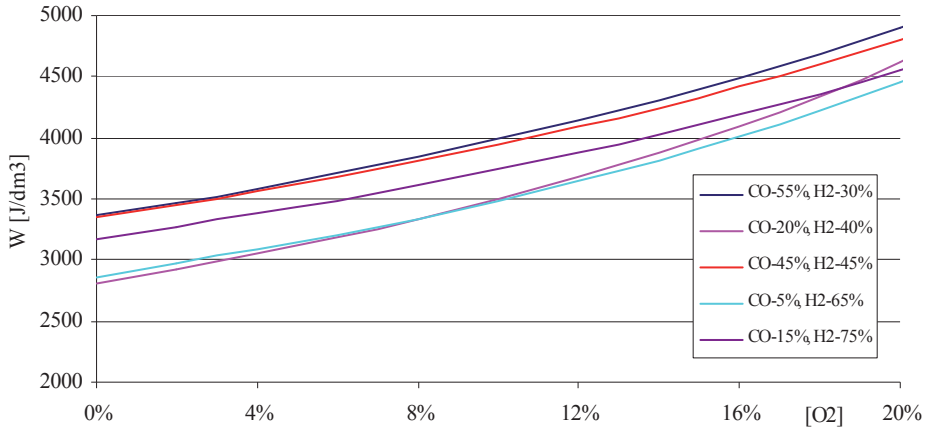

Fig. 7. Effect of the oxygen content in the synthesis gas on the calorific value of the combustible mixture for λ = 1

Conclusions

In summarizing the results on the effect of the composition of low calorific gaseous fuels on combustion chamber air filling and the calorific value of the obtained air-gaseous fuel mixture with the combustible mixture formed outside the combustion chamber, it must be concluded that:

- feeding the engine with gaseous fuels significantly reduces combustion chamber fresh air filling, which limits the burnable amount of fuel. When the engine is fed with pure methane with λ = 1, the combustion chamber volume fillable by air decreases by around 10%. When the engine is fed with pure carbon monoxide or methane, the volume of induced air under the same conditions decreases by 30%. This reduces the amount of burnable fuel, which limits the amount of heat released in the combustion chamber;
- when the engine is fed with low calorific fuels containing ballast compounds besides combustible components, the amount of heat obtainable in the combustion chamber is still lower, which causes a further decrease not only in the obtainable engine power, but also causes increased losses of heat absorbed by gases not participating in the combustion reaction;
- for fuels containing oxygen, e.g. synthesis gases, the oxygen contained in fuel increases the calorific value of the formed combustible mixture along with an increasing oxygen percentage in the fuel;
- it should, however, be stressed that despite the above limitations, low calorific gaseous fuels positively affect the share of renewable fuels in the overall energy balance. It is also important to stress that the use of these fuels for energy purposes reduces the emission of methane released spontaneously from, among others, dumping sites, which is ca. 25 times more harmful to the ozone layer than carbon dioxide [3].

Acknowledgment

This paper was partially financed by research grant No N N509 573039, given by Polish Ministry of Science and Higher Education.

References

[1] Cebula J.: *Biogas purification by sorption techniques*. ACEE Journal, 2/2009.

[2] Dubiński J.: *Produkcja paliw ciekłych i gazowych z węgla - szanse i perspektywy*, Wiadomości Górnicze, 2007. Vol. 58, nr 5 str. 273-278

[3] Fahey D. W.: *Twenty questions and answers about the ozone layer*. United Nations Environment Programme. Ozone Secretariat, 2002, Q.12.

[4] Piskowska-Wasiak J.: *Uzdatnianie gazów pochodzenia biologicznego w celu wytwarzania biopaliw i biokomponentów*. Nafta – Gaz. 2013, R. 69, nr 3 241-255.

[5] Piętak A.: *Paliwa dla silników spalinowych*. Czysta Energia, 2011, nr 3, str. 21-24.

[6] Skorek J., Kalina J.: *Gazowe układy kogeneracyjne*. WNT, Warszawa, 2005.

[7] Usidus J., Kryłowicz A. Chrzanowski K.: *Budowa elektrowni, elektrogazowni i gazowni biometanowych w skali przemysłowej*. Spektrum. 2010, nr 9-10.

[8] Wandrasz J. W., Wandrasz A. J.: *Paliwa formowane. Biopaliwa i paliwa z odpadów w procesach termicznych*. Wydawnictwo Seidel-Przywecki, 2006.

[9] Żyła M., Kreiner K.: *Wykorzystanie energii ze złóż naturalnych paliw węglowych*. Gospodarka Surowcami Mineralnymi. 2007, t. 23, z. 3, str. 257-264.

GDAŃSK UNIVERSITY OF TECHNOLOGY

Journal of POLISH CIMAC

Faculty of Ocean Engineering & Ship Technology
GDAŃSK UNIVERSITY OF TECHNOLOGY

RESEARCH ON ENERGETIC PROCESSES IN A MARINE DIESEL ENGINE DRIVING A SYNCHRONOUS GENERATOR FOR DIAGNOSTIC PURPOSES PART 1 – PHYSICAL MODEL OF THE PROCESSES

Aleksy Cwalina

Gdańsk University of Technology
Ul. Narutowicza 11/12, 80-950 Gdańsk, Poland
e-mail: A.Cwalina@amw.gdynia.pl

Marcin Zacharewicz

Polish Naval Academy
Ul. Śmidowicza 69, 81-103 Gdynia, Poland
Tel.: +48 626 23 82
e-mail: M.Zacharewicz@amw.gdynia.pl

Abstract

In the paper a physical model of certain processes taking place when marine diesel engine is driving a synchronous generator is presented. This physical model will be a basis for a mathematical model realization in a form of equations describing the relationships between the designated parameters of the diesel engine and the generator. The method of theoretical and operational investigations which enables identification of the technical condition of the set is presented. Systematic collecting the results in the database will allow to refine the model, and to conclude about the technical condition of real objects.

Keywords: *diagnostic, marine diesel generator*

NOMENCLATURE

PARAMETERS

F	- force
I	- current
J	- mass polar moment of inertia
i	- enthalpy
M	- torque
m	- mass
$\dot{m}$	- mass flow rate
p	- pressure
R	- gas constant
$\dot{Q}$	- heat flux
S	- area

T	- temperature
U	- voltage
w	- linear velocity
V	- volume
ε	- generalized losses
κ	- isentropic exponent
ω	- angular velocity

ABBREVIATIONS AND INDEXES

cyl.	- cylinder
g	- gas
K	- connecting rod
L	- phase
oK	- connecting rod response
oMP	- engines machinery response
oP	- generator response
oWK	- crankshaft response
p	- back pressure
P	- generator
pk	- exhaust gases in the manifold
sp	- exhaust gases in the outlet channel
t	- piston
wk	- crankshaft
*	- total value of parameter
1,2,3…n	- subsequent cylinder, phase, etc.

1. INTRODUCTION

One of the maintain problems of the generating set consisting of the marine diesel engine and the synchronous generator is to determine their technical condition. The generators on the ship are frequently driven by a combustion engines that are not equipped with indicator valves. Such engines with limited monitoring susceptibility, are operated according to so-called overhaul life strategy. The current trend is to implement economically advantageous operating strategy according to the technical condition of the ship's mechanisms and appliances. Such attempts have also been made with respect to diesel-electric generating sets. Technical condition of selected elements of the structure design based on endoscopic examination [4] and vibration testing was evaluated. An alternative method currently developed by the authors of the paper is to determine the technical state of the ship generating set by means of testing pressure pulsations in the exhaust gas channels, phase-to-phase generator voltages, and vibrations of selected parts of the engine and the driven generator [2, 3].

2. PLAN AND METHODOLGY OF RESEARCH

The first stage of research directed on developing methods for evaluation technical condition of the generating set of the ship power station was to develop a research plan. Similar plans were worked out in previous works by the authors, for example [2, 3, 5, 8] in the form of block diagram presenting successive stages of the investigation. The diagram

shows the interactions between particular stages of work. In general, the starting point for the development of the plan is a real object, in this case a diesel- electric generating set consisting of a combustion engine type SW 400 and synchronous generator GCPf-94c/1. Basic technical data of the investigated engine are shown in Table 1.

Table 1. Technical characteristic of diesel engine type SW 400 [9]

Rated output	54,06 kW	Injection type	Direct
Rated crankshaft Speed	1500 rpm	Injection order	1-5-3-6-2-4
Number of cylinders	6	Injection pressure	16,18 – 16,67 MPa
Piston stroke	120,65 mm	Specific fuel consumption	190 g/kWh
Cylinder bore	107,19 mm	Intake valve opening commencement	10^0 before the TDC

General view and schematic diagram of the generating set is shown in Figure 1.

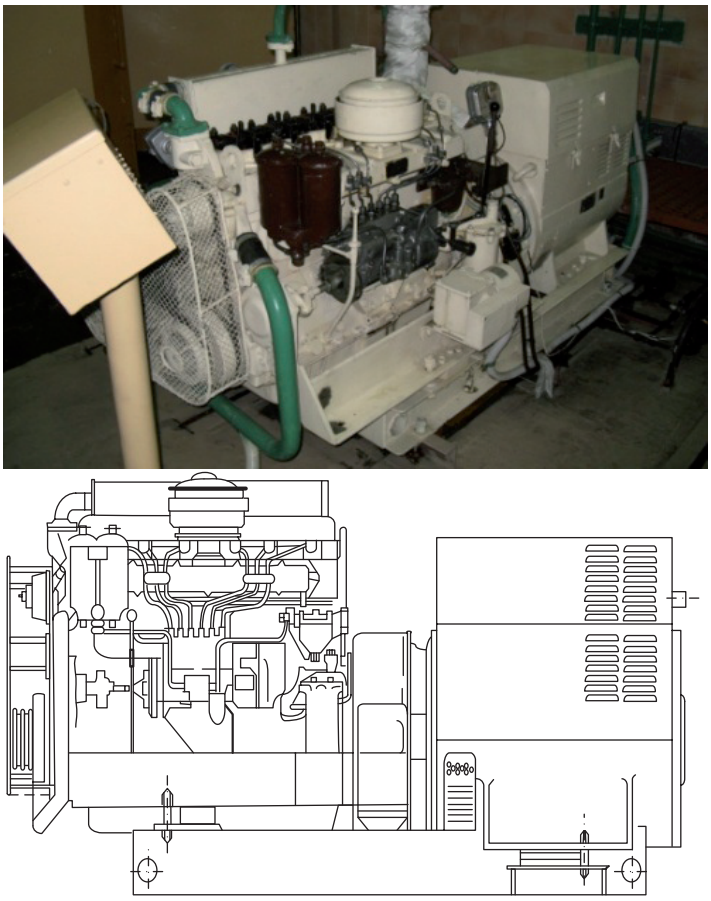

Fig.1. General view and schematic diagram of the diesel-electric generating set being the object of the research

In the proposed research plan the real object is a base for developing a physical model of the selected processes occurring in diesel-electric generating set. In this physical model the possibility to simulate damages to the combustion engine and synchronous generator by means of changing values of selected structural parameters was taken into account [6]. The physical model is a base for preparing a mathematical model in a form of set of equations describing the interdependence between selected mechanical, electrical, and gas dynamical parameters.

The equations of the mathematical model recorded as a computer programme will allow for conducting the model studies of the effects of simulated damage on the waveforms of the generating set analyzed energetic parameters. At the same time we are going to conduct the research on the real object, generating set. There will be introduced the same known and recognizable damage to the model and the real object. The results obtained from simulation studies and research conducted on the real object will be compared in the time domain and frequency domain. Following the results of the comparative analysis the adequacy of the physical model and based on it the mathematical model will be evaluated. If the simulation results will differ to a greater extent than assumed by the results of a real object, the physical model will be modified to increase its relevance. The results of all studies, both the model and simulation will be collected in a database technical condition – symptom. Creation of such a comprehensive database will help in the future to identify the technical state of the generating set and the proper diagnosis. The proposed flow chart of the investigation is shown in Figure 2 [1].

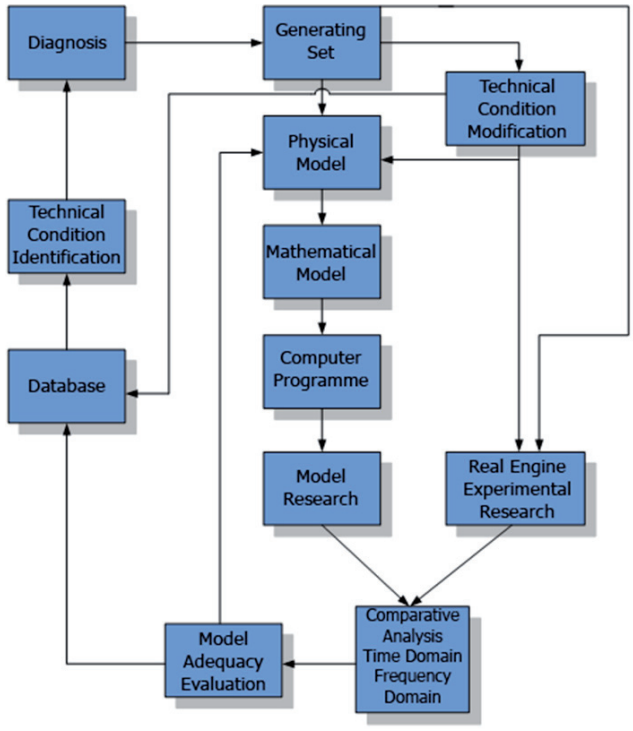

Fig.2. Diagram of realization the diagnostics research

3. A PHYSICAL MODEL

The proposed physical model is a certain conception of theoretical representation of phenomena and processes which occur in considered real object – generating set. This model includes a set of assumptions that define a simplified image of the investigated object, and takes into account whole physical quantitative and qualitative relationships. The degree of model simplification results from both objective and subjective factors. The objective factors include the state of the art – the possibility to identify all the phenomena and processes, and competency to describe them by means of appropriate relationships. The subjective factors are the needs and technical conditions for the model analysis of the given object (generating set). In general, only selected stages of considered processes are modeled, with far-reaching simplification [6].

In this model, the physical input parameters are:

- gas pressure in engine cylinders $p_{cyl} = f(\alpha)$,
- cylinder volume $v_{cyl} = f(\alpha)$,
- gas parameters inside cylinders, such as gas constant $R_{cyl} = f(\alpha)$ and isentropic exponent $\kappa_{cyl} = f(\alpha)$,
- engine load expressed by generator voltage and current $U, I = f(\alpha)$.

All these parameters are a function of the engine crank angle α. The next group of input parameters are the design parameters of the structure of the generating set (diesel engine, synchronous generator, coupling). The main of them are the piston diameter, connecting rod length, and crank arm length. Another group of parameters are connecting rod, piston, piston pin masses distribution, rotating elements moments of inertia (engine crankshaft, clutch, rotor of the generator, driven mechanisms etc.).

Output parameters are:

- exhaust gas pressure in the outlet channel $p_{pk}^{*} = f(x, \tau)$,
- exhaust gas temperature in the outlet channel $T_{pk}^{*} = f(x, \tau)$,
- speed of movement of peak amplitude exhaust gas pressure wave $w_{pk} = f(x, \tau)$.

All these exhaust gas parameters in the outlet channel are a function of time and the channel length (coordinate cross-section in which they are measured). The last group of the output parameters are those measured on the synchronous generator driven by the diesel engine. In the presented model instant values of phase-to-phase voltages as time functions are taken into account. The proposed physical model is shown in Figure 3.

In this model the engine cylinder were treated as zero-dimensional objects i.e. independent variable for them is only time of the process. Engine cylinders are able to store a mass of thermodynamic medium marked as m_{cyl}. The input parameters relating to the engine cylinders are pressures inside cylinders, cylinder volumes and parameters of working medium inside cylinders such as individual gas constant and isentropic exponent. In the model of the engine cylinder section mass of the piston with connecting rod was taken into account, and marked as m_T, and considered as carrying out reciprocating motion only.

Engine cylinders output thermodynamic parameters being the input parameters for the exhaust channel are pressure p_{cyl}^{*}, and temperature T_{cyl}^{*} of the exhaust gases, their mass flux

$\dot{m}_{cyl}$, enthalpy flux i^*_{cyl}, and speed of moving working medium w_{cyl}. Additionally, the model takes into account influence of the gas pressure from the outlet channel on cylinder sections p^*_p. Exhaust gas output channel is modeled as a one-dimensional object, which means that the independent variables are time and channel length determining the position of control cross-sections in which exhaust gas measurements are taken. The physical model takes into account dynamics of elements reciprocating and those in rotating motion. For this purpose weight distribution of selected structural elements of the engine and generator were taken into consideration.

This refers mainly to the piston with piston pin and rings involved in reciprocating motion, connecting rod that moves in a mixed way – its one part is reciprocating and the other is rotating, and engine crankshaft with a flywheel that rotate together with the rotor of the generator. The complicated character of movement of the connecting rod can be examined as a sum of a motion of reciprocating mass and a motion of rotating mass, calculated by means of the "weighing system" [7]. In the model gas forces acting on the piston F_g and connecting rod forces F_{oK} were considered as well as moments of inertia of the piston-crank mechanism J_K. Engine crankshaft is another element of the model. Turning moment acting upon the crankshaft, originating from gas forces, is a product of these forces and the length of the crankshaft crank M_{WK}. In a similar way as in the case of the piston-connecting rod set, in the assembly connecting rod-crankshaft the moment M_{oWK} from the crankshaft acting on the connecting rod was taken into account . It is assumed in the model that all the masses and moments of inertia of mechanisms driven by the engine are treated globally.
Torque derived from the crankshaft is transmitted to the generator rotor M_{WK}. The generator influence on the engine is the load torque M_{oP}. It was assumed in the model of the generator that the only rotating mass is the mass of the rotor m_p. The synchronous generator unit produces three-phase alternating voltage with a frequency of 50Hz which meets double frequency of rotating speed of the engine crankshaft. Electric load of the generator brings about passage of current I_L at the assumption that phase-to-phase voltage is U_L. As the generator load is resistive, power can be calculated as the product of voltage and current because power factor is equal to 1. Consumption of power produced by the synchronous generator is the source of the diesel engine load torque M_{oP}.

There are feedback loops in the model because increasing of the generator load results in decreasing of electric voltages in phases L_1, L_2 and L_3 what in turn increases generator excitation current. This process is controlled by AVG (Automatic Voltage Regulator) which senses the generator output voltage and acts to alter the field current to maintain the voltage at its set value V_1, V_2, and V_3. As a result of such a regulation the generator voltage increases or decreases to ±2,5% (or better), so changing the angular speed of the diesel crankshaft ω. The angular speed is an input signal to the speed governor of the diesel engine that, by means of changing the fuel charge, keeps the speed at the set value. This speed is an input to the speed governor of a piston engine, which is a drop in the value of increasing the flow of fuel supplied to the engine cylinders thus increasing the angular velocity of the crankshaft to the specified value.

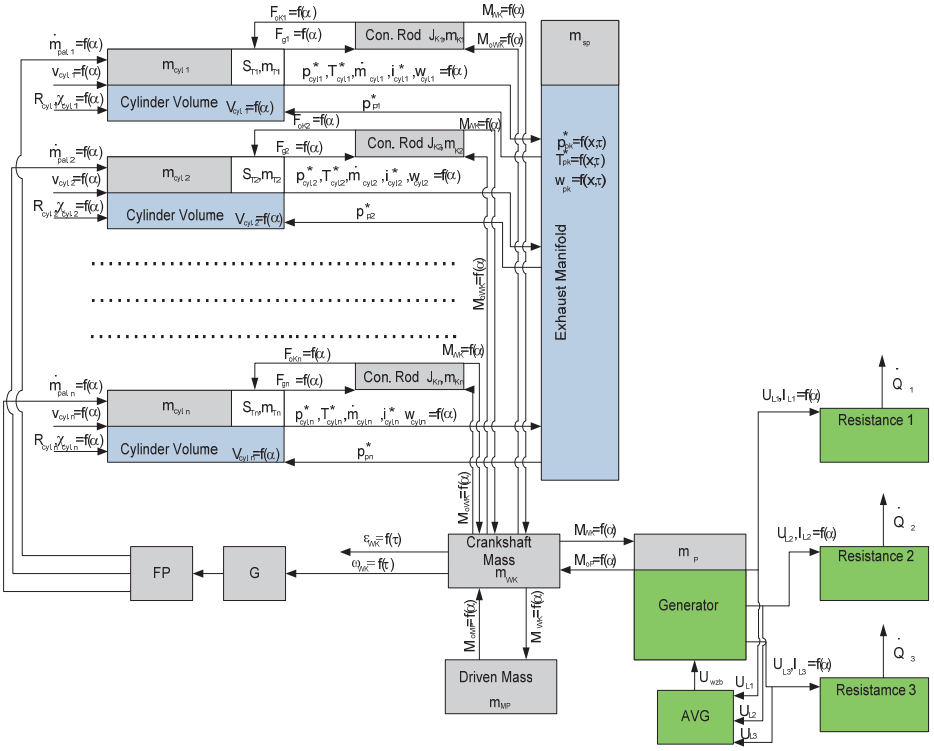

Fig.3. Physical model of energetic processes taking place in the generating set diesel engine – synchronous generator

4. SUMMARY

The presented above research plan and physical model of the marine generating set should allow to work out a non-invasive method for evaluation the technical condition of a diesel electric set, and further a diagnostic methodology, when the engine is not equipped with indicator valves. It is estimated that diagnostic inference there will be possible about combustion process in engine cylinders. Technical state of the engine fuel system, its regulation and the tightness of the set piston-piston rings-cylinder liner, and the condition of the timing system, have the greatest influence on it. Moreover, it will be possible to assess the technical condition of the electrical elements of the synchronous generator and its bearings.

REFERENCES

[1] Cannon, R. h., *Dynamika układów fizycznych*, WNT, Warszawa 1973.

[2] Cwalina A., Zacharewicz M., *Preminary investigations of gebnerating set of the ship's power station in the apspect of diagnosing selected parts of its construction structure,* Combustion Engines nr 3/2011 (146

[3] Cwalina A.,Zacharewicz M., *The conception of diagnosis in auxiliary diesel engine at limited monitoring susceptibility in automated ship power plant,* Polish Journal of Environmental Studies 2011, Vol 20, No 5A/2011

[4] Korczewski Z., *Endoskopia silników okrętowych*, AMW, Gdynia 2008

[5] Korczewski Z., Zacharewicz M., *Metodyka diagnozowania silników okrętów wojennych o ograniczonej możliwości pomiaru ciśnień wewnątrzcylindrowych na podstawie wyników badania procesów gazodynamicznych w układzie turbodoładowania*. Opracowanie w ramach projektu badawczego nr: 0T00B02129
[6] Sobieszczański, M., *Modelowanie procesów zasilania w silnikach spalinowych*, WKŁ, Warszawa 2000
[7] Szczeciński S., *Lotnicze silniki tłokowe*, MON, Warszawa 1969
[8] Zacharewicz M., *Metoda diagnozowania przestrzeni roboczych silnika okrętowego na podstawie parametrów procesów gazodynamicznych w kanale zasilającym turbosprężarkę*, Rozprawa Doktorska, AMW, Gdynia 2009.
[9] Dokumentacja techniczno - ruchowa zespołu prądotwórczego ZE500/52

GDAŃSK UNIVERSITY OF TECHNOLOGY

Journal of POLISH CIMAC

Faculty of Ocean Engineering & Ship Technology
GDAŃSK UNIVERSITY OF TECHNOLOGY

MODELLING OF TOXIC COMPOUNDS EMISSION IN MARINE DIESEL ENGINE DURING TRANSIENT STATES AT VARIABLE ANGLE OF FUEL INJECTION

Ryszard Zadrąg

Polish Naval Academy
Faculty of Mechanical and Electrical Engineering
ul. Śmidowicza 69, 81-103 Gdynia, Poland
r.zadrag@amw.gdynia.pl

Marek Zellma

Polish Naval Academy
Faculty of Mechanical and Electrical Engineering
ul. Śmidowicza 69, 81-103 Gdynia, Poland
m.zellma@amw.gdynia.pl

Abstract

Transient states are an important part of the spectrum of engine loads, especially the traction engines. In the case of marine diesel engines, transient states are of particular importance in reducing the analysis of motion units for special areas and maneuvering in port, the participation of transient states in the load spectrum significantly increases, also, the emission of toxic compounds from this period increases proportionally. The factors which determine the value of the emission are the forces shaping transient states and the technical condition of the engine itself. This paper presents a description of transient states using multi-equation models, and the analysis of their relevance. It also presents a comparison of toxic compounds concentration at modified angles of fuel injection advance.

Keywords: *diagnostic, theory of experiments, marine diesel engine, exhaust gas toxicity, multi-equation models*

1. Introduction

Transient states are exceptional marine diesel engine operating conditions. They arise in the absence of thermodynamic equilibrium in the engine cylinders and are an important part of the engine load spectrum, especially of traction engines, thereby without affecting the emission of toxic compounds. Engine research in this area is forced because of homologation, where the main problem comes down to the optimization of the combustion course with variable engine load described even through urban driving tests.

In the case of marine diesel propulsion, the importance of transient states, in the above sense, is less prominent because of the relatively small proportion of transients in the engine load spectrum. If, however, such an analysis is subjected to the movement of individuals in

specific areas or maneuvering in port, the proportion of transients in the engine load spectrum grows significantly and is worthy of special consideration. Proportionately to this growth increases the emission of toxic compounds, caused by the impact of those states. This should be explained by the fact that transients interfere with cylinder thermodynamic equilibrium, which occurs during the fixed charges. This interrupts the combustion process by causing temporary changes, primarily to the stream of fresh charge of the cylinder, but also the amount of fuel delivered. Thus, the air-fuel ratio changes temporarily, which results in the changes in air excess ratio, leading to increased emissions of combustion products created due to the local oxygen deficit. A further consequence of the appearance of increased amounts of carbon monoxide (CO) and unburned hydrocarbons (HC) is to lower the combustion temperature, which determines the reduced NOx emissions.

The deciding factor in the emissions of toxic compounds derived from transient states is primarily the value of force, which causes these conditions . But this is not the only factor. Another factor affecting the emission of toxic compounds derived from transients that has to be taken into consideration, is the condition of the engine. This condition, described with the structure parameters while using the engine, is constantly changing, which is responsible for the processes of wear. This change enhances the formation of toxic compounds during transient states, as these processes, though short, are so dynamic that the instantaneous concentrations frequently exceed ZT values of the steady states . Therefore, it is expected that the engine with its structure parameters changed due to wear, will be more sensitive to the effects of transients and thus it will be easier to determine its technical condition [5].

The basic parameter deciding about the correctness of combustion process in spark-ignition engines is the fuel injection timing. Even small deviations result in the significant changes in the key indicators of the engine, including the exhaust emission indicators. In the case of conventional engine design, a "self-acting" change of fuel injection timing is rather unlikely. However, in modern constructions, where most of the control parameters is controlled electronically, it is possible for the control system to be damaged and the settings of injection timing to be changed.

The paper will present the modeling of transient states with a variable angle of injection timing and their impact on the changes in the basic concentration of toxic compounds.

2. Identification of a dynamic process of multi-equation model

Building on the experience of authors [6,7,8,9,10] with modeling of toxic compounds concentrations, it was decided to implement the multi-equation models, proven during steady state, for the analysis of dynamic processes, whereby it is assumed that the change process of gas toxicity occurs throughout a time, which makes it dynamic. Therefore, the model can be described as multi-equation system of linear differential equations. Since the measurement of the concentration of toxic compounds is a discrete measurement, discrete-time signal (time series) is a function whose domain is the church of integers. Thus, a discrete-time signal is a sequence of numbers. Such sequences are referred to as recorded in the functional notation. The adoption of such a notation was striving to minimize the impact of errors including the approximation of functions that would have to occur when using the continuous functions.

Discrete-time signal $x[k]$ is often determined by sampling $x(t)$, a continuous signal in time. If the sampling is uniform, then $x[k] = x(kT)$. Constant T is called the sampling period. Course of the dynamic process in time depends not only on the value of force at a given time but also the value of extortion in the past. Thus, the dynamic process (system) has a memory where it stores consequences of past interactions.

The relations between the input signals $x_1[k], x_2[k], \cdots, x_n[k]$, and output signals $y_1[k], y_2[k], \cdots, y_m[k]$, $k = 0,1,2,\ldots$, will be described by a system of linear differential equations.

$$\begin{cases} y_1[k+1] = a_{11}y_1[k] + a_{12}y_2[k] + \cdots + a_{1m}y_m[k] + b_{11}x_1[k] + b_{12}x_2[k] + \cdots + b_{1n}x_n[k] + \xi_1 \\ y_2[k+1] = a_{21}y_1[k] + a_{22}y_2[k] + \cdots + a_{2m}y_m[k] + b_{21}x_1[k] + b_{22}x_2[k] + \cdots + b_{2n}x_n[k] + \xi_2 \\ \cdots\cdots\cdots\cdots\cdots\cdots\cdots\cdots\cdots\cdots\cdots\cdots\cdots\cdots\cdots\cdots\cdots\cdots\cdots\cdots\cdots\cdots\cdots\cdots\cdots\cdots\cdots\cdots \\ y_m[k+1] = a_{m1}y_1[k] + a_{m2}y_2[k] + \cdots + a_{mm}y_m[k] + b_{m1}x_1[k] + b_{m2}x_2[k] + \cdots + b_{mn}x_n[k] + \xi_m \end{cases} \quad (1)$$

where:

$y_i[k], i = 1,2,\ldots,m$ - output signal values at k,

$x_j[k], j = 1,2,\ldots,n$ - input signal values at k,

a_{ij} – is a coefficient found in i-th equation with j-th output signal, $i, j = 1,2,\cdots,m$

b_{ij} - is a coefficient found in i-th equation with j-th input signal, $i = 1,2,\cdots,m$, $j = 0,1,\cdots,n$,

ξ_i - is a non-observable random component in i-th equation.

In analogy to (1), the system of equations (2) can be written in matrix form

$$\mathbf{y}[k+1] = \mathbf{A}\mathbf{y}[\mathbf{k}] + \mathbf{B}\,\mathbf{x}[\mathbf{k}] + \boldsymbol{\xi} \quad (2)$$

where:

$$\mathbf{B} = \begin{bmatrix} b_{11} & b_{12} & \cdots & b_{1m} \\ b_{21} & b_{22} & \cdots & b_{2m} \\ \cdots & \cdots & \cdots & \cdots \\ b_{m1} & b_{m2} & \cdots & b_{mm} \end{bmatrix}, \qquad \mathbf{A} = \begin{bmatrix} a_{11} & a_{12} & \cdots & a_{1n} \\ a_{21} & a_{22} & \cdots & a_{2n} \\ \cdots & \cdots & \cdots & \cdots \\ a_{m1} & a_{m1} & \cdots & a_{mn} \end{bmatrix},$$

$$\mathbf{y}[k] = \begin{bmatrix} y_1[k] \\ y_2[k] \\ \cdots \\ y_m[k] \end{bmatrix}, \quad \mathbf{y}[k+1] = \begin{bmatrix} y_1[k+1] \\ y_2[k+1] \\ \cdots \\ y_m[k+1] \end{bmatrix}, \quad \mathbf{x}[\mathbf{k}] = \begin{bmatrix} x_1[k] \\ x_2[k] \\ \cdots \\ x_n[k] \end{bmatrix}, \quad \boldsymbol{\xi} = \begin{bmatrix} \xi_1 \\ \xi_2 \\ \cdots \\ \xi_m \end{bmatrix}.$$

Later denoting:

$$\boldsymbol{C} := [\boldsymbol{A}|\boldsymbol{B}] = [c_{ij}]_{m\mathrm{x}(m+n)} \quad (3)$$

and

$$\boldsymbol{z}[k] := \begin{bmatrix} \boldsymbol{y}[k] \\ \boldsymbol{x}[k] \end{bmatrix},$$

the system of equations (1) is shown in reduced form

$$\boldsymbol{y}[k+1] = \boldsymbol{C}\boldsymbol{z}[k] + \boldsymbol{\xi} \quad (4)$$

Identification of the system of equations (1) and (4) will be based on the selection of the coefficients using the set of measurements on the real object of input and output signals. The problem of aforementioned selection the authors present, among others, in [6,7,8,9,10].

3. Study of dynamic process in engine fuel supply system through multi-equation models

The object of this research was the engine fuel supply system (fuel injection) of a single-cylinder test engine 1-SB installed in the Laboratory of the Exploitation of Marine Power Plants at the Naval Academy [8]. The experimental material was collected by trivalent developed a complete plan [4]. The implementation of specific measuring systems (measuring points) of the above experiment design were performed using a programmable controller, which allowed a high repeatability of dynamic processes. The period between an onset of the clipping of injection system components and the re-stabilization of output quantities was adopted as the duration of the dynamic process. This period was chosen through a series of experiments, and it averaged to about 106 seconds.

In order to identify the impact of the technical condition of the fuel supply system on the parameters of the engine power during dynamic processes, sets of input quantities (preset parameters) and output quantities (observed parameters) were defined. For the purpose of this study a set of input quantities X was limited to three elements, that is: x_1 - engine speed n [r/min]; x_2 – engine torque T_{tq} [N·m]; x_3 – fuel injection timing α_{ww} [ºREC]. The study was conducted in accordance with the approved complete plan, for three values of speed, ie 850, 950 and 1100 [r / min]. For each speed, torque (T_{tq}) increased and thus created a transient state, consequently for the load of 10, 20, 30, 50, 70 [N]. For speed of 850 r / min, afraid of a large engine overload, the loads of 50 and 70 N were omitted. Similarly, this was done to the speed of 950 r / min and a 70 N load. Fuel Injection timing varied by ± 5 ºREC, yielding three values, i.e. face value - N, accelerated angle - W, delayed angle - P. 36 repetitive transients were obtained this way. Graphic interpretation of the test program is shown in Figure 1.

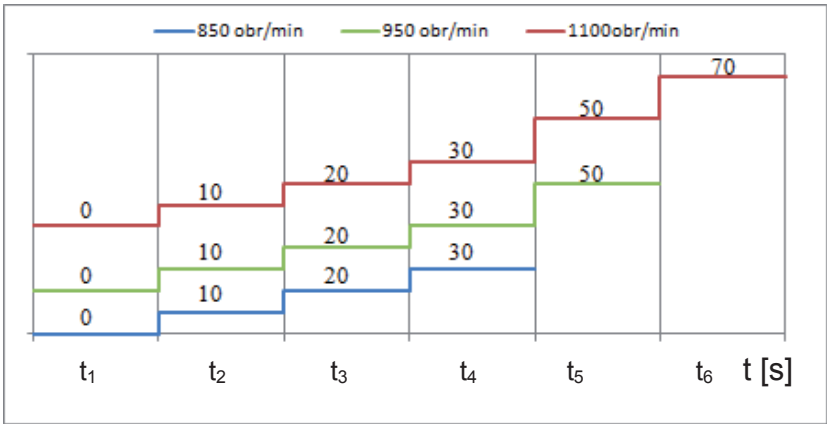

Figure 1. Schematic of the program of research

Similar treatment was applied to the set Y of output quantities, limiting the number of its elements to only the primary toxic compounds in exhaust manifold: y_1 – concentration of carbon monoxide in the exhaust manifold $C_{CO(k)}$ *[ppm];* y_2 – concentration of hydrocarbons in the exhaust manifold $C_{HC(k)}$ *[ppm];* y_3 – concentration of nitrogen oxides in the exhaust manifold $C_{NOx(k)}$ *[ppm],* y_4 – tsp exhaust gas temperature [º C], y_5 – air-fuel ratio λ.

Statistical identification was made using GRETL [1]. Estimation of the equation coefficients for specific output variables was performed using the least-squares method and it had to verify the significance of its parameters and, consequently, the rejection of insignificant values, which consequently led to a significant simplification of the models. Given the large amount of experimental material, for the purpose of this study is selected the most typical cases, while limited to the greatest loads that occur during the experiment. Tables 1, 2, 3, 4 are coefficients of equations for nominal output variable injection timing. Significance values of model parameters are shown in the last column of the tables. Equations describing the changes in concentration of hydrocarbons (y_2) and the concentration of nitrogen oxides (y_3) have undergone the greatest simplification. (Table 1, 2, 3). In the case of equations describing changes in carbon monoxide and hydrocarbons, they depend on the excess air ratio λ (y5) significantly, a parameter directly related to the parameter of the structure, which was the fuel injection timing (x3). Both CO and HC significantly dependent on each other. Furthermore, in the case of CO, speed has a greater impact, while in the case of HC it is the load, which seems to be logical, considering the creation processes of these compounds in the cylinder.

Table 1. Least-squares estimation of the dependent variable y_1

Variable	*Coefficient*	*Mean error*	*Student t*	*p value*	*i significance*
x1_1	0,785212	0,297116	2,6428	0,00952	***
y5_1	-640,111	84,9526	-7,5349	<0,00001	***
y2_1	6,00076	0,536841	11,1779	<0,00001	***

Table 2. Least-squares estimation of the dependent variable y_2

Variable	*Coefficient*	*Mean error*	*Student t*	*p value*	*i significance*
y5_1	52,7105	9,26814	5,6873	<0,00001	***
x2_1	2,23258	0,472489	4,7252	<0,00001	***
y1_1	0,0605765	0,0102887	5,8876	<0,00001	***

Table 3. Least-squares estimation of the dependent variable y_3

Variable	*Coefficient*	*Mean error*	*Student t*	*p value*	*i significance*
x2_1	0,104014	0,0251446	4,1366	0,00007	***
x1_1	0,216752	0,00166072	130,5167	<0,00001	***
y4_1	0,025725	0,00437145	5,8848	<0,00001	***

Table 4. Least-squares estimation of the dependent variable y_4

Variable	*Coefficient*	*Mean error*	*Student t*	*p value*	*i significance*
x1_1	-0,483745	0,23243	-2,0813	0,03994	**
y1_1	-0,0155244	0,00653628	-2,3751	0,01943	**

y3_1	4,6947	0,975664	4,8118	<0,00001	***
y5_1	-118,888	10,9896	-10,8182	<0,00001	***

The graphical presentation (Fig. 2) of the matching can prove having a good model fit to the values obtained in the experiment on the engine, as well as equal distribution of residuals from the regression of mean values (Fig. 3).

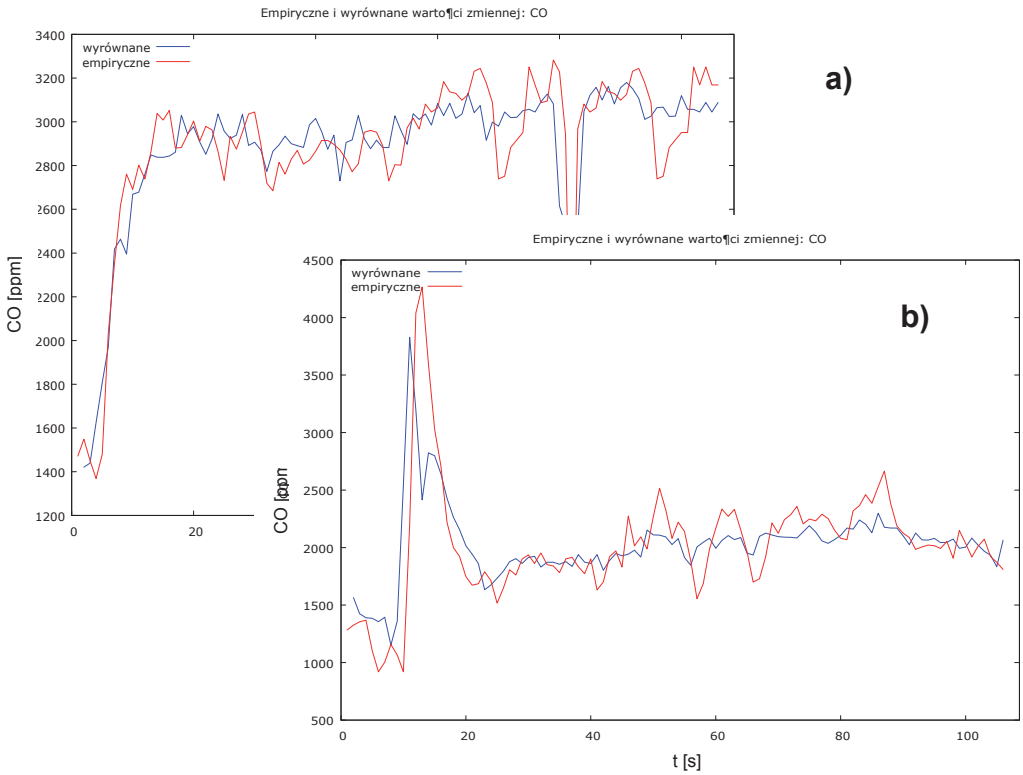

Figure 2. Graphical matching of the CO model to the empirical data for the transient at n = 1100 r / min and load change with Ttq = 50 to N = 70 N Ttq a) delayed (P) injection timing angle, b) accelerated (W) injection timing angle

The analysis of Figure 3 shows that the worse adjustment, due to the higher residue values, exists for accelerated (earlier) fuel injection timing angle.

The results of the presented analysis highlight the significant advantage of multi-equation models, the possibility of multi-criteria analysis of the variables in the case where these values are in mutual correlation. Analysis of these relationships in one model reflects the reality more accurately (because there are obvious interactions between, for example, CO and HC and, for example, λ), and thus allows for a broader interpretation of the test problem.

Despite the undeniable advantages of multi-equation models do not provide direct information on the quality of changes, in this case, differences between the concentration of

various toxic compounds due to changes in fuel injection timing. Only the juxtaposition of courses of the experiment or the analysis of the obtained models provides some picture of the phenomenon. Nonetheless, analysis still remains difficult due to the similarity of transient waveforms, irrespective of the value of extortion.

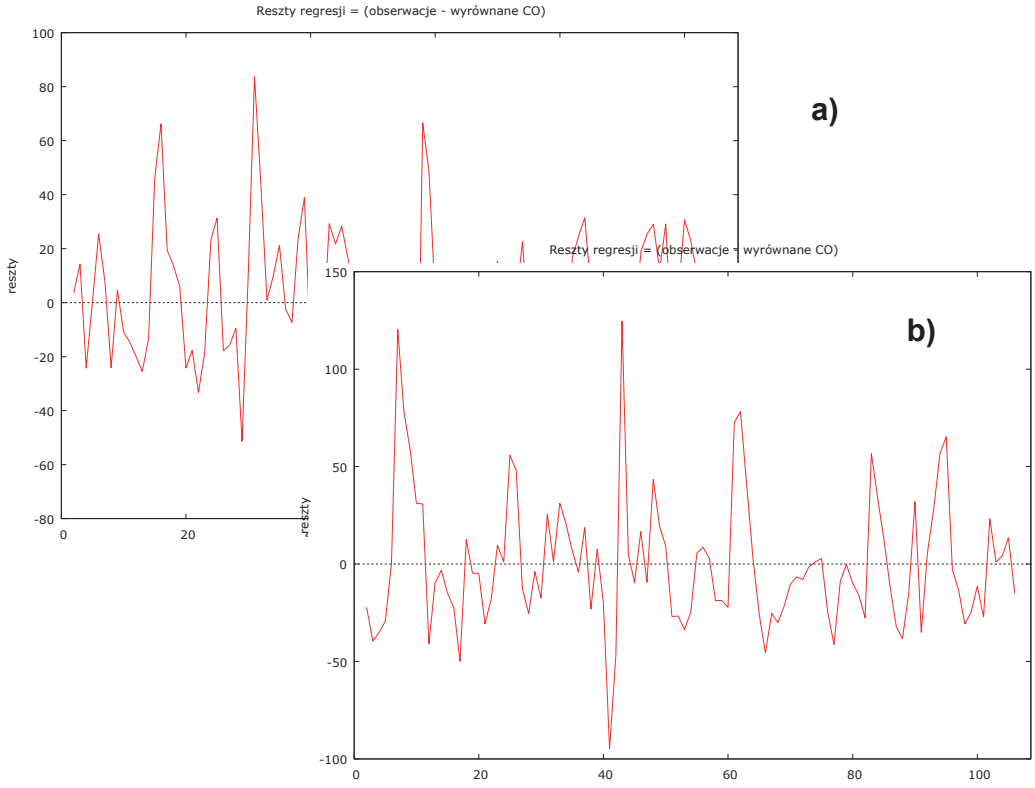

Figure 3. Graph of the CO regression residuals for the transient at n = 1100 r / min and load change from T_{tq} = 50 N to T_{tq} = 70 N a) delayed (P) injection timing, b) accelerated (W) injection timing.

In such case, it is desired to apply the criteria that would be useful in the objective assessment of the comparative levels or emissions from transients. The use of an evaluation index is one of the commonly used methods in such cases. The basic hourly evaluation is an individual emission of toxic fumes, which is calculated by the formula [3]:

$$E_{i,j} = a_j \cdot C_{j,i} \cdot G_{sp,i} \text{ [g/h]} \tag{5}$$

where:

j – CO, HC, NO_x,

a_i – characteristic factor for a given compound j:

a_{CO} = 0,000966, a_{HC}=0,000478, a_{NOx}=0,001587,

$C_{j,i}$ – concentration of individual compounds [ppm],

$G_{sp,i}$ – exhaust gas flow [kg/h].

This evaluation is, however, difficult to apply in the case of the analysis of transient processes, since determining the exhaust flow would require the estimation, thus introducing significant errors, which obviously excludes this method. Another view was proposed by the authors in [3], using the following relationship evaluation:

$$W_i = a_i \int_0^t C_{j.i}(t)dt \tag{6}$$

where:
$C_{j,i}(t)$ – the concentration of any toxic compound in time t [ppm],
t – the duration of the transient state [s].

Thus, by integrating the area under the curve obtained from an experiment or from a model, an indicator that accurately describes the direction of change was obtained. On the other hand, this indicator continues to not describe the nature of the changes. As is known from observation, depending on the value of force, the course of the transient can vary significantly. These differences depend largely on the intensity of the experience of individual phases of the transient. Frequently, in the course of a typical transient, two phases can be noticed. First, characterized by the highest growth rate, accompanied by a sharp increase in the concentration of TS, typically several times more than the concentration in the steady state. The second phase of the transient is characterized by a much less violent course, it has a monotonic character and approaches the steady-state of concentrations in an asymptotic manner.

As mentioned above, the concentrations of individual toxic compounds derived from transients are characterized by a certain regularity and repetition, and therefore a tool had to be found that would be deprived of the above-mentioned disadvantages of the indicators, while being able to be described in the precise and objective nature of the changes in the concentrations of individual toxic. It seems that the described method would be the analysis of the correlation of individual transients. This method determines the correlation of the researched transient state and that of the transient adopted as a model describing the phenomenon. Analysis of the correlation function allows you to specify the degree of correlation and its nature. Analyzing the components of the function can infer the said transient nature, that is, the participation and intensity of the individual phases.

The graphic imagining of the analysis correlation is a scatter diagram presented in Figure 4 and 5. Figure 4 shows the linear correlation function of the concentration of unburnt hydrocarbons HC at early injection timing angle (30 ° HVAC - red) relative to the nominal injection timing (26 º HVAC) , where the correlation coefficient was r = 0.75. The color green indicates the correlation function and the HC concentration at the delayed angle (22 º HVAC) also with respect to the nominal injection timing. The correlation coefficient in this case was smaller, and was r = 0.59. Smaller values of the correlation coefficient were affected by the dispersion of points around the correlation function, which indicates an unstable transient process (matching multi-equation model is significant even in this case, as the greatest value of the residue is 60 ppm). Analogously, correlation analysis may be performed for NOx (Fig. 5).

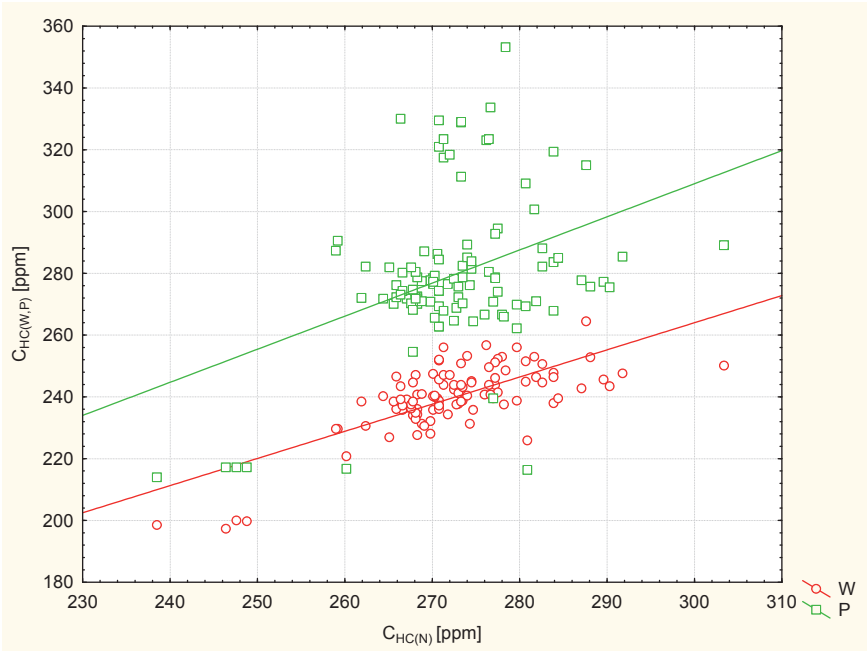

Figure 4. The concentration of hydrocarbons HC for the transient at n = 1100 r / min and load change from T_{tq} = 30 N to T_{tq} = 50 N: P - late, W - accelerated injection timing, CHC (N, S, P) - HC concentration for (N) nominal, (W) accelerated, (P) delayed injection timing

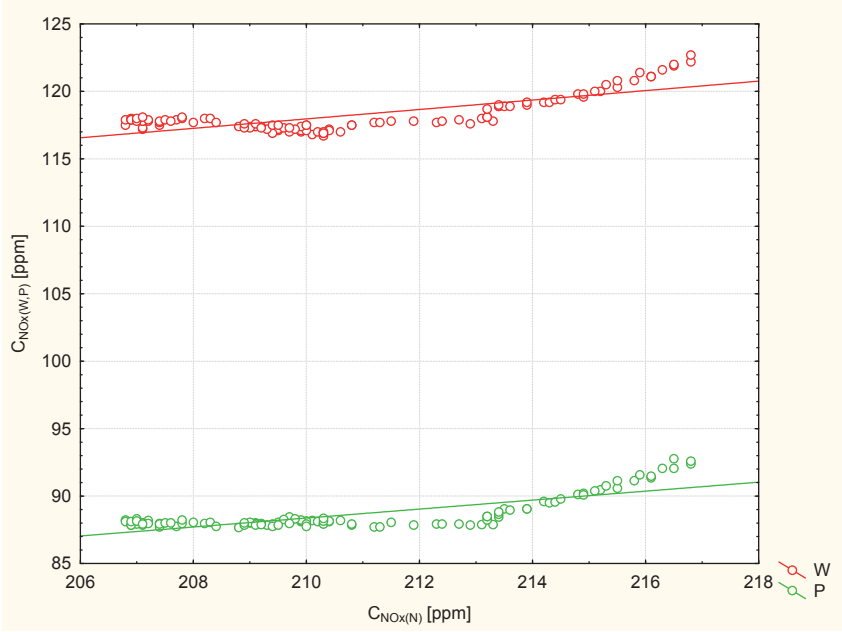

Figure 5. The concentration of NOx for the transientat n = 1100 r / min and load change from T_{tq} = 30 N to T_{tq} = 50 N: P - late, in - accelerated injection timing, CNOx (N, S, P) - NOx concentration (N) nominal, (W) accelerated, (P) delayed injection timing

The correlation coefficients indicate a high matching of correlation functions in the two cases. And, for the accelerated angle (red), correlation coefficient is r = 0.79, while for delayed angle, r = 0.80. Another regularity can be noted, namely, much higher concentrations of NOx fall for the former angle, which of course is consistent with the theory of combustion (with the increase of injection timing, the share of kinetic combustion increases, at the same time increasing the pressure and temperature of combustion) , are thus improved conditions , at which nitrogen oxides are formed. For HC the situation is reversed (Fig. 4), delayed injection timing results in a higher proportion of diffusion combustion, which often goes into burnout and thus creates favorable conditions for the formation of unburned hydrocarbons.

4. Summary:

In the course of this study, the following conclusions have raised:

- multi-equation models provide a good match to the empirical results,
- using a multi-equation model makes it possible to predict, and thus greaten the modeling of concentration change (emission) during the transient,
- a discussion of the accuracy of different methods to estimate emissions, even using the method of spline functions is possible.

REFERENCES

[1] Kufel T.: Econometrics. Solving Problems Using GRETL Software, in Polish, Polish Scientific Publishers PWN, Warszawa. 2007.

[2] Kukiełka L.: Basics of Engineering Research, in Polish, Polish Scientific Publishers PWN, Warszawa 2002.

[3] Piaseczny L. Zadrąg R.: The influence of selected damages of engine SI type on the changes of emission of exhaust gas components, Diesel Engines, Opole 2009.

[4] Polański Z.: Design of Experiments in Technology, Polish Scientific Publishers PWN, Warszawa 1984.

[5] Zadrąg R.: Criteria for the selection of the diagnostic parameter for diagnosis of marine diesel engine, LOGISTYKA No. 4/2010, ISSN 1231-5478, Poznań 2010.

[6] Zadrąg R.: The Multi-equational models of leakproofness of charge exchange system of ship engine, in Polish, in monography 'Gaseous engines – selected issues'' edited by Adam Dużyński, University of Czestochowa Publishing, ISBN 978-83-7193-461-2, ISSN 0860-501., Częstochowa 2010.

[7] Zadrąg R.: The multi-equational models in the analysis of results of marine diesel engines research, International Conference Eksplodiesel & Gas Turbine'2009, Międzyzdroje- Kopenhaga 2009.

[8] Zadrąg R. et al.: Indentification models for the technical condition of the engine on the basis of exhaust component emissions, in Polish, The report of the research project no. 4T12D 055 29, AMW, Gdynia 2008.

[9] Zadrąg R., Zellma M.: Analysis of the results of internal combustion engines using multivariate models, in Polish, Symposium on Marine Power Plants Symso'2009, Gdynia 2009.

[10] Zadrąg R., Zellma M.: The usage of multi-equation models in analysis of dynamic process in marine diesel engine research. JOURNAL OF POLISCH CIMAC, Vol.7, No 1, ISSN 1231-3998, str. 295-304, Gdańsk 2012.